Reviewer 1

This article presents clumped isotope measurements in scleractinian and gorgonian deep-sea corals. The data are very interesting, but I think that the discussion needs to be rewritten. As it is, the discussion gives the feeling that gorgonian and scleractinian share identical processes of biomineralization, which absolutely not the case. The discussion should be clearly separated between the two types of deep-sea corals. For example, as far as I know, calicoblastic cells were not detected in gorgonian corals, as well as ECF (see Noé and Dullo, 2006). There are also a lot of imprecisions in the text.

Reviewer comment: *A lot of references miss in the reference section: Dunbar and Wellington (1981), Came et al (2004), Eagle et al (2010), Dennis and Schrag (2010), Douglas et al (2014), Ghosh et al (2007), Gabitov et al (2012), Kimball et al (2014), McConnaughey (2003), Nielsen et al (2012), Petrizzo et al (2014), Saenger et al (2013), Swart et al (1991), Watson and Liang (1995), Watson (2004), Watkins et al (2013), Weber and Woodhead (1972), Thiagarajan et al (2013), Zeebe (1999).*

Also some references in the reference section are not cited in the text:

Bigeleisen and Mayer (1947), Ehrlich et al (2006), Jimenez-Lopez et al (2004), McCrea (1950), Noé et al (2008), O'Neil et al (1969), Urey (1947), Wang et al (2004)

Author response: These have been removed or cited.

Reviewer comment: *19117-l18: I think that it is not an 'emerging' approach anymore as it is now known for 10 years.*

The word emerging has been removed.

Reviewer comment: *19118-l14: what is the difference between aragonitic scleractinian corals and aragonitic deep-sea corals?*

Author response: We have clarified this sentence that now reads:

"Proxy material calibrations thus far have included aragonitic scleractinian zooxanthellate corals (Ghosh et al., 2006; Saenger et al., 2012; Tripati et al., 2015), aragonitic scleractinian non-zooxanthellate deep-sea corals (Ghosh et al., 2006; Thiagarajan et al., 2011), aragonitic otoliths (Ghosh et al., 2007)"

Reviewer comment: *19118-l17: Is there any aragonite in brachiopod shells?*

Author response: To clarify we have removed the word aragonite, this sentence now reads:

"… mollusks and brachiopods."

Reviewer comment: *19118-l19: It is 'Daëron' instead of 'Daeron'. Please correct.*

Author response: Corrected

Reviewer comment*: 19118-l20: In the reference section, it is Petryshyn et al (2015).*

Author response: Corrected

Reviewer comment*: 19118-l27: It is Wacker et al (2013) in the reference section.*

Author response: Corrected

Reviewer comment*: 19119- l10: Is it Defliese et al 2015a or b?*

Author response: These have been specified throughout the text.

Reviewer comment*: 19120-l11-14: please add references*

Author response: Reference added, fractionation (Adkins et al., 2003; Gaetani et al., 2011).

Reviewer comment*: 19120-l20: I am not sure that there are some d18O data for deep-sea corals in McConnaughey (1989a or b?; 2003). Please add references of Lutringer et al (2005), Rollion-Bard et al (2003, 2010).*

Author response: Done

Reviewer comment*: 19120-l23: Please add the reference to Lutringer et al (2005).*

Author response: Done

Reviewer comment*: 19121-l1: please remove one 'Ghosh et al' In this section, I found it very unclear what is attributed to gorgonian or scleractinian (doesn't need to be)*

Author response: Done

Reviewer comment: *19122-l6: Replace 'was' by 'were' (no)*

Author response: Done

Reviewer comment: *19122-l27: What do you mean by 'sufficient'?*

Author response: Changed to: "the required weight of sample for replica …"

Reviewer comment: *19123-l25: It is Henkes et al (2014) in the ref*

Author response: Henkes 2013 is the correct reference.

Reviewer comment: *19125-l8-9: Is it in PDB? (look at table)*

Author response: Its V-SMOW, this has been corrected.

Reviewer comment: *19126-l6: 'Tables' instead of 'Table'. I am not sure that you have to refer to Table 3 here.*

Author response: Now reads: "Measured and predicted coral isotopic measurements are presented in Table 4."

Reviewer comment: *19126-l12-13: R2 instead of R. It is not consistent with the rest of the paragraph.*

Author response: Corrected

Reviewer comment: *19126-l25: 'Noé' instead of 'Noe'*

Author response: Corrected

Reviewer comment: *19130-l4: AFF is not defined.*

Author response: Now reads: "suggests there may be mineral-specific acid digestion fractionation factors (AFF),"

Reviewer comment: *19132-l3: Please add references.*

Author response: References added.

Reviewer comment: *19132-l10: It is Roark et al (2005) in the ref. In this article, I did not see any d13C and/or d18O data. Please verify. Please add references to Lutringer et al (2005), Rollion-Bard et al (2003, 2010).*

Author response: Reference removed and others included.

Reviewer comment: *Between the centres of calcification and fibres, in scleractinian corals, you can have these two end-members. So why do you write that the mixing would be between less extreme differences? Also, note that there are no COC in gorgonian corals. Again, for this section, it would be clearer to separate the discussion between gorgonian* *and scleractinian corals.*

Author response: This is a good point and we have added statements about these differences between scleractinian and gorgonian coral, and revised this section to better explain what sets the endmembers for mixing.

"we estimate the maximum artifacts in our data arising from mixing. The estimate for mixing artifacts from Thiagarajan et al. (2011) is based on observed variability in stable isotope values in scleractinian deep-sea coral, and represents an extreme example for this study, as they use δ13C and δ^{18}O values of end members that differ by 12‰ and 7‰, respectively. Such differences in scleractinian coral represent systematic isotopic depletions in centers of calcification compared to fibers (Adkins et al., 2003), as well as variability associated with density bands; no centers of calcification have been reported in gorgonian corals. The calculations from Thiagarajan et al. (2011) represent an estimate of the maximum artifact to arise from mixing for either taxa given the range of carbon and oxygen isotope values observed in scleractinian and gorgonian deep-sea coral. We also observed little variability in δ^{13}C and δ^{18}O of different preparations of the same coral, with standard deviations of <1‰."

As described in more detail in the response to reviewers below we have separated the models of scleractinian and gorgonian corals.

Reviewer comment: *19133-l18: Is there any reference for the observation of calicoblastic cells in gorgonian corals? Same remark concerning the scheme for the calcifying region. This model was developed for scleractinian corals, not for gorgonian.*

Author response: The potential differences in calcification between the two groups of corals is now more acknowledged by creating separate subsections in the manuscript discussing each. The gorgonian coral section now reads:

"The growth structure, mineralogy, and biomineralization of gorgonian coral skeletons is distinctly different from scleractinian corals (Noé and Dullo, 2006). Additionally, the organic matrix-mediated calcification process is largely unexplored and unknown for most gorgonian families. The biomineralization models described for scleractinian corals therefore are not valid when interpreting potential vital effect signals in gorgonian corals.

An exhaustive study of the growth structure and fabric of deep-sea isidid gorgonians in the same family as those investigated here, was done by Noé and Dullo (2006). Their findings are based on characterization of the isidid skeletal micro- and ultrastructure in combination with absolute age determinations. From their reconstructions of growth mode and fabric, they propose a biomineralization model. With no calicoblastic cells observed in gorgonians, they propose gorgonin produced from the endodermal epithelium acts as the structural framework, while a viscous slime surrounding the skeleton acts as the matrix, facilitating and regulating mineral growth. Their model however relies on physical observations and lacks geochemical data to inform their interpretations. So while offering some insight into the uniqueness of Isidid biomineralization, the findings are not useful in interpreting the geochemical data observed in this study.

Despite the lack of proposed biomineralization models in gorgonian corals, the trends in d^{13}C and d^{18}O have been explored and found to be similar in pattern to scleractinian corals, but with an offset that agrees with theoretical mineralogical fractionation predictions. The similarity in d^{13}C, d^{18}O and d_{47} patterns suggests that while the particular biomineralization process is necessarily different in the two groups, there is a functional similarity that results in the conserved patterns in both gorgonian and scleractinian corals."

Reviewer comment: *19134-l19: It is 'Mavromatis et al'. This article is only about fractionation factor for Mg-calcite. I do not see why it is cited here (because isidids are high-Mg calcite)*

Author response: Reference removed.

Reviewer comment: *19135-l4: Are you sure that brachiopod shells are aragonitic?*

Author response: This statement has been removed.

Reviewer comment: *19135-l24: Please add 'e.g.' before the list of references as a lot of studies deal with this aspect. Here McConnaughey is misspelled. Is it 1989a or b? Watson (2004), DePaolo (2011), Gabitov et al (2012) and Watkins et al (2013) study inorganic precipitations. Why are they cited here concerning the calcification processes in calcifying organisms?*

Author response: This section now reads:
"Non-equilibrium partitioning of oxygen and carbon isotopes have been observed in numerous calcifying organisms and inorganic precipitation experiments, and linked to calcification processes (e.g. McConnaughey, 1989a; Spero et al., 1997; Zeebe, 1999; Adkins et al, 2003: Watson, 2004; DePaolo, 2011; Gabitov et al., 2012; Watkins et al., 2013)."

Reviewer comment: *19136-l5: This model is for scleractinian corals! I am not convinced that you can apply it to gorgonian corals.*

Author response: See response to comment above which also covers this comment.

Reviewer comment: *19136-l12: Again McConnaughey is misspelled.*

Author response: Corrected

Reviewer comment: *19136-l28: Again McConnaughey is misspelled.*

Author response: Corrected

Reviewer comment: *19137-l1: It is also calculated/noted in Zeebe and Wolf-Gladrow (2001), Beck et al (2005) and Rollion-Bard et al (2011). Please add.*

Author response: Added

Reviewer comment: *19137-l8: It is 'Usdowski et al, 1991'. Please add reference to McCrea (1950)*

Author response: Done.

Reviewer comment*: 19137-l15-18: So how do you explain the kinetic effects for carbon isotopes if the exchanges are very rapid (please add ref) between DIC species?*

Author response: The model referred to in this section accounts for the range in carbon isotopes by proposing it to be a function of two sources of CO_2, membrane diffused and seawater leaked, and the proportion of them, a function of pH gradients across the membrane.

Reviewer comment*: 19137-l27: Please add references to Lutringer et al (2005), Rollion-Bard et al (2003, 2010).*

Author response: Done

Reviewer comment*: Please note that the model of Adkins et al (2003) is not compatible with boron isotope data (see Blamart et al, 2007; Rollion-Bard et al, 2010).*

Author response: Done

Reviewer comment*: 19138-l1: Correct McConnaughey and Rollion-Bard. Please add the models of Allison et al (2010) for zooxanthellate corals and the model of Rollion-Bard et al (2010) for deep-sea scleractinian corals.*

Author response: Done

Reviewer comment: *19139-l9: Ref? 19139-l20: Again, please add references to Rollion-Bard et al (2003, 2010). See also the work of Brahmi et al (2012) concerning the different growth rates.*

Author response: Tripati et al., 2015 is referenced. Here we discuss clumped isotopes only - that is only the reason we have not referenced other work.

Reviewer comment: *19139-l29: Again McConnaughey is misspelled*

Author response: Corrected

Reviewer comment: *19139-l8: same remark 19139-18: It was already shown that the Adkins' model is not compatible with d11B data (see Rollion-Bard et al, 2010)*

Author response: This has now been previously addressed in the text.

Reviewer comment: *19140-l26: Please add references*

Author response: Added.

Reviewer comment: *19141-l1-3: Please add references*

Author response: Done

Reviewer comment: *19141-l12: Is it Ehrlich or Ehrlick?*

Author response: Ehrlich, corrected.

Reviewer comment: *19142- l16: See the work of Furla et al (2000) 19142-l19: See the work of Tambutté et al(1995)*

Author response: We thank the reviewer for the references. In this case the paragraph is meant to be a summary of our previous discussion and not introducing new work.

Reviewer comment: *19142-l2: 'corals' instead of 'coral'*

Author response: Corrected

Reviewer Comment: *Between Figures 4 and 5, please use the same colors for the symbols.*

Author response: *Corrected. All symbols are black.*

Reviewer Comment: Figure 6: Precise if it is Defliese et al 2015a or b. Please add error bars

Author response: (done).

Figures 7, 8, 9: Please add error bars (done). Figure 9: Please enlarge the symbols (done). Figure 11: Please specify that this model is for scleractinian corals. For example, the data of Farmer et al (2015) are not in favor of an elevation of pH

Author response: (done)

Reviewer 2

In this contribution, the authors present traditional O and clumped isotope data from carbonates precipitated by deep-sea corals over a range of temperatures. The authors compare their temperature-dependent _47 data to existing biogenic and abiotic temperature calibrations. Differences between scleractinian and gorgonian corals are pointed out and discussed, as are similarities and differences among the observed temperature dependences in deep-sea corals and those in existing temperature calibrations. Overall, in this paper the authors present the data clearly, and although no far-reaching insight is obtained regarding calcification mechanisms in corals, the temperature dependence of carbonate clumped isotope compositions, or the validity of the various temperature calibration curves existing in the literature, the new data from corals are exhaustively compared with the existing calibrations, including a consideration of the effect of the acid digestion fractionation used. A nice contribution of the current paper is the schematic diagram showing expected trajectories for the various processes that can cause a deviation from equilibrium O and clumped isotope composition (Figure 10).

As I am no expert on models of coral precipitation, I cannot speak to the accuracy of this aspect of the paper. In terms of the analytical details, the presentation and interpretation of the data, this paper requires only minor modifications prior to publication. Once revised and published, this paper will be a valuable source of isotopic data on disequilibrium isotopic compositions in corals, which may one day inform models of coral mineralization, as well as the validity of the various clumped temperature calibrations.

Minor comments:

Reviewer comment: *1. There are many references that appear in the text but not in the bibliography and vice versa.*

Author response: This has been corrected.

Reviewer comment: *2. 19122 line 25: 'mortor' should be mortar.*

Author response: Corrected

Reviewer comment: *3. 19123 line 24: 'John' should be Johns.*

Author response: Corrected

Reviewer comment*: 4. 19126 lines6-8: Why does it matter that this coral was only partly alive ("Mostly dead is partly alive!" - Miracle Max)? When measured in the geologic record, corals are quite dead, yet we are happy to use their isotopic composition to inform problems of interest. I'm not sure I see a reason for excluding this data point (because this is a calibration)*

Author response: We agree that the wording of this is imprecise so have revised it. This coral was not alive. Our aim is to focus on data for live-collected specimens to compare with in situ temperature measurements to eliminate any uncertainty in growth temperatures or post-formation dissolution when considering proxy systematics. For proxy validation, or for reconstruction purposes, using this specimen would be reasonable. The text has been revised to indicate this:

"Since specimen PV 703-7 was mostly a dead coral except in small sections when collected and therefore could have had a more complicated life history, it was excluded from calibration analysis"

Reviewer comment: *5. 19127 sentence ending in line 6 is grammatically incorrect.*

Author response: *Corrected, now reads:*

"In a plot of Δ_{47} vs. $10^6/T^2$, the linear regression through data derived from 9 gorgonian deep-sea corals analyzed in this study gives a significantly shallower slope (slope: 0.025±0.01, intercept: 0.403±0.129, R^2=.48) and Δ_{47} offset of ca. 0.04-0.07‰ in the temperature range of 3.2-11.2°C compared to scleractinian corals as well as compared to the Ghosh et al. (2006) calibration."

Reviewer comment: *6. 19130 line 1: 'used' should be uses.*

Author response: Corrected

Reviewer comment: *7. 19130 line 7: 'predications' should be predictions.*

Corrected

Reviewer comment: *8. 19131 line 5: The uninitiated do not know what an 'autoline' is. How about 'auto-mated sample extraction line'?*

Author response: Clarified as suggested

Reviewer comment: *9. 19135 line 20: 'effects' should be affects.*

Author response: I think effects is the correct one here.

Data figures 7, 8, 9 are much less well prepared and presented than figures 3-6, in terms of marker sizes, font readability, legend location and readability, etc.

We have modified figures 7-9 to address this comment.

Carbonate "clumped" isotope signatures in aragonitic scleractinian and calcitic gorgonian deep-sea corals

J. Kimball[1,2], R. Eagle[1,3], R. Dunbar[2],

[1] {Department of Atmospheric and Oceanic Sciences, Institute of the Environment and Sustainability, University of California, Los Angeles, CA, 90095, USA}

[2]{Department of Environmental Earth System Science, Stanford University, Stanford, CA 94025, USA}

[3]{European Institute of Marine Sciences (IUEM), Université de Brest, UMR 6538/6539, Rue Dumont D'Urville, and IFREMER, Plouzané, France}

Corresponding author: robeagle@g.ucla.edu

Abstract

Deep-sea corals are a potentially valuable archive of the temperature and ocean chemistry of intermediate and deep waters. Living in near constant temperature, salinity and pH, and having amongst the slowest calcification rates observed in carbonate-precipitating biological organisms, deep-sea corals can provide valuable constraints on processes driving mineral equilibrium and disequilibrium isotope signatures. Here we report new data to further develop "clumped" isotopes as a paleothermometer in deep-sea corals as well as to investigate mineral-specific, taxon-specific, and growth-rate related effects. Carbonate clumped isotope thermometry is based on measurements of the abundance of the doubly-substituted isotopologue $^{13}C^{18}O^{16}O_2$ in carbonate minerals, analyzed in CO_2 gas liberated on phosphoric acid digestion of carbonates and reported as Δ_{47} values. We analyzed Δ_{47} in live-collected aragonitic scleractinian (*Enallopsammia* sp.) and calcitic gorgonian (Isididae and Coralliidae) deep-sea corals, and compared results to published data for other aragonitic scleractinian taxa. Measured Δ_{47} values were compared to *in situ* temperatures and the relationship between Δ_{47} and temperature was determined for each group to investigate taxon-specific effects. We find that aragonitic scleractinian deep-sea corals exhibit higher values than calcitic gorgonian corals and the two groups of coral produce statistically different relationship between Δ_{47} -

Rob Tripati 7/25/2016 10:33 AM
Deleted: E.

Revisions 7/25/2016 10:32 AM
Deleted: A. E. Tripati[1,3]

Revisions 7/25/2016 10:32 AM
Deleted: Institute of the Environment and Sustainability,

Revisions 7/25/2016 10:32 AM
Deleted: Department

Revisions 7/25/2016 10:32 AM
Formatted: English (US)

Revisions 7/25/2016 10:32 AM
Deleted: Earth, Planetary,

Revisions 7/25/2016 10:32 AM
Formatted: English (US)

Revisions 7/25/2016 10:32 AM
Deleted: Space Sciences

Revisions 7/25/2016 10:32 AM
Formatted: English (US)

Revisions 7/25/2016 10:32 AM
Deleted: Correspondence to: R. E. Tripati (robert.tripati@gmail.com)

temperature calibrations. These data are significant in the interpretation of all carbonate "clumped" isotope calibration data as they show that distinct Δ_{47} -temperature calibrations can be observed in different materials recovered from the same environment and analyzed using the same instrumentation, phosphoric acid composition, digestion temperature and technique, CO_2 gas purification apparatus, and data handling.

There are three possible explanations for the origin of these different calibrations. The offset between the corals of different mineralogy is in same direction as published theoretical predictions for the offset between calcite and aragonite although the magnitude of the offset is different. One possibility is that the deep-sea coral results reflect that crystals may attain nominal mineral equilibrium clumped isotope signatures only under conditions of extremely slow growth. In that case, a possible explanation for the attainment of disequilibrium bulk isotope signatures and equilibrium clumped isotope signatures by deep-sea corals is that extraordinarily slow growth rates can promote the occurrence of isotopic reordering in the interfacial region of growing crystals. We also cannot rule out a component of a biological "vital-effect" influencing clumped isotope signatures in one or both orders of coral. Based on published experimental data and theoretical calculations, these biological "vital" effects could arise from kinetic isotope effects due to the source of carbon used for calcification, temperature- and pH-dependent rates of CO_2 hydration and/or hydroxylation, calcifying fluid pH, the activity of carbonic anhydrase, the residence time of dissolved inorganic carbon in the calcifying fluid, and calcification rate. A third possible explanation is the occurrence of variable acid digestion fractionation factors. Although a recent study has suggested that dolomite, calcite, and aragonite may have similar clumped isotope acid digestion fractionation factors, the influence of acid digestion kinetics on Δ_{47} is a subject that warrants further investigation.

Introduction

"Clumped"-isotope paleothermometry is an approach to determining carbonate mineral formation temperatures (Ghosh et al., 2006; Schauble et al., 2006; Eiler, 2007), which like the oxygen isotope thermometer before it, is founded on thermodynamic predictions of the distribution of isotopes. Crucially, instead of relying on an isotopic exchange reaction between different phases (e.g. $CaCO_3$ and H_2O), clumped isotope thermometry relies on internal isotopic exchange between isotopes in a single phase (Schauble et al., 2006). This means that, in theory, all that is needed to determine mineral formation temperatures is the clumped isotope composition of the solid, and not the water from which it grew (Schauble et al., 2006; Eiler, 2007). When considering carbonate minerals, statistical thermodynamics predicts that heavy stable isotopes of carbon (^{13}C) and oxygen (^{18}O) will increasingly bond or "clump" in a mineral as temperature decreases and will conform to isotopic equilibrium constants for reactions such as:

Revisions 7/25/2016 10:32 AM
Deleted: emerging

Revisions 7/25/2016 10:32 AM
Deleted: for

Revisions 7/25/2016 10:32 AM
Deleted: eg

$$[1]\ X^{12}C^{18}O^{16}O_2 + X^{13}C^{16}O_3 <-> X^{12}C^{16}O_3 + X^{\mathbf{13}}\mathbf{C}^{\mathbf{18}}\mathbf{O}^{16}O_2$$

where X refers to cations such as Ca^{2+}, Mg^{2+}, Sr^{2+}, Ba^{2+}. In practice, the determination of ^{13}C-^{18}O bonds in carbonate minerals is accomplished by measurement of mass-47 CO_2 (predominantly $^{13}C^{18}O^{16}O$) liberated by phosphoric acid digestion Ghosh et al., 2006). ^{13}C-^{18}O bonding is reported as a per mil enrichment from that which would be expected in the liberated CO_2 if the sample had a stochastic distribution of C and O isotopes among all isotopologues and is designated by the parameter Δ_{47}. Following the initial calibration of synthetic calcites and some coral taxa (Ghosh et al., 2006), several studies have focused on in-depth calibrations of biogenic carbonates that represent potential paleoclimate proxies. Proxy material calibrations thus far have included aragonitic scleractinian zooxanthellate corals (Ghosh et al., 2006; Saenger et al., 2012; Tripati et al., 2015), aragonitic scleractinian non-zooxanthellate deep-sea corals (Ghosh et al., 2006; Thiagarajan et al., 2011), aragonitic otoliths (Ghosh et al., 2007), calcitic and aragonitic foraminifera (Tripati et al., 2010), mollusks and brachiopods (Came et al., 2007, 2014; Eagle et al., 2013; Henkes et al., 2013) and land snails (Zaarur et al., 2011; Eagle et al., 2013), calcitic speleothems (Affek et al.,

Revisions 7/25/2016 10:32 AM
Deleted: coral

Revisions 7/25/2016 10:32 AM
Deleted: aragonitic

2008; Daëron et al., 2011), bioapatite (Eagle et al., 2010), and calcitic microbialites (Petryshyn et al., 2015).

Revisions 7/25/2016 10:32 AM
Deleted: Daeron

Revisions 7/25/2016 10:32 AM
Deleted: 2014

It has been noted that calibration data on different biogenic carbonates generated in the same laboratory at Caltech and using similar analytical methods produce a relationship between temperature and Δ_{47} values that was similar to the initial inorganic calcite calibration (Ghosh et al., 2006; Eagle et al., 2013). However there are differences in inorganic calcite calibrations produced in different laboratories (Ghosh et al., 2006; Dennis and Schrag et al., 2010; Zaarur et al., 2013; Tang et al., 2014; Wacker et al., 2013; Kluge et al., 2015), that are thought to either reflect methodological differences in clumped isotope measurements or differences in how synthetic carbonates were precipitated (Tripati et al., 2015). It is clear from studies in mollusks (Henkes et al., 2013; Eagle et al., 2013; Douglas et al., 2014; Petrizzo et al., 2014) and brachiopods (Henkes et al., 2013; Came et al., 2014) that calibrations of the same types of materials in different laboratories can yield different relationship between temperature and Δ_{47} values.

Revisions 7/25/2016 10:32 AM
Deleted: 2014

More recent studies have discussed some possible sources of methodological effects on clumped isotope calibrations relating to data handling and mass spectrometric effects (Wacker et al., 2013; Petrizzo et al., 2014; Defliese et al., 2015). It is also possible that phosphoric acid digestion technique and temperature may be playing a role (Wacker et al., 2013; Defliese et al., 2015), as is known to be the case for conventional $\delta^{18}O$ measurements (Swart et al., 1991). Nonetheless carbonate standards and a deep-sea scleractinian coral were found to yield broadly comparable results in an inter-lab comparison study between four different laboratories (Dennis et al., 2011).

Revisions 7/25/2016 10:32 AM
Deleted: 2014

Revisions 7/25/2016 10:32 AM
Deleted: 2015

Revisions 7/25/2016 10:32 AM
Deleted: 2014

Revisions 7/25/2016 10:32 AM
Deleted: 2015

To date, there is relatively little published data attempting to resolve these whether different biogenic calibrations may originate from methodological differences between laboratories, by simply measuring multiple types of biogenic carbonates interspersed with each other using the same methods. Therefore it remains difficult at this time to distinguish between methodological differences and genuine differences in clumped isotope compositions of different materials, for example biologically mediated fractionations or “vital-effects”. The little work that has been done includes *Porites* corals that appears to exhibit a kinetic isotope effect that drives their Δ_{47} values significantly out of equilibrium (Ghosh et al., 2006; Saenger et al., 2012), and a temperate coral *Oculina arbuscula* cultured at the same temperature and variable pH that exhibits large kinetic effects (Tripati et al., 2015).

Here we explore ^{13}C-^{18}O bond abundances in deep-sea coral species from the orders Scleractinia and Gorgonacea, that precipitate aragonite and high-Mg calcite respectively. As these corals were recovered from the same environment, analyzed by the same methods and mass spectrometer during the same analytical period, and subject to the same data processing, they represent an opportunity to explore the potential role of mineralogy and biology in governing clumped isotope signatures. We discuss results in the context of recent studies including of acid digestion fractionation (Defliese et al., 2015) and theoretical models and experimental data that have been used to constrain differences in clumped isotope composition between different dissolved inorganic carbon (DIC) species (Hill et al., 2014; Tripati et al., 2015), as it has been suggested that in cases where a carbonate mineral may inherit an isotopic signature of DIC then factors effecting DIC speciation such as pH, salinity, and temperature may also influence carbonate clumped isotope signatures (Hill et al., 2014; Tripati et al., 2015).

Revisions 7/25/2016 10:32 AM
Deleted: 2015

1.1 Deep-sea corals in paleoceanography

Deep-sea corals represent a potentially valuable archive of intermediate and deep ocean temperatures, and have been a target for models of stable isotope fractionation (Adkins et al., 2003; Gaetani et al., 2011). These archives could give valuable insight into the natural variability of regions of the ocean that play an active role in large-scale climate dynamics. With fossil deep-sea coral recorded for at least the last 225,000 years (Robinson et al., 2007; Thiagarajan et al., 2013) it is a proxy with potential to extend our observations of ocean physics and climate into the Pleistocene with decadal to centennial resolution. It has been established that deep-sea corals have significant skeletal "vital" effects (disequilibrium stable isotope fractionations) that compromise the classic δ^{18}O paleotemperature method (Emiliani et al., 1978; McConnaughey, 1989a, 2003; Adkins et al., 2003; Smith et al., 2000; Rollion-Bard et al, 2003, 2010; Lutringer et al., 2005; Hill et al., 2011, Kimball et al., 2014). Attempts to circumvent these kinetic effects have focused on the "lines" method that recovers an average temperature over the lifetime of a coral (Smith et al., 2000; Lutringer et al., 2005; Hill

Revisions 7/25/2016 10:32 AM
Deleted: .

Revisions 7/25/2016 10:32 AM
Deleted: 1989

Revisions 7/25/2016 10:32 AM
Deleted: ,

et al., 2011; Kimball et al., 2014) and a Rayleigh-based multi-element (e.g. Mg/Ca, Sr/Ca, Ba/Ca) paleotemperature method (Gaetani et al., 2011).

Despite deep-sea coral species showing significant disequilibrium in $\delta^{13}C$ and $\delta^{18}O$ values, sometimes termed "vital effects", initial calibration work using clumped-isotopes in scleractinian corals (Thiagarajan et al., 2011) revealed a good agreement between aragonitic scleractinian deep-sea coral Δ_{47} and the inorganic calcite calibration of Ghosh et al. (2006). Therefore at least some species that show significant "vital effects" on $\delta^{13}C$ and $\delta^{18}O$ yield apparent equilibrium Δ_{47} values, an observation also made on foraminifera and coccoliths (Tripati et al., 2010). Recently scleractinian deep-sea coral Δ_{47} measurements have been used in applied paleoceanographic reconstructions (Thiagarajan et al., 2014).

Revisions 7/25/2016 10:32 AM
Deleted: (Ghosh et al.,

2 Samples and Methods

2.1 Samples

Thirteen live-collected specimens of deep-sea coral were examined. One specimen, PV 703-7 was mostly dead with patches of living tissue. Specimens were collected by deep-sea submersible diving on Warwick Seamount, Gulf of Alaska (DSRV Alvin, 2002), the Hawaiian Islands (DSRV Pisces V, 2007) and Line Islands (DSRV Pisces IV, 2005) (**Fig. 1**). The thirteen corals belong to the Gorgonacea (gorgonian) and Scleractinia (scleractinian) orders. Gorgonian corals represent the Isididae and Coralliidae families and scleractinian corals are *Enallopsammia rostrata*. Isididae samples were identified as *Keratoisis*, *Isidella*, or *Acanella* spp. (collectively referred to as bamboo corals) and the Coralliidae sample as *Corallium* sp., most likely *Corallium secundum* (**Table 1**). Identification at the time of collection represents the current and best available taxonomic understanding.

Revisions 7/25/2016 10:32 AM
Deleted: at the base and so a

Revisions 7/25/2016 10:32 AM
Deleted: branch was analyzed instead

Temperature data from Warwick Seamount is averaged from two Seabird CTD casts taken at the dive location during the dive, while *in situ* temperature was measured on DSRV Pisces V and IV at the time of collection for Hawaiian and Line Island corals. Temperature ranges from Hawaiian Island coral were calculated from Hawaiian Ocean Time Series (HOTS) (data collected at Station ALOHA during the years 1990-2012. Although Station ALOHA is located about 328 miles east of our samples, a comparison between the HOTS vertical temperature profile matches closely to CTD profiles taken from the sample locations.

Additionally, Station ALOHA was originally chosen as a monitoring station because it is believed to be representative of the North Pacific subtropical gyre and we take it to represent conditions experienced by Hawaiian corals. Temperature ranges from Warwick Seamount are estimated from CTD casts taken at approximately 48.02N, -130.66W from 11 cruises during 1972-1998 at different times of the year. Temperature data was extracted from National Oceanic Data Center at 634± 5 m, 704± 5 m, 720±5 m and 872±5 m to assess temperature variability at the depths the corals were collected at, in the same oceanic region. Similarly temperature ranges from the Line Islands are estimated from CTD casts extracted from National Oceanic Data Center taken at approximately 6°N, -160°W from 9-27 cruises (depending on depth) during 1972-1998.

2.2 Sample preparation

Disks were cut from near the base for all coral skeletons, except PV 703-7 which was dead at the base. For this specimen, a disk was cut from the living branch for sampling. Disks were cleaned by the simple method of sonication in nanopure water and air-drying at room temperature (~ 25°C). All specimens lacked visual organic contamination of any kind and following the findings of Thiagarjan et al. (2011) and Eagle et al. (2013), which found cleaning steps to be unnecessary in deep-sea corals and mollusks, respectively, no further cleaning was performed. For most corals, sample powders of ca. 50-70 mg were milled using a Merchantek micromill from the outer portions of disks which represents the most recently accreted part of the skeleton (**Fig. 2**). In one sample, PV-703-5, a sample was milled from both the center and outer edge of the disk. In a few cases (PIV 148-2, PV 703-2 PIV 146-6, PV 694-3, PV 694-13) samples were first milled from the outer edge and later, to obtain additional sample, whole disks were ground into powder using a mortar and pestle. Although milling was preferred, in some cases, disks were small enough that the entire disk was necessary to yield the required weight of sample for replica Δ_{47} measurements.

In order to explore intra-coral heterogeneity and sampling effects, specimen PIV 146-6 is sampled both along the outer edge by micromilling as well as by grinding and homogenizing an entire disk, while PV 703-5 was micromilled in the center and outer edge (**Fig. 2**). In this way, intra-specimen reproducibility and the effects of sampling were assessed.

Revisions 7/25/2016 10:32 AM
Deleted:)

Revisions 7/25/2016 10:32 AM
Deleted: mortor

Rob Tripati 8/5/2016 5:21 PM
Deleted: sufficient sample for repeated

2.3 Notation and reference frame

The parameter Δ_{47} is a measure of the enrichment in per mil of $^{13}C^{18}O^{16}O$ in CO_2 relative to the predicted stochastic abundance:

$$\Delta_{47} = (R_{47}/ R_{47}^* -1) - (R_{46}/ R_{46}^* -1) - (R_{45}/ R_{45}^* -1) \times 1000$$

where R_{47}, R_{46}, R_{45} are the measured abundance ratios of masses 47/44, 46/44 and 45/44 in the sample and R_{47}^*, R_{46}^*, R_{45}^* are the predicted abundance ratios of the same masses in the sample if it had a stochastic distribution of C and O isotopes among CO_2 isotopologues.

Standard gases of different bulk compositions were equilibrated at different temperatures (25 or 1000°C) and measured each day. Values of Δ_{47} are reported in the absolute reference frame (ARF) and calculated as described in another publication using equilibrated gases(Dennis et al., 2011). Published data are presented in the absolute reference frame with conversion of data from Thiagarajan et al., (2011) and Ghosh et al. (2006) to the ARF, as reported in Eagle et al. (2013).

2.4 Analytical measurement of Δ_{47}

Revisions 7/25/2016 10:32 AM
Deleted:

Isotopic measurements were conducted on a dual inlet Thermo Scientific MAT 253 mass spectrometer coupled to a custom-built semi-automated sample digestion and purification system located at the University of California, Los Angeles. The set-up is modeled on that used at Caltech and Johns Hopkins, which are described in Passey et al. (2010) and Henkes et al. (2013). Samples were run during two separate time periods (winter: January 2013-March 2013, summer: May 2013-July 2013) and samples of scleractinian (aragonite) and gorgonian (high-Mg calcite) were run interchangeably during both time periods. For each analysis (previously referred to as extraction) 8-10 mg of material was used to yield sufficient gas to maintain a steady signal at extended counting times. Also, recent results suggest that digestion of samples that are significantly smaller might undergo secondary equilibration with water, resulting in elevated Δ_{47} values compared to >7 mg size samples (Wacker et al., 2013).

Revisions 7/25/2016 10:32 AM
Deleted: John

Mass spectrometric configuration was set to measure ion beams corresponding to m/z= 44, 45, 46 (amplified by 3×10^8 to 1×10^{11} Ω resistors) and 47, 48, 49 (amplified by 10^{12} Ω resistors) with the ion bean m/z=44 fixed at ~16V. Each analysis contains 8 measurements of 7 cycles between sample and reference gas with 26 seconds of integration per cycle. The total integration time of 1456 seconds is sufficiently long that errors should be able to approach shot noise error predictions (Thiagarajan et al., 2011; Huntington et al., 2009). Internal precision of Δ_{47} was ca. 0.005-0.012‰, 1σ (based on 8 measurements of 7 cycles of sample and reference gas comparison within a single analysis, (**Table 2, Suppl. 1**) and external precision was ca. 0.004-0.008‰, 1σ (determined from repeat analyses of standards, **Table 3**) To increase external precision, samples were measured 3-7 times each, which resulted in standard errors for Δ_{47} of 0.002-0.010‰ for the corals in this study (**Table 2**).

The semi-automated sample digestion system allows for sample to be introduced as either a carbonate powder or a gas. Carbonate powders are introduced via a Costech autosampler which drops samples *in vacuo* into a common ~103% phosphoric acid (ρ ≈ 1.91 mg/ml) bath held at 90°C and allowed to react for 20 minutes. Evolved CO_2 from acid digestion is then passed through a cooled ethanol trap (-78°C) and collected in a liquid nitrogen trap (-200°C). CO_2 is liberated by warming with the same ethanol trap (-78°C), and with a helium carrier gas, passes through a Porapak Q 120/80 mesh GC (gas chromatograph) column at -20°C and silver wool which removes organic contaminants and scavenges sulfur compounds, respectively. After GC passage, CO_2 is again collected in liquid nitrogen and undergoes one final cryogenic purification step *in vacuo* before introduction to the mass spectrometer. Gaseous CO_2 can also be prepared on a vacuum line and introduced using quartz tubes. A tube cracker which leads into the second cooled ethanol trap prior to the GC step allows CO_2 to pass through the autoline in the same way as carbonate samples, minus the common acid bath.

In addition to carbonate powders, on most days, at least one gaseous "equilibrated CO_2" sample is analyzed for use in defining the absolute reference frame for Δ_{47} measurements. Producing equilibrated CO_2 gases with varying bulk isotopic ($\delta^{13}C$ and $\delta^{18}O$) composition is accomplished by utilizing a very depleted CO_2 ($\delta^{13}C$= -25‰, $\delta^{18}O$= 3.6‰ VSMOW) and equilibrating Oztech CO_2 ($\delta^{13}C$= -3.6‰ VPDB, $\delta^{18}O$= 23.6‰ VSMOW) with isotopically "heavy" water (^{18}O enriched and produced by boiling house DI). These two isotopically end member gases are then either heated at 1000°C for 2 hours to produce a nearly stochastic distribution of isotopes among isotopologues, or equilibrated in a water bath held at 25°C. Equilibrated CO_2 is then cryogenically purified on a vacuum line and captured into quartz tubes. This procedure produces four isotopically unique gaseous CO_2 samples which define the empirical transfer function (ETF) used to covert Δ_{47} values to the ARF scale (Dennis et al., 2011). The carbonate standards Carrara Marble, Carmel Chalk, TV01, and 102-GC-AZ01

Revisions 7/25/2016 10:32 AM
Deleted: -30‰)

Revisions 7/25/2016 10:32 AM
Deleted: PDB

Revisions 7/25/2016 10:32 AM
Deleted: -15.83‰ PDB

were run in concert with samples and were shown to have values that were indistinguishable from those determined in the Caltech lab (**Table 3**).

An acid fractionation factor of 0.092‰ was applied to all data and to theoretical predictions to normalize to previously reported data at 25°C (Henkes et al., 2013). In tables and figures, we also report results calculated using a value of 0.082‰ (Passey et al., 2010; Defliese et al, 2015b) as well as other acid digestion fractionation factors (e.g., Wacker et al., 2013).

3 Results

3.1 Scleractinian coral Δ_{47}

When compared with previously reported deep-sea coral data the aragonitic scleractinian coral results from this study agree very closely to those measured in Thiagarajan et al. (2011) and Ghosh et al. (2006) (**Figs. 3** and **4**). Measured and predicted coral isotopic measurements are presented in **Table 4**. Since specimen PV 703-7 was mostly a dead coral except in small sections when collected and therefore could have had a more complicated life history, it was excluded from calibration analysis. For the purpose of calibration, we focus on data from live-collected specimens to compare with *in situ* temperature measurements to eliminate any uncertainty in growth temperatures or post-formation dissolution when considering proxy systematics. When the scleractinian corals are combined with the data from Thiagarajan et al. (2011), a similar Δ_{47} –T relationship to that originally reported is found. In a plot of Δ_{47} vs. $10^6/T^2$ the linear regression of the 11 corals from Thiagarajan et al., (2011) (slope: 0.0643±0.008, intercept: -0.029±0.103, R^2=0.934) is almost identical to that of the combined data set of 14 scleractinian corals (slope: 0.0582±0.008, intercept: 0.0452±0.103, R^2=0.81). As noted in Thiagarajan et al., (2011) this is closely similar to that of the Ghosh et al. (2006) calibration of inorganic calcite (slope: 0.0620; intercept: -0.0021).

The temperature sensitivity of the combined scleractinian coral calibration (slope: 0.0582±0.008, intercept: 0.0452±0.103, R^2=0.81) was examined. At high (17.4°C) and low (2.3°C) temperatures, 95% confidence intervals of Δ_{47} give ±0.0165‰ and ±0.0105‰, which correspond to temperature uncertainties of ca. ±4-5°C and ±3-4°C, respectively. At the average temperature of the data set (9.6°C) uncertainty can be as good as ±0.0075‰ or ±2°C.

Revisions 7/25/2016 10:32 AM
Deleted: 2

Revisions 7/25/2016 10:32 AM
Deleted: 081

aradhna tripati 8/11/2016 3:39 PM
Deleted: ,

Revisions 7/25/2016 10:32 AM
Deleted: Passey…enkes et al., 2010 ... [1]

aradhna tripati 8/11/2016 3:40 PM
Deleted: W… also show …eport resu ... [2]

Revisions 7/25/2016 10:32 AM
Deleted: Henkes

aradhna tripati 8/11/2016 3:40 PM
Deleted: Passey et al., 20132010; …a ... [3]

Rob Tripati 8/5/2016 6:04 PM
Deleted: Measured and predicted coral isotopic measurements are presented in **Table 3** and **4**

Revisions 7/25/2016 10:32 AM
Formatted: Font:Not Bold

Revisions 7/25/2016 10:32 AM
Deleted: , respectively.

Rob Tripati 8/6/2016 11:58 AM
Deleted: not completely alive

Revisions 7/25/2016 10:32 AM
Formatted: Font:11 pt, Italic, German

aradhna tripati 8/11/2016 3:40 PM
Formatted: Font:Italic

Revisions 7/25/2016 10:32 AM
Deleted: R…^{2}=0.934) is almost identi ... [4]

Revisions 7/25/2016 10:32 AM
Deleted: 0631…582±0.008, intercept ... [5]

Uncertainty in Δ_{47} is converted to uncertainty in temperature in accordance with Huntington et al. (2009).

3.2 Gorgonian coral Δ_{47}

Gorgonian deep-sea corals precipitate skeletal carbonate in the form of high-Mg calcite, with 5-10 mol % $MgCO_3$ (Noé and Dullo, 2006; Kimball et al., 2014). Compared to scleractinian deep-sea coral and all other previously reported biogenic carbonates, Δ_{47} is depleted in gorgonian deep-sea corals. In a plot of Δ_{47} vs. $10^6/T^2$, the linear regression through data derived from 9 gorgonian deep-sea corals analyzed in this study gives a significantly shallower slope (slope: 0.025±0.01, intercept: 0.403±0.129, R^2=.48) and Δ_{47} offset of ca. 0.04-0.07‰ in the temperature range of 3.2-11.2°C compared to scleractinian corals as well as compared to the Ghosh et al. (2006) calibration. It is however more similar to the inorganic calibration of Dennis and Schrag (2010) (**Fig. 3**). Temperature sensitivity of the gorgonian coral calibration was not examined due to poorness of fit (R^2=0.48).

3.3 Intra-specimen sampling

Intraspecimen measurements from sampling different portions of the skeleton gives insight into the Δ_{47} heterogeneity present in an individual coral. Specimen PIV 146-6 was sampled both along the outer edge by micromilling as well as by grinding and homogenizing an entire disk, while PV 703-5 was micromilled in the center and outer edge. In both corals, aliquots produced from a given sampling method are significantly different in bulk isotopes. PIV 146-6 has differing bulk isotopic compositions between the two aliquots of more than 1‰ in $\delta^{13}C$ and 0.4‰ in $\delta^{18}O$. PV 703-5 has almost a 3‰ difference in $\delta^{13}C$ and 0.5‰ in $\delta^{18}O$ (**Table 5**). Δ_{47} of the aliquots are approximately 0.03 and 0.02 different from each other in PIV 146-6 and PV 703-5, respectively. For PIV 146-6, the average of all 7 measurements is 0.791±0.008 and for the two aliquots the averages are 0.779±0.007 and 0.803±0.01. For PV 703-5 the average of all 6 measurements is 0.744±0.007 and the averages for the two aliquots are 0.734±0.005 and 0.754±0.010.

Revisions 7/25/2016 10:32 AM
Deleted: Noe

Revisions 7/25/2016 10:32 AM
Deleted: of the

Revisions 7/25/2016 10:32 AM
Deleted: (slope: 0.018±0.012, intercept: 0.511±0.157, R^2=.23)

Revisions 7/25/2016 10:32 AM
Deleted: from

Revisions 7/25/2016 10:32 AM
Deleted: ,

Revisions 7/25/2016 10:32 AM
Deleted: is

Revisions 7/25/2016 10:32 AM
Deleted: =.23

Revisions 7/25/2016 10:32 AM
Deleted: 804

Revisions 7/25/2016 10:32 AM
Deleted: 808

Revisions 7/25/2016 10:32 AM
Deleted: 008

Revisions 7/25/2016 10:32 AM
Deleted: 823

Revisions 7/25/2016 10:32 AM
Deleted: 750

Revisions 7/25/2016 10:32 AM
Deleted: 740

Revisions 7/25/2016 10:32 AM
Deleted: 760

4 Discussion

4.1 Trends in deep-sea coral data

The scleractinian corals analyzed in this study are solely *Enallopsammia* sp. In contrast, the deep-sea corals presented in Ghosh et al. (2006) and Thiagarajan et al. (2011) are scleractinian *Desmophyllum*, *Enallopsammia*, and *Caryophyllia* sp . All scleractinian species precipitate a skeleton composed of aragonite, although growth habits vary between species. *Desmophyllum* sp, also known as cup corals, grow in a rosette shape, whereas *Caryophyllia* and *Enallopsammia* sp have a dendritic growth habit. The *E.rostrata* specimens measured in Thiagarajan et al. (2011) allow comparison between deep-sea corals of the same species measured in this study.

Revisions 7/25/2016 10:32 AM
Deleted:

Revisions 7/25/2016 10:32 AM
Deleted:

The scleractinian deep-sea coral data from this study have values that overlap with those reported by Thiagarajan et al. (2011). In contrast, the gorgonian corals show significantly lower Δ_{47} values compared to the scleractinian corals for the same temperature range. An analysis of covariance (ANCOVA) between the scleractinian and gorgonian coral data gives a P value <0.01 which indicates that the differences between the two groups are statistically significant. This 0.04-0.07 ‰ offset between scleractinian and gorgonian corals is observed in non-acid digestion corrected Δ_{47} values. Possible explanations for this offset are discussed below.

4.2 Comparison with other published Δ_{47} calibration data sets

Since its inception, numerous theoretical, inorganic and biogenic calibrations have been put forward to calibrate the Δ_{47}- T relationship in different carbonate materials. To date, at least seven synthetic calibrations have been published (Ghosh et al., 2006; Dennis and Schrag, 2010; Zaruur et al., 2013; Tang et al., 2014; Defliese et al., 2015; Kluge et al., 2015; Tripati et al., 2015). Numerous biogenic carbonate materials have been studied to assess their agreement with inorganic and theoretical studies (Ghosh et al., 2006; Thiagarajan et al., 2011; Saenger et al., 2012; Eagle et al., 2013; Henkes et al., 2013). The scleractinian corals in this study agree well with the inorganic calibrations of Ghosh et al. (2006) and Zaruur et al. (2014) and Tripati et al., 2015, while the gorgonian corals show agreement with the Dennis

Revisions 7/25/2016 10:32 AM
Deleted: 2015

and Schrag (2010), Tang et al. (2014), and Kluge et al., 2015 inorganic calibrations (e.g., **Fig. 4)**.

4.3 Comparison with theoretical predictions

Theoretical modeling of Δ_{63} for different carbonate minerals (Schauble et al., 2006; Hill et al., 2014; Tripati et al., 2015) have been combined with theoretical acid digestion fractionations to give predicted Δ_{47} values for a variety of carbonate minerals. These predictions generally agree with measured inorganic and biogenic studies however are more depleted in Δ_{47} for a given temperature. Further, offsets due to mineralogy, while predicted in these theoretical modeling studies, have not been resolved in measured samples. Compared to deep-sea coral Δ_{47}, theoretical predictions are more depleted for aragonite, however the calcite prediction agrees well with the calcitic gorgonians from this study (**Fig. 5**). The offset of 0.03 ‰ between aragonite and calcite is on the lower end of what we observe. A recent theoretical modeling effort (Hill et al., 2014) has produced similar predicted Δ_{47} values for aragonite and calcite although with more depleted (less agreement) between predicted and observed aragonite Δ_{47} and a smaller offset between aragonite and calcite.

4.4 Acid digestion fractionation factor uncertainties

It is possible that uncertainties in the acid digestion fractionation factor for carbonates digested at 25 and 90 °C may account for some of the above offsets. Three values have been proposed for the acid digestion fractionation factor (AFF) for reporting data at 90 °C and converting to 25 °C on the absolute reference frame. To explore the sensitivity of results to choice of acid digestion fractionation factor, **Fig. 6-9** show calculations using a range of acid digestion fractionation factors of isotope ratios, and apparent deviations of measured isotopic ratios from isotopic equilibrium. Passey et al. (2010) calculates and uses a value of 0.081‰, whereas Henkes et al. (2013) suggests a value of 0.092‰ ± 0.012‰, which is within error of the Passey et al. (2010) value. Defliese et al. (2015) proposes a value of 0.082‰ ± 0.014‰, which is within error of both values,. In a recent study Wacker et al. (2013) suggests there may be mineral-specific acid digestion fractionation factors (AFF), which is also predicted in the theoretical study by Guo et al. (2009). Application of the Wacker et al. $\Delta^*_{25\text{-}90}$ correction to the aragonite and calcite Δ_{47} data can explain 0.009‰ of the 0.03-0.07‰ offset observed in our aragonite and calcite data. Based on theoretical predictions for dolomite (Guo et al.,

Revisions 7/25/2016 10:32 AM
Deleted: used

aradhna tripati 8/11/2016 2:51 PM
Deleted: and the

Revisions 7/25/2016 10:32 AM
Deleted: 2015

aradhna tripati 8/11/2016 2:56 PM
Deleted: a

aradhna tripati 8/11/2016 2:51 PM
Deleted: 91

Revisions 7/25/2016 10:32 AM
Deleted: a

Revisions 7/25/2016 10:32 AM
Deleted: ,

Revisions 7/25/2016 10:32 AM
Deleted: predications

2009), a further offset might be expected due to Mg incorporation in calcite. Still, experimental (Wacker et al., 2013; Defliese et al., 2015) and theoretical (Guo et al., 2009) studies suggest acid digestion differences due to mineralogy may not be large enough to explain the ca. 0.04-0.07‰ offset that we observe.

Revisions 7/25/2016 10:32 AM
Deleted: 2015

Deep-sea coral Δ_{47} were corrected using $\Delta_{25\text{-}90}$ AFF of 0.082‰ (Defliese et al., 2015) - identical to the value from Passey et al., 2010, 0.092‰ (Henkes et al., 2013) and 0.066‰ (Wacker et al., 2013, aragonite) and 0.075‰ (Wacker et al., 2013, calcite). **Figure 6** shows the result of the AFF sensitivity analysis and indicates that although the absolute values of the Δ_{47} change with application of AFF values, the offset between aragonite and calcite is unaffected except for in the case of application of mineral specific AFF from Wacker et al. (2013). Application of Wacker et al. (2013) mineral specific AFF values results in a decrease of the offset between the aragonite and calcite deep-sea coral Δ_{47} of only 0.009‰, therefore not altering our conclusions.

aradhna tripati 8/11/2016 3:40 PM
Deleted: 1

aradhna tripati 8/11/2016 3:40 PM
Deleted: (Passey et al., 2010)

aradhna tripati 8/11/2016 2:50 PM
Deleted: – near identical to the value of 0.091‰ from Defliese et al., 20152015a

However, we acknowledge the kinetics of acid digestion and effects on clumped isotope signatures on Δ_{47} values is relatively poorly constrained. It is possible there are variable acid digestion fractionation factors that are influencing these observations, possibly due to cation substitution into carbonates (Guo et al., 2009), mineral bulk isotope composition (Guo et al., 2009), the presence of organic matter, as well as other factors. Until systematic studies of acid digestion is undertaken to investigate each of these factors, the contribution of acid digestion fractionation to the observed differences between aragonitic scleractinian and high-Mg calcitic gorgonian corals cannot be accurately quantified.

4.5 Analytical procedure, data comparison

Since its inception, the analytical measurement of Δ_{47} has improved in precision and accuracy due to advances in mass spectrometric analysis (e.g. development of automated sample digestions and purification systems, abbreviated to autoline, and higher counting times) and standardization of reporting procedures (Huntington et al., 2009; Dennis et al., 2011). Because the methods involved in producing and reporting Δ_{47} have changed over time, the comparison of data between laboratories and even within laboratories can be an issue. For relevant comparisons between previously reported data and this study's data, we refer to the recalculations of Δ_{47} performed in Eagle et al., (2013) using standard values to project into the absolute reference frame. Still, we can not exclude the possibility that analytical artifacts remain. For instance, Zaruur et al. (2013) noted that the shorter counting times and fewer replications of the trailblazing work of Ghosh et al., (2006) may contribute to any discrepancies between data sets. We assess interlaboratory comparability from standards, which indicate accuracy and precision comparable to what has been reported for other laboratories (**Table 2**; Dennis et al., 2011). Furthermore, we note that good agreement between the aragonitic scleractinian corals of this study and that of Thiagarajan et al. (2011) reinforces the comparability of our data to the wider body of measurements reported from other laboratories.

Interlaboratory comparability should not be a critical issue for the interpretation of data presented herein since the offset between aragonitic and calcitic corals was observed in data generated within our lab, while running samples interchangeably using the same analytical procedure. Standards were also run concurrently during these time periods (**Table 3**) and found to be in good agreement with accepted values. We therefore conclude it is unlikely that the offset is due to internal analytical variability.

4.6 Mixing and intraspecimen Δ_{47} heterogeneity

It has been shown that both scleractinian and gorgonian deep-sea corals exhibit significant disequilibrium in δ^{13}C and δ^{18}O of several per mil within an individual coral (eg. Smith et al., 2000; Adkins et al., 2003; Rollion-Bard et al., 2003, 2010; Lutringer et al., 2005; Kimball et al., 2014). Because of the subtle saddle-shaped curvature in Δ_{47} relative to δ^{13}C and δ^{18}O (Eiler and Schauble, 2004; Thiagarajan et al., 2011; Defliese and Lohmann, 2015), Δ_{47} is sensitive to mixing of end member δ^{13}C and δ^{18}O values and will result in non-conservative mixing (**Fig. 10**). Deep-sea corals, with their several per mil range in δ^{13}C and δ^{18}O values will be particularly susceptible to this effect. In fact, both banding and spatial variability in δ^{13}C and δ^{18}O values within deep-sea coral skeletons varies on the scale of 10s to 100s of microns (Smith et al., 2000; Adkins et al., 2003; Rollion-Bard et al., 2003, 2010; Lutringer et al., 2005; Kimball et al., 2014). Any small-scale spatial variability makes the possibility of sampling within a skeletal band or an area with homogenous δ^{13}C and δ^{18}O values for Δ_{47} measurements unfeasible, and therefore there is the potential for mixing effects in Δ_{47} which we address here.

Both Thiagarajan et al. (2011) and Henkes et al. (2013) have addressed mixing in biogenic carbonates by calculating the Δ_{47} effect from mixing samples of differing bulk isotope

Revisions 7/25/2016 10:32 AM
Deleted: .

Revisions 7/25/2016 10:32 AM
Deleted: 2015

aradhna tripati 8/11/2016 2:57 PM
Deleted: b

Revisions 7/25/2016 10:32 AM
Deleted: : Roark

Revisions 7/25/2016 10:32 AM
Deleted: 2006

Revisions 7/25/2016 10:32 AM
Deleted:) making

Revisions 7/25/2016 10:32 AM
Formatted: Font:Arial, 9.5 pt, Font color: Custom Color(RGB(34,34,34)), German, Pattern: Clear (White)

composition. The end members from the Thiagarajan et al. (2011) calculations are similar to the most extreme values that we observe (δ^{13}C= 2‰, δ^{18}O= 5‰ and δ^{13}C= -10‰, δ^{18}O= -2‰). Using these end member values, Thiagarajan et al. (2011) calculated a positive Δ_{47} increase as large as 0.02‰ for the resulting mixture, if 50% of each end member is used. They note that while this mixing effect is not consistent with their data, mixing and then re-equilibration could potentially result in the trend seen in their data. Since sampling an isotopically homogenous area of a deep-sea coral is unfeasible (especially given the sample size requirements for clumped isotopes), we estimate the maximum artifacts in our data arising from mixing. The estimate for mixing artifacts from Thiagarajan et al. (2011) is based on observed variability in stable isotope values in scleractinian deep-sea coral, and represents an extreme example for this study, as they use δ^{13}C and δ^{18}O values of end members that differ by 12‰ and 7‰, respectively. Such differences in scleractinian coral represent systematic isotopic depletions in centers of calcification compared to fibers (Adkins et al., 2003), as well as variability associated with density bands; no centers of calcification have been reported in gorgonian corals. The calculations from Thiagarajan et al. (2011) represent an estimate of the maximum artifact to arise from mixing for either taxa given the range of carbon and oxygen isotope values observed in scleractinian and gorgonian deep-sea coral. We also observed little variability in δ^{13}C and δ^{18}O of different preparations of the same coral, with standard deviations of <1‰.

Revisions 7/25/2016 10:32 AM
Deleted: what

Revisions 7/25/2016 10:32 AM
Deleted:) we must assume that this mixing effect is indeed occurring. However, the extreme example of end members and the 50% contribution from each would be an unlikely occurrence. More likely is mixing between skeletal carbonate of less extreme differences in bulk isotopic composition. This is also supported by replicate analyses of the same sample aliquot. Standard errors for δ^{13}C and δ^{18}O in different preparations of the same coral measured range from 0.019 to 0.204‰ and 0.018 to 0.095‰, respectively (excluding those specimens which included multiple aliquots). This is consistent with relative small mixing effects.

As a further investigation into intraspecimen heterogeneity effects on Δ_{47} portions of two coral samples that differed in bulk isotopic composition were analyzed. In two corals, PIV 146-6 (scleractinian) and PV 703-5 (gorgonian), δ^{13}C, δ^{18}O and Δ_{47} were measured from intraspecimen aliquots of carbonate produced from sampling portions of the skeleton which differed significantly in their bulk isotopic composition (**Table 5**). Although Δ_{47} of the aliquots are approximately 0.02‰ different from each other in both corals, this is similar to that reported in other studies between a few replicates (Huntington et al., 2009; Thiagarajan et al., 2011). Additionally there is not a consistent trend observed between δ^{18}O and Δ_{47}, as for coral PIV 146-6, the aliquot with the more positive δ^{18}O also has the higher Δ_{47}, but the opposite is observed for coral PV 703-5. We therefore interpret the difference in Δ_{47} values between the aliquots as noise in the measurements, which further reinforces the need to run many replicates.

Revisions 7/25/2016 10:32 AM
Deleted: however,

4.7 Diffusion

Both Thiagarajan et al. (2011) and Saenger et al. (2013) have suggested the diffusion of CO_2 across the calicoblastic membrane in corals as a possible mechanism for fractionation of Δ_{47}. A generalized schematic of a scleractinian coral calcifying region is shown in **Fig. 11**. Thiagarajan et al. (2011) calculated 0.7‰ and 1.6‰ decreases in $\delta^{18}O$ and $\delta^{13}C$, respectively and a 0.036‰ increase in Δ_{47} for liquid phase diffusion of CO_2 (**Fig. 10**). For this Δ_{47} fractionation to be heritable by the mineral, however, the mineral must preserve the isotopic state of ordering of the DIC rather than obtain internal equilibrium within the mineral carbonate itself. Additionally carbonate mineral growth would have to occur before isotope clumping could reach equilibrium. Furthermore this fractionation only applies to DIC produced from diffused CO_2 and therefore the ratio of DIC from diffused DIC to 'DIC derived from seawater "leaking" directly to the calcifying environment would also have to be known. Both Thiagarajan et al. (2011) and Saenger et al. (2013) found fractionation associated with CO_2 diffusion across the calicoblastic layer or, additionally proposed by Saenger et al. (2013), across a boundary layer developed between the growing mineral and calcifying fluid, to be an unlikely explanation of the trends observed in their data. Additionally, gorgonian corals are not known to have calicoblastic cells (Noé and Dullo, 2006) so this is relevant to scleractinian corals, or if there is a similar functional cell playing a role in this for gorgonian corals.

Revisions 7/25/2016 10:32 AM
Deleted: the

It is possible the observed pattern could be explained if scleractinian deep-sea corals contain a larger fraction of diffused CO_2 compared to gorgonian coral, if this CO_2 then underwent relatively little isotopic equilibration in the calcifying fluid (**Fig. 10**). In cross plots of $\delta^{18}O$ and Δ_{47} residuals, scleractinian corals do exhibit elevated Δ_{47} and depleted $\delta^{18}O$ values, relative to Zaruur et al. (2013), Dennis and Schrag (2010) and theoretical aragonite (Schuable et al., 2006; Guo et al., 2009) in accordance with calculated diffusion effects. However, since scleractinian deep-sea corals generally conform to the majority of reported biogenic and synthetic calibrations, this would have be a widespread effect occurring in other materials reported as well.

4.8 Mineralogy and Δ_{47}

Despite Epstein et al.'s (1953) original finding that the nacreous layer (aragonite) and prismatic layer (calcite) of mollusks showed no oxygen isotopic offset, it has since been recognized that aragonite is enriched in ^{18}O and ^{13}C relative to calcite both in theory and experiment (Tarutani et al., 1969; Kim and O'Neil, 1997; Kim and O'Neil, 2007; Mavtomatis, 2012). An analogous mineralogical offset is predicted for Δ_{47} (with aragonite predicted to have greater abundance of ^{13}C-^{18}O bonds than calcite that formed at the same temperature) (Schauble et al., 2006; Guo et al., 2013; Hill et al., 2014; Tripati et al., 2015).

The corals in this study differ in mineralogy, with scleractinian corals precipitating a fully aragonitic skeleton and gorgonian corals secreting carbonate in the form of high-Mg calcite. To date, a combination of aragonitic and calcitic biogenic materials have been analyzed. Calcitic specimens have been represented by certain species of mollusks (Eagle et al, 2013; Henkes et al., 2013), brachiopods (Came et al., 2007; Henkes et al., 2013), and foraminifera (Tripati et al., 2010). Aragonitic specimens have included deep-sea (Thiagarajan et al., 2011) and shallow (Ghosh et al., 2006; Saenger et al., 2013) scleractinian corals, mollusks (Eagle et al., 2013; Henkes et al., 2013), and land snails (Zaarur et al., 2011), all of which have not revealed statistically significant mineralogical offsets from the synthetic calibrations of calcite (Ghosh et al., 2006; Dennis et al., 2010; Zaruur et al., 2013). More careful study, however of the XRD data of Ghosh et al. (2006) has revealed aragonite was also present in their precipitates (Zaruur et al., 2013).

Revisions 7/25/2016 10:32 AM
Deleted: brachiopods (Came et al., 2007)

Despite not observing this offset between calcite and aragonite Δ_{47} in synthetic or biogenic carbonates, it has been predicted in theoretical studies. By combining a previous theoretical model of ^{13}C-^{18}O clumping in carbonate minerals (Schauble et al., 2006) with their theoretical model of kinetic isotope effects associated with phosphoric acid digestion, Guo et al. (2009) proposed predicted Δ_{47}- T relationships for a number of carbonate minerals. For the temperature range 0-30°C, $\Delta_{47,\ \text{aragonite-calcite}} \approx 0.02‰$ and $\Delta_{47,\ \text{aragonite-dolomite}} \approx 0.04‰$ with the direction of fractionation in agreement with the offset that we observe (**Figure 5**). A similar pattern was reported by Hill et al. (2014) and Tripati et al. (2015). If these models of mineral-specific Δ_{47}-T relationships is correct, then this could potentially explain a substantial portion of the offset we observe between the aragonite and high-Mg calcite corals in this study. We discuss possible reasons for observed mineralogical effects in deep-sea corals and not in other types of carbonates in more detail below.

Revisions 7/25/2016 10:32 AM
Deleted: an

4.8 Calcification in scleractinian deep-sea corals

Non-equilibrium partitioning of oxygen and carbon isotopes have been observed in numerous calcifying organisms and inorganic precipitation experiments, and linked to calcification processes (e.g. McConnaughey, 1989a; Spero et al., 1997; Zeebe, 1999; Adkins et al, 2003: Watson, 2004; DePaolo, 2011; Gabitov et al., 2012; Watkins et al., 2013). Clumped isotopes represent another tool that can be used to probe mechanisms for disequilibrium isotopic signals in biological carbonates, and to determine when equilibrium precipitation has occurred, through the coupling of theoretical calculations and inorganic precipitation experiments with culturing studies (Thiagarajan et al., 2011; Tripati et al., 2015). **Fig. 10** shows a framework for how multiple paired stable isotope measurements can be used to trace the origin of disequilibrium effects.

Revisions 7/25/2016 10:32 AM
Deleted: McConnaughy, 1989

In scleractinian corals, precipitation of carbonate is believed to occur in a space between the calicoblastic layer and the hard skeleton (**Fig. 11**). It is likely that calcifying fluid chemistry (pH, salinity) as well as growth rate and DIC equilibrium can all be potential sources of non-equilibrium signals preserved in the solid. The chemical composition and DIC sources from which the carbonate mineral forms have been a main focus for understanding non-equilibrium δ^{13}C and δ^{18}O values observed in corals. Biomineralization in shallow symbiotic scleractinian corals has been well-studied over the past few decades (see Cohen and McConnaughey, 2003 for a review). Early studies of shallow symbiotic scleractinian corals revealed time independent δ^{18}O and δ^{13}C offsets from theoretical carbonate-water fractionation curves. This was addressed through species-specific calibration studies, which allowed offsets to be corrected for, revealing the underlying environmental signals (Weber and Woodhead, 1972; Dunbar and Wellington, 1981). In contrast, linear trends between δ^{18}O and δ^{13}C with depletions of several per mil, are observed in an individual deep-sea coral. Living in near constant temperature, salinity and pH environments, these large disequilibrium signals are attributed to their biomineralization mechanism (i.e. “vital effects”). Different mechanistic models aimed at explaining non-equilibrium δ^{13}C and δ^{18}O values seen in deep-sea corals have been proposed to account for these so-called “vital effects”.

Revisions 7/25/2016 10:32 AM
Deleted: seen

Revisions 7/25/2016 10:32 AM
Deleted: McConnaughy

The first of these models, proposed by McConnaughey (1989a) calls on a kinetic fractionation during the hydration and hydroxylation steps of DIC speciation in which precipitation outpaces the ability of the system to reach isotopic equilibrium (“Kinetic model” in **Fig. 11**).

The range of $\delta^{13}C$ and $\delta^{18}O$ values is therefore a reflection of a spectrum of varying amounts of equilibrium being attained amongst DIC species. The master variable in this case being time, McConnaughey (1989b), using calcification rates, calculated that calcification could outpace the time it took for isotopic equilibrium to be reached. Henkes et al. (2013) further noted that at lower temperatures, days to weeks are required for oxygen isotopic equilibrium to be reached in DIC.

Revisions 7/25/2016 10:32 AM
Deleted: McConnaughy

The second model proposed by Adkins et al. (2003) extensively examines potential sources of DIC to the extracellular calcifying fluid and introduces the concept of a variable pH environment as the master controller on skeletal $\delta^{13}C$ and $\delta^{18}O$ ("pH model" in **Fig. 11**). For oxygen isotope processes, they draw on work characterizing the oxygen isotopic fractionation between DIC species (i.e. CO_2, H_2CO_3,, HCO_3^-, CO_3^{2-}) (McCrea, 1950; Usdowski et al., 1991; Zeebe and Wolf-Gladrow, 2001; Beck et al., 2005; Zeebe, 2007; Rollion-Bard et al., 2011). Their model suggests that the mineral preserves the oxygen isotopic ratio of HCO_3^-/CO_3^{2-}. Because each DIC species has a unique oxygen fractionation relative to water, the oxygen isotope fractionation between the sum of DIC (DIC_{sum}) species and water will vary depending on the proportion of the DIC species. For seawater, at high pH (pH >9), DIC will be dominated by CO_3^{2-}, which has the lowest fractionation factor and will therefore result in a more depleted $\delta^{18}O$ value of the DIC_{sum} from which the mineral precipitates. At lower (pH 6-9) fluid pH, as the HCO_3^-/CO_3^{2-} ratio of the fluid rises, so does the precipitated mineral's $\delta^{18}O$ value. $\delta^{13}C$ is not expected to be sensitive to pH effects since the exchange of carbon between DIC species is very rapid. $\delta^{13}C$, therefore, is proposed to be a function of two sources of CO_2, membrane diffused and seawater leaked, and the proportion of them, a function of pH gradients across the membrane. The 'break' that they uncover at the most depleted isotopic values in which $\delta^{18}O$ continues to decrease but $\delta^{13}C$ plateaus, is interpreted as the point at which the maximum flux of diffused CO_2 across the membrane is reached (during rapid calcification). Qualitatively their model captures the isotopic trends that they see in their corals and although numerical modeling is able to reproduce the 'break' and range of $\delta^{18}O$ and $\delta^{13}C$ that they report, it fails to reproduce the numerical value of the $\delta^{18}O$ vs. $\delta^{13}C$ slopes that they observe. $\delta^{18}O$ vs. $\delta^{13}C$ slopes have been observed in other studies and appear to be a conservative property of biomineralization in deep-sea corals (Smith et al., 2000; Adkins et al., 2003; Rollion-Bard et al. 2003, 2010; Lutringer et al 2005; Hill et al., 2010; Kimball et al., 2014). Discrepancies between the biomineralization model of Adkins et al., 2003 and boron

Revisions 7/25/2016 10:32 AM
Formatted: No widow/orphan control, Don't adjust space between Latin and Asian text, Don't adjust space between Asian text and numbers

Revisions 7/25/2016 10:32 AM
Deleted: 2009

isotope data are yet to be resolved (Blamart et al., 2007; Rollion-Bard et al., 2010).

Additional biomineralization models have been proposed in shallow symbiotic corals which incorporate the presence and activity of zooxanthellae (Cohen and McConnaughey, 2003; Rollion-Bard et al., 2003; Allison et al., 2010) and for deep-sea corals (Rollion-Bard et al., 2010; Gaetani et al., 2010). However only those models that examine effects on δ^{18}O and δ^{13}C are considered with respect to the data presented herein.

More generally, models for equilibrium/disequilibrium stable isotope signatures have been proposed that examine processes that influence the ion-by-ion growth of crystals (Nielsen et al., 2012; Watkins et al., 2013; Tripati et al., 2015), as well as diffusional/reordering processes that occur near the calcifying fluid/crystal interface (Watson and Liang, 1995; Watson, 2004; Gabitov et al., 2012; Tripati et al., 2015).

4.9 Calcification in gorgonian deep-sea corals

The growth structure, mineralogy, and biomineralization of gorgonian coral skeletons is distinctly different from scleractinian corals (Noé and Dullo, 2006). Additionally, the organic matrix-mediated calcification process is largely unexplored and unknown for most gorgonian families. The biomineralization models described for scleractinian corals therefore are not valid when interpreting potential vital effect signals in gorgonian corals.

An exhaustive study of the growth structure and fabric of deep-sea isidid gorgonians in the same family as those investigated here, was done by Noé and Dullo (2006). Their findings are based on characterization of the isidid skeletal micro- and ultrastructure in combination with absolute age determinations. From their reconstructions of growth mode and fabric, they propose a biomineralization model. With no calicoblastic cells observed in gorgonians, they propose gorgonin produced from the endodermal epithelium acts as the structural framework, while a viscous slime surrounding the skeleton acts as the matrix, facilitating and regulating mineral growth. Their model however relies on physical observations and lacks geochemical data to inform their interpretations. So while offering some insight into the uniqueness of Isidid biomineralization, the findings are not useful in interpreting the geochemical data observed in this study.

Revisions 7/25/2016 10:32 AM
Formatted: German

Revisions 7/25/2016 10:32 AM
Deleted: McConnaughy

Revisions 7/25/2016 10:32 AM
Deleted: Rollian

Rob Tripati 8/5/2016 7:06 PM
Deleted: , based on trace elements

Revisions 7/25/2016 10:32 AM
Deleted: Additionally, as of yet, a model that addresses the distinct high-Mg calcite mineralogy of gorgonians has not been proposed.

Despite the lack of proposed biomineralization models in gorgonian corals, the trends in $\delta^{13}C$ and $\delta^{18}O$ have been explored and found to be similar in pattern to scleractinian corals, but with an offset that agrees with theoretical mineralogical fractionation predictions. The similarity in $\delta^{13}C$, $\delta^{18}O$ and δ_{47} patterns suggests that while the particular biomineralization process is necessarily different in the two groups, there is a functional similarity that results in the conserved patterns in both gorgonian and scleractinian corals.

4.9 Δ_{47} in deep-sea coral skeletal carbonate: biomineralization model implications

The Δ_{47} of a mineral is predicted to conform to the K_{eq} of a homogenous isotope exchange reaction (**Reaction 1**) and be independent of the fluid composition from which is forms, as well as the bulk isotopic composition of the crystal. Recent experimental and theoretical studies have suggested that mineral equilibrium with respect to Δ_{47} might not always be attained however (Saenger et al., 2013; Tripati et al., 2015). Because of this, Δ_{47} can be utilized as an additional geochemical skeletal signal which could give more insight into the mechanisms involved in skeletal precipitation in deep-sea corals and other biological carbonates.

In a recent study, (Tripati et al., 2015) the impact of DIC speciation on mineral Δ_{47} signatures was examined with respect to Δ_{47}. Contrary to initial theoretical modeling by Hill et al. (2014) which calculated differences of ~0.03‰ in the Δ_{47} values of DIC species at equilibrium, Tripati et al. (2015), using experimental results, found that HCO_3^- Δ_{63} could be as much as 0.05 to 0.07‰ higher than CO_3^{2-}. They further propose that this fractionation could be partially or fully inheritable by the solid. Central to their mechanism of preservation of disequilibrium mineral Δ_{63} signals is the concept of differing mineral isotopic archival effects occurring during "slow" and "fast" crystal growth, with "slow" and "fast" being defined as particular to a specific temperature, salinity and pH growth environment, rather than conforming to a particular value. Depending on the proportion of HCO_3^- and CO_3^{2-} incorporated into the growing crystal and the ability of the crystal lattice to conform to K_{eq} (Reaction 1), disequilibrium in Δ_{63} and therefore Δ_{47} could be preserved. Only during "slow" crystal growth, they argue, is the mineral able to fully conform to K_{eq} (Reaction 1). In this scenario, disequilibrium in Δ_{63} and bulk isotopes are not correlated and it would therefore be possible to attain equilibrium with respect to Δ_{63}, but not in bulk isotopes (Tripati et al., 2015).

Revisions 7/25/2016 10:32 AM
Deleted: .

Deep-sea corals, being one of the slowest calcifiers, are a likely potential candidate for attainment of Δ_{63} mineral equilibrium, if the mechanism proposed by Tripati et al. (2015) is correct. Bulk isotopes, as previously mentioned, vary greatly within an individual deep-sea coral, while Δ_{47} values are reproducible within instrumental error. This indicates that while bulk isotopes are controlled by processes such as in the biomineralization models outlined above, Δ_{47} values are independent and possibly conform to equilibrium values. While a complete quantitative biophysical model has yet to be proposed, one possibility is that the range in bulk isotopes is controlled by processes related to the chemical environment (eg. calcifying solution pH, kinetics) while the slow growth rates in deep-sea corals allow isotopic reordering at the crystal-solution interface resulting in attainment of nominal mineral equilibrium for Δ_{47} (**Fig. 11**).

Adkins et al. (2003), however, finds that in the more dense (interpreted as faster calcification) growth bands, $\delta^{18}O$ is depleted compared to the less dense (more slowly growing) bands. In the Tripati et al. (2015) model, they predict that during rapid calcification both $\delta^{18}O$ and Δ_{47} would be more positive. Relative to the calcification rates required for inheritance of these signals however, perhaps even at the most elevated calcification rates, deep-sea corals, are still able to reach mineral isotopic equilibrium with respect to Δ_{47}, while bulk $\delta^{18}O$ and $\delta^{13}C$ is still under the control of processes associated with the calcifying fluid environment.

Cross plots of $\delta^{18}O$ and Δ_{47} residuals (**Figs 7, 8, and 9**) can be used to assess conformation to proposed biomineralization models. For the McConnaughey et al. (2003) model of coral biomineralization, a range of depletions in $\delta^{18}O$ is expected, with coral $\delta^{18}O$ approaching or potentially reaching mineral equilibrium $\delta^{18}O$, depending on the calcification rate. Similarly in the Adkins et al. (2003) model, a range of pH would result in a range of depletions in recorded mineral $\delta^{18}O$, assuming that the proportion of HCO_3^-/CO_3^{2-} incorporated into the skeleton is independent of calcification rate (**Fig. 10**). Although neither model addresses Δ_{63}, in both cases, all else being equal, and assuming a mechanism for inheritance of DIC Δ_{63} into mineral Δ_{63}, a decrease in $\delta^{18}O$ would be tied to a decrease in Δ_{63}. For the McConnaughey et al. (2003) model, an increase in calcification rate resulting in only partial equilibration of the DIC-water system would result in depleted $\delta^{18}O$ and Δ_{63} values of HCO_3^- and CO_3^{2-}.

Revisions 7/25/2016 10:32 AM
Deleted: McConnaughy

Revisions 7/25/2016 10:32 AM
Deleted: McConnaughy

Similarly, in Adkins et al. (2003) model, varying solution pH would have the same effect on δ^{18}O and Δ_{63} with both values decreasing (increasing) as pH increases (decreases). Comparing residual cross plots from various Δ_{47} calibrations however, fails to capture a positive relationship between δ^{18}O and Δ_{47} and instead appears that δ^{18}O and Δ_{47} are varying independently from each other. This suggests that either the models are not accurately portraying the mechanism by which variable δ^{18}O values are inherited in the mineral or the Δ_{63} is not under the same controls as δ^{18}O (i.e. not inheriting the Δ_{63} value of the fluid).

4.10 Other biomineralization effects

Unlike scleractinian zooxanthellate and azooxanthelate corals, gorgonian corals have been much less studied. In particular, biomineralization in gorgonian corals has yet to be addressed from a geochemical perspective. The fact that gorgonians precipitate high-Mg calcite however, in contrast to the aragonitic skeletons of scleractinians, is a simple indication of differing biomineralization mechanisms (Ries, 2010). Additionally, although it has been shown that deep-sea gorgonian corals exhibit δ^{18}O and δ^{13}C trends similar to their scleractinian counterparts, they have not been shown to exhibit the 'break' that is observed in Adkins et al. 2003 (Kimball et al., 2014). When growing inorganic carbonate precipitates, mineralogy can be controlled through the Mg/Ca ratio of the precipitating fluid, with molar Mg/Ca>2 producing aragonite and high-Mg calcite and molar Mg/Ca<2 producing calcite (reviewed by Ries, 2010). Current seas are ca. Mg/Ca=5.2 (Ries, 2010) and the biomineralization mechanism responsible for precipitation of high-Mg calcite in gorgonians is unknown.

Revisions 7/25/2016 10:32 AM
Deleted: (

Revisions 7/25/2016 10:32 AM
Deleted: .

One possibility is that biomineralization is regulated in gorgonians through an organic template. The presence of an insoluble organic matrix in both isidid bamboo and *Corallium* sp. (Allemand et al., 1994; Ehrlich et al., 2006; Noé and Dullo, 2006) supports the possibility that an organic template may be directing mineral precipitation. The presence of an organic matrix is unique to gorgonian corals (has not been observed in scleractinians) and only preliminary studies have been undertaken to characterize the amino acid composition of the organic matrixes (Allemand et al., 1994; Ehrlick et al., 2006).

Revisions 7/25/2016 10:32 AM
Deleted: Ehrlick

Revisions 7/25/2016 10:32 AM
Deleted: Noe

It seems plausible, that the organic template, in addition to directing lattice structure, could also be influencing isotopic fractionation within a growing mineral, as has recently been shown for Mg/Ca ratios in carbonates (Wang et al., 2009). Therefore, in addition to theoretical depletions expected in Δ_{63} due to mineralogy, the presence of an organic template might act as an additional control on bond ordering. Carbonate anhydrase has also been implicated in scleractinian hermatypic coral biomineralization models, and presence/absence and variable activities of carbonic anhydrase may another factor to be considered.

4.11 Suggestions for future work

In-depth experimental studies are needed to explore the role of multiple processes on acid digestion kinetics, such as Wacker et al. (2013) and Defliese et al. (2015). Possible factors influencing acid digestion fractionation factors that still need to be examined include (but are not limited to) organic matter content, the influence of cation substitution (e.g., high vs low Mg-calcite), variations in bulk composition (δ^{13}C, δ^{18}O), the type of reaction vessel and clean-up method used, and phosphoric acid composition.

Revisions 7/25/2016 10:32 AM
Deleted: 2015

aradhna tripati 8/11/2016 2:56 PM
Deleted: a

Direct constraints on the impact of variable cation concentrations on the clumped isotopic composition of carbonate minerals from theory and synthetic experiments may be a useful tool to distinguish between whether these different deep-sea corals orders in fact are recording equilibrium mineral-specific offsets. Additionally, measurement of coral calcifying fluid pH and the use of labeled carbon sources during growth experiments would provide important constraints on whether the observed patterns reflect kinetic effects.

Revisions 7/25/2016 10:32 AM
Deleted: coral

A unifying model which explains the observed patterns of isotopic and trace element variability that have been observed could also help to test the different explanations posed in this study and other publications, and could help us advance our understanding of biomineralization in scleractinian and gorgonian deep-sea corals. For clumped isotopes, such a model would need to include the factors that influence equilibrium fractionation, i.e., temperature and well-constrained mineral-specific fractionation factors. Additional factors that need to be included to accurately model kinetic isotope effects include temperature, the carbon source used for calcification (the relative fraction of seawater-derived DIC versus CO_2 diffused across cellular membranes), DIC speciation as controlled by multiple factors (pH, temperature, salinity), the timescale for DIC equilibration vs precipitation rate (affected by the residence time of DIC in the calcification space), as modulated by the occurrence and activity of the enzyme carbonic anhydrase.

5 Conclusions

Two groups of deep-sea corals with differing mineralogy (aragonite and calcite) were analyzed for $\delta^{13}C$, $\delta^{18}O$ and Δ_{47}. Aragonitic scleractinian deep-sea coral exhibit a nearly coincident Δ_{47}-T relationship to previously reported scleractinian deep-sea corals (Thiagarjan et al., 2011) and can be used to predict temperatures to ±2°C at the mean temperature and ±3-5°C at the extreme ends of the data set. Calcitic gorgonian deep-sea corals show lower Δ_{47} values. This offset between taxa is consistent with theoretical predictions for mineralogic differences, albeit significantly larger in magnitude than expected. Therefore the offset between gorgonian and scleractinian deep-sea corals may reflect, at least in part, as a difference in mineralogy that is only observed in deep-sea corals and not in data published for other carbonates simply because of their very slow growth rates as compared to all other studied carbonates. Another equally likely explanation is that differences in carbon sources and biomineralization pathways in coral taxa result in distinctive clumped isotope vital effects in gorgonian and scleractinian deep-sea coral. Finally, we can not preclude that offsets may reflect variable acid digestion kinetics for the different types of materials that we have surveyed.

Data availability

All raw data for samples and standards and equilibrated gas lines are in Supplement 1.

Acknowledgements

This work was supported by a NSF Graduate Fellowship, NSF OCE-1437166, DOE BES grant DE-FG02-13ER16402, and the "Laboratoire d'Excellence" LabexMER (ANR-10-LABX-19), co-funded by a grant from the French government under the program "Investissements d'Avenir". We thank Aradhna Tripati and the Tripati Lab Group for their assistance with analyses and discussion of this work, and Ben Elliott for assistance with drafting figures.

Revisions 7/25/2016 10:32 AM
Deleted:) and

References

Adkins, J.F., Boyle, E.A., Curry, W.B., Lutringer, A., 2003, Stable isotopes in deep-sea corals and a new mechanism for "vital effects". *Geochim. Cosmochim. Acta*,. 6, 129-1143

Affek, H. P., M. Bar-Matthews, A. Ayalon, A. Matthews, and J. M. Eiler (2008), Glacial/interglacial temperature variations in Soreq cave speleothems as recorded by 'clumped isotope' thermometry *Geochim. Cosmochim. Acta*, 72(22), 5351-5360. doi: 10.1016/j.gca.2008.06.031

Allemand D, Cuif J-P, Watabe N, Oishi M, Kawaguchi T., 1994, The organic matrix of skeletal structures of the Mediterranean Red Coral, Corallium rubrum. In: Allemand D, Cuif J-P (eds) Biomineralisation '93: 7th Int Symp Biomineralisation. *Bulletin de l'Institut oceanographique*, Monaco, Numero special 14, 1:129–140.

Allison N., Finch A., EIMF. 2000 δ^{11}B, Sr, Mg and B in a modern *Porites* coral: the relationship between calcification site pH and skeletal chemistry *Geochim. Cosmochim. Acta*, 74, 1790-1800.

Beck W.C., Grossman E. L., Morse, J. W. Experimental studies of oxygen isotope fractionation in the carbonic acid system at 15, 25, and 40 C. *Geochim. Cosmochim. Acta* 69, 3493-3503.

Blamart D., Rollion-Bard C., Meibom A., Cuif J.-P., Julliet-Leclerc A., and Dauphin Y. Correlation of boron isotopic composition with ultrastructure in the deep-sea coral Lophelia pertusa: Implications for biomineralization and paleo-pH. *Geochem. Geophys. Geosys*. DOI: 10.1029/2007GC001686.

Boyer, T.P., J. I. Antonov, O. K. Baranova, C. Coleman, H. E. Garcia, A. Grodsky, D. R. Johnson, R. A. Locarnini, A. V. Mishonov, T.D. O'Brien, C.R. Paver, J.R. Reagan, D. Seidov, I. V. Smolyar, and M. M. Zweng, 2013: World Ocean Database 2013, NOAA Atlas NESDIS 72, S. Levitus, Ed., A. Mishonov, Technical Ed.; Silver Spring, MD, 209 pp.

Came, R. E., J. M. Eiler, J. Veizer, K. Azmy, U. Brand, and C. R. Weidman (2007), Coupling of surface temperatures and atmospheric CO_2 concentrations during the Palaeozoic era, *Nature*, 449(7159), 198-201. doi: 10.1038/nature06085

Revisions 7/25/2016 10:32 AM
Moved (insertion) [1]

Revisions 7/25/2016 10:32 AM
Deleted: Geochimica Et Cosmochimica

Revisions 7/25/2016 10:32 AM
Deleted: .

Rob Tripati 8/5/2016 7:10 PM
Deleted: v.

Rob Tripati 8/5/2016 7:10 PM
Deleted: p.1

Revisions 7/25/2016 10:32 AM
Formatted: Font:Italic

Revisions 7/25/2016 10:32 AM
Formatted: Font:Italic

Revisions 7/25/2016 10:32 AM
Formatted: Font:Italic

Rob Tripati 8/5/2016 7:10 PM
Formatted: English (US)

Revisions 7/25/2016 10:32 AM
Moved (insertion) [2]

Revisions 7/25/2016 10:32 AM
Formatted: English (US)

Revisions 7/25/2016 10:32 AM
Formatted: Font:Italic

Revisions 7/25/2016 10:32 AM
Moved (insertion) [3]

Revisions 7/25/2016 10:32 AM
Deleted: Bigeleisen, J., and Mayer, M.G., 1947, Calculation of Equilibrium Constants for Isotopic Exchange Reactions: Journal of Chemical Physics, v. 15, p. 261-267.

Revisions 7/25/2016 10:32 AM
Formatted: Subscript

Revisions 7/25/2016 10:32 AM
Formatted: Font:Italic

Came, R. E., Brand, U., Affek, H.P. (2014), Clumped isotope signatures in brachiopod carbonate. *Chem. Geol.* 377, 20-30.

Cohen A.L., McConnaughey T.A., 2003, A geochemical perspective on coral mineralization. In: Dove M, Weiner S, de Yoreo J (eds) Biomineralization. *Rev Miner Geochem* 54:151–187

Daëron, M., W. Guo, J. Eiler, D. Genty, D. Blamart, R. Boch, R. Drysdale, R. Maire, K. Wainer, and G. Zanchetta (2011), ^{13}C^{18}O clumping in speleothems: Observations from natural caves and precipitation experiments, *Geochim. Cosmochim. Acta,* 75(12), 3303-3317. doi: 10.1016/j.gca.2010.10.032.

Defliese, W. F., Hren, M. T., & Lohmann, K. C. (2015). Compositional and temperature effects of phosphoric acid fractionation on Δ$_{47}$ analysis and implications for discrepant calibrations. *Chem. Geol.,* 396, 51-60.

Defliese, W. F., & Lohmann, K. C. (2015). Non-linear mixing effects on mass-47 CO$_2$ clumped isotope thermometry: Patterns and implications. *Rapid Comm. in Mass Spec.,* 29(9), 901-909.

Dennis, K. J., and Schrag, D. P. (2010), Clumped isotope thermometry of carbonatites as an indicator of diagenetic alteration: *Geochim. Cosmochim. Acta*, v. 74, no. 14, p. 4110–4122.

Dennis, K. J., H. P. Affek, B. H. Passey, D. P. Schrag, and J. M. Eiler (2011), Defining an absolute reference frame for 'clumped' isotope studies of CO$_2$, *Geochim. Cosmochim. Acta* 75, 7117-7131.

Douglas P. M. J., Affek H. P., Ivany L. C., Houben A., Sijp W., Sluijs A., Schouten S, and Pagani M. Pronounced zonal heterogeneity in Eocene southern high-latitude sea surface temperatures. *Proc. Natl. Acad. Sci. USA*. 111, 6582–6587.

Dunbar R. and Wellington G. 1981, Stable isotopes in a branching coral monitor seasonal temperature variation, *Nature* vol. 293.

Eagle R., Schauble E., Tripati A., Tutken T, Hulbert R, Eiler J. 2010. Body temperatures of modern and extinct vertebrates from 13C-18O bond abundances in bioapatite. 107, 10377-10382.

Eagle, R., Eiler, J., Tripati, A., Ries, J., Freitas, P., Hiebenthal, C., Wanamaker Jr., A., Taviani, M., Elliot, M., Richardson, C., Marenssi, S., Nakamura, K., Ramirez, P., Roy, K.

Revisions 7/25/2016 10:32 AM
Moved (insertion) [4]

Rob Tripati 7/25/2016 10:47 AM
Formatted: Font:Italic

Revisions 7/25/2016 10:32 AM
Formatted: Font:Italic

Revisions 7/25/2016 10:32 AM
Formatted: Superscript

Revisions 7/25/2016 10:32 AM
Formatted: Superscript

Revisions 7/25/2016 10:32 AM
Formatted: Font:Italic

Revisions 7/25/2016 10:32 AM
Deleted: 10.1016/j.gca.2010.10.032

Revisions 7/25/2016 10:32 AM
Deleted: 2015

aradhna tripati 8/11/2016 2:55 PM
Deleted: a

Revisions 7/25/2016 10:32 AM
Deleted: Δ 47

Revisions 7/25/2016 10:32 AM
Deleted: Chemical Geology,

Revisions 7/25/2016 10:32 AM
Deleted: 2015

aradhna tripati 8/11/2016 2:55 PM
Deleted: b

Revisions 7/25/2016 10:32 AM
Deleted: □

Revisions 7/25/2016 10:32 AM
Deleted: □

Revisions 7/25/2016 10:32 AM
Formatted: Subscript

Revisions 7/25/2016 10:32 AM
Formatted: Font:Italic

Revisions 7/25/2016 10:32 AM
Deleted: Communications

Revisions 7/25/2016 10:32 AM
Formatted: Font:Italic

Revisions 7/25/2016 10:32 AM
Deleted: Spectrometry,

Revisions 7/25/2016 10:32 AM
Formatted: Subscript

Revisions 7/25/2016 10:32 AM
Formatted: Font:Not Italic

Revisions 7/25/2016 10:32 AM
Moved (insertion) [5]

(2013), The influence of temperature and seawater carbonate saturation state on ^{13}C-^{18}O bond ordering in bivalve mollusks, *Biogeosciences*. doi:10.5194/bgd-10-157-2013.

Eiler, J. M. (2007), "Clumped-isotope" geochemistry – The study of naturally-occurring, multiply-substituted isotopologues, *Earth Planet. Sci. Lett.*, 262, 309-327. doi: 10.1016/j.epsl.2007.08.020

Emiliani, C., Hudson, J.H., Shinn, E.A., and George, R.Y., 1978, Oxygen and Carbon Isotopic Growth Record in a Reef Coral from the Florida Keys and a Deep-sea Coral from Blake Plateau: *Science*, v. 202, p. 627-629.

Epstein, S., Buchsbaum, R., Lowenstam, H.A., and Urey, H.C., 1953, Revised Carbonate-Water Isotopic Temperature Scale: *Geol. Soc. of Am. Bull.,* v. 64, p. 1315-1325.

Gabitov R. I., Watson E. B., Sadekov A. Oxygen isotope fractionation between calcite and fluid as a function of growth rate and temperature: An in situ study. *Chem Geol.* 4, 92-102.

Gaetani, G.A., Cohen, A.L., Wang, Z., and Crusius, J., 2011, Rayleigh-based, multi-element coral thermometry: A biomineralization approach to developing climate proxies: Geochimica Et Cosmochimica Acta, v. 75, p. 1920-1932.

Ghosh, P., J. Adkins, H. Affek, B. Balta, W. Guo, E. A. Schauble, D. Schrag, and J. M. Eiler 2006, ^{13}C-^{18}O bonds in carbonate materials: A new kind of paleothermometer, *Geochim. Cosmochim. Acta*, 70, 1439-1456. doi: 10.1016/j.gca.2005.11.014

Ghosh P., Eiler J, Campana S, Feeney R. 2007. Calibration of the carbonate 'clumped isotope' paleothermometer for otoliths. *Geochim. Cosmochim. Acta*, 71, 2736-2744.

Guo, W., J. L. Mosenfelder, W. A. Goddard III, and J. M. Eiler (2009), Isotopic fractionations associated with phosphoric acid digestion of carbonate minerals: Insights from first-principles theoretical modeling and clumped isotope measurements, *Geochim. Cosmochim. Acta*, 73(24), 7203-7225. doi: 10.1016/j.gca.2009.05.071

Grossman, E.L., and Ku, T.-L., 1986, Carbon and oxygen isotopic fractionation in biogenic aragonite- temp effects: Chemical Geology v. 59, p. 74.

Henkes G.A., Passey B.H., Wanamaker A.D., Grossman E.L., Ambrose W.G., and Carroll M.L. (2013), Carbonate clumped isotope compositions of modern marine mollusk and brachiopod shells, *Geochim. Cosmochim. Acta*, 106, 307-325. doi: 10.1016/j.gca.2012.12.020.

Revisions 7/25/2016 10:32 AM
Formatted: Superscript

Revisions 7/25/2016 10:32 AM
Formatted: Superscript

Revisions 7/25/2016 10:32 AM
Formatted: Font:Italic

Revisions 7/25/2016 10:32 AM
Deleted: Ehrlich, H., Etnoyer,

Revisions 7/25/2016 10:32 AM
Moved up [3]: P.,

Revisions 7/25/2016 10:32 AM
Deleted: Litvinov, S. D., Olennikova, M.

Revisions 7/25/2016 10:32 AM
Moved down [6]: M.,

Revisions 7/25/2016 10:32 AM
Deleted: Domaschke, H., Hanke, T., Born, R., Meissner, H., and Worch, H., 2006. Biomaterial structure in deep-sea bamboo coral (Anthozoa : Gorgonacea : Isididae): perspectives for the development of bone implants and templates for tissue engineering. Materialwissenschaft Und Werkstofftechnik 37, 552-557.

Revisions 7/25/2016 10:32 AM
Deleted: 10.1016/j.epsl.2007.08.020

Revisions 7/25/2016 10:32 AM
Formatted: Font:Italic

Revisions 7/25/2016 10:32 AM
Deleted: Geological Society of America Bulletin,

Revisions 7/25/2016 10:32 AM
Moved (insertion) [7]

Revisions 7/25/2016 10:32 AM
Deleted: (

Revisions 7/25/2016 10:32 AM
Deleted:),

Revisions 7/25/2016 10:32 AM
Formatted: Superscript

Revisions 7/25/2016 10:32 AM
Formatted: Superscript

Revisions 7/25/2016 10:32 AM
Deleted: (6),

Revisions 7/25/2016 10:32 AM
Deleted: 10.1016/j.gca.2005.11.014

Revisions 7/25/2016 10:32 AM
Deleted: 10.1016/j.gca.2009.05.071

Revisions 7/25/2016 10:32 AM
Formatted: Font:Italic

Henkes, G. A., Passey, B. H., Grossman, E. L., Shenton, B. J., Pérez-Huerta, A., & Yancey, T. E. (2014). Temperature limits for preservation of primary calcite clumped isotope paleotemperatures. *Geochim. Cosmochim. Acta*,139, 362-382.

Hill, P. S., Tripati, A. K., & Schauble, E. A., 2014, Theoretical constraints on the effects of pH, salinity, and temperature on clumped isotope signatures of dissolved inorganic carbon species and precipitating carbonate minerals. *Geochim. Cosmochim. Acta*, 125, 610-652.

Hill, T.M., Spero, H. J., Guilderson, T., Lavigne, M., Clague, D., Macalello, S., and Jang, N. 2011. Temperature and vital effect controls on bamboo coral (Isididae) isotope geochemistry: A test of the "lines method". *Geochem. Geophys. Geosys.*, v. 12, n. 4.

Huntington, K. W., J. M. Eiler, H. P. Affek, W. Guo, M. Bonifacie, L. Y. Yeung, N. Thiagarajan, B. Passey, A. Tripati, M. Daëron, and R. Came (2009), Methods and limitations of 'clumped' CO_2 isotope (Δ_{47}) analysis by gas-source isotope ratio mass spectrometry, *J. Mass. Spectrom.*, 44(9), 1318-1329. doi: 10.1002/jms.1614

Karl, D.M. and Lukas, 1996, The Hawaii Ocean Time-series (HOT) Program: Background, rationale and field implementation. *Deep Sea Res. Part II*, 43, 129-156.

Kim, S.-T., O'Neil, J. R., Hillaire-Marcel, C., and Mucci, A., 2007. Oxygen isotope fractionation between synthetic aragonite and water: Influence of temperature and Mg2+ concentration. *Geochim. Cosmochim. Acta.,* 71, 4704-4715.

Kim, S. T. and O'Neil, J. R., 1997. Equilibrium and nonequilibrium oxygen isotope effects in synthetic carbonates. *Geochim. Cosmochim. Acta.,* 61, 3461-3475.

Kimball, J. B., Dunbar R. B., and Guilderson T. P. 2014. Oxygen and carbon isotope fractionation in calcitic deep-sea corals: Implications for paleotemperature reconstructions. *Chem. Geol. 381, 223-233.*

Kluge, T., John, C. M., Jourdan, A. L., Davis, S., & Crawshaw, J. (2015). Laboratory calibration of the calcium carbonate clumped isotope thermometer in the 25–250° C temperature range. *Geochim. Cosmochim. Acta*, 157, 213-227.

Lutringer, A., Blamart, D., Frank, N., Labeyrie L. 2005. Paleotemperatures from deep sea corals: scale effects. Cold Water Corals and Ecosystems. pp 1081-1096. ed. Freiwald A., and Murray Roberts J. Springer.

Revisions 7/25/2016 10:32 AM
Deleted: Geochimica et cosmochimica acta

Revisions 7/25/2016 10:32 AM
Deleted: Geochimica et cosmochimica acta

Revisions 7/25/2016 10:32 AM
Deleted: Geochemistry Geophysics Geosystems,

Revisions 7/25/2016 10:32 AM
Formatted: Subscript

Revisions 7/25/2016 10:32 AM
Formatted: Subscript

Revisions 7/25/2016 10:32 AM
Deleted: 10.1002/jms.1614

Revisions 7/25/2016 10:32 AM
Moved up [1]: *Geochim. Cosmochim.*

Revisions 7/25/2016 10:32 AM
Deleted: Jimenez-Lopez, C., Romanek, C.S., Huertas, F.J., Ohmoto, H., and Caballero, E., 2004, Oxygen isotope fractionation in synthetic magnesian calcite:

Revisions 7/25/2016 10:32 AM
Deleted: *Acta.*, v. 68, p. 3367-3377.

Revisions 7/25/2016 10:32 AM
Formatted: Font:Italic

Revisions 7/25/2016 10:32 AM
Moved (insertion) [8]

Revisions 7/25/2016 10:32 AM
Deleted: Geochimica et Cosmochimica

Revisions 7/25/2016 10:32 AM
Formatted: Font:Italic

Revisions 7/25/2016 10:32 AM
Deleted: Mavromatis V., Schmidt M, Botz, R. Comas-Bru, L. Oelkers, E.H., 2012, Experimental quantification of the effect of Mg on calcite–aqueous fluid oxygen isotope fractionation, Chemical Geology, v.310–311, p.97-105.

McConnaughey, T., 1989a, C-13 and O-18 Isotopic Disequilibrium in Biological Carbonates.I. Patterns: *Geochim. Cosmochim. Acta*, v. 53, p. 151-162.

McConnaughey, T., 1989b, C-13 and O-18 Isotopic Disequilibrium in Biological Carbonates.II. In vitro simulation of kinetic isotope effects: *Geochim. Cosmochim. Acta*, v. 53, p. 163-161.

McConnaughey, T., 2003. Sub-equilibrium oxygen-18 and carbon-13 levels in biological carbonates: carbonate and kinetic models. *Coral Reefs* v 22, p. 316-327.

McCrea, J.M, 1950, On the Isotopic Chemistry of Carbonates and a Paleotemperature Scale. *J. Chem. Phys.* v 18, p. 849

Nielson L. C., DePaulo D. J., De Yoreo J. J. Self-consistent ion-by-ion growth model for kinetic isotopic fractionation during calcite precipitation. *Geochim. Cosmochim. Acta.* 86, 166-171.

Noé , S.U., and Dullo, W.C., 2006, Skeletal morphogenesis and growth mode of modern and fossil deep-water isidid gorgonians (Octocorallia) in the West Pacific (New Zealand and Sea of Okhotsk): Coral Reefs, v. 25, p. 303-320.

Passey, B. H., & Henkes, G. A. (2012). Carbonate clumped isotope bond reordering and geospeedometry. Earth and Planetary Science Letters, 351, 223-236.

Passey, B. H., N. E. Levin, T. E. Cerling, F. H. Brown, and J. M. Eiler (2010), High-temperature environments of human evolution in East Africa based on bond ordering in paleosol carbonates, *Proc. Natl. Acad. Sci. USA*, 107(25), 11245-11249. doi: 10.1073/pnas.1001824107.

Petrizzo D., Young E., Runnegar B. 2014. Implications for high-precision measurement of ^{13}C-^{18}O bonds in CO_2 and effects on carbonate clumped-isotope thermometry in modern bivalved mollusc shells. *Geochim. Cosmochim. Acta.* 142, 400-410.

Petryshyn, V., Lim, D., Brady, A., Slater, G., Laval, B., and Tripati A., 2015, Reconstruction of hydrology from microbialites using carbonate clumped isotope paleothermometer, *Geobiology,* 13, 53-67.

Revisions 7/25/2016 10:32 AM
Deleted: Geochimica Et Cosmochimica

Revisions 7/25/2016 10:32 AM
Formatted: Font:Italic

Revisions 7/25/2016 10:32 AM
Deleted: Geochimica Et Cosmochimica

Revisions 7/25/2016 10:32 AM
Formatted: Font:Italic

Revisions 7/25/2016 10:32 AM
Deleted: .,

Revisions 7/25/2016 10:32 AM
Formatted: English (US)

Revisions 7/25/2016 10:32 AM
Deleted: .

Revisions 7/25/2016 10:32 AM
Formatted: English (US)

Revisions 7/25/2016 10:32 AM
Moved (insertion) [9]

Revisions 7/25/2016 10:32 AM
Formatted: Font:Italic, English (US)

Revisions 7/25/2016 10:32 AM
Deleted: : Journal of Chemical Physics,

Revisions 7/25/2016 10:32 AM
Formatted: English (US)

Revisions 7/25/2016 10:32 AM
Deleted: .

Revisions 7/25/2016 10:32 AM
Formatted: English (US)

Revisions 7/25/2016 10:32 AM
Deleted: -857

Revisions 7/25/2016 10:32 AM
Formatted: English (US)

Revisions 7/25/2016 10:32 AM
Deleted: Noe

Revisions 7/25/2016 10:32 AM
Deleted: Noe, S.U., Lembke-Jene, L., and Dullo, W.C., 2008, Varying growth rates in bamboo corals: sclerochronology and radiocarbon dating of a mid-Holocene d ... [6]

Revisions 7/25/2016 10:32 AM
Moved up [4]: Chem.

Revisions 7/25/2016 10:32 AM
Moved up [9]: *Phys.*

Revisions 7/25/2016 10:32 AM
Formatted: Font:Italic, English (US)

Revisions 7/25/2016 10:32 AM
Deleted: 51, 5547. doi: 10.1063/1.1671982 .

Revisions 7/25/2016 10:32 AM
Deleted: 10.1073/pnas.1001824107

Revisions 7/25/2016 10:32 AM
Formatted: Font:Italic

Robinson, L.F., Adkins, J.F., Scheirer, D.S., Fernandez, D.P., Gagnon,A., Waller,R.G., 2007. Deep-seascleractinian coral age and depth distributions in the WN Atlantic for the last 225 thousand years: *Bull.Mar.Sci.* 81,371–391.

Rollion-Bard C., Chaussidon M. and France-Lanord C. 2003 pH control on oxygen isotopic composition of symbiotic corals. *Earth Planet. Sci. Lett.* 215, 275–288.

Rollion-Bard C., Blamart D., Cuif J-P., Dauphin Y. 2010. *In situ* measurements of oxygen isotopic composition in deep-sea coral, *Lophelia pertusa*: Re-examination of the current geochemical models of biomineralization. *Geochim. Cosmochim. Acta*, 74, 1338-1349.

Rollion-Bard C., Blamart D., Trebosc J., Tricot G., Mussi A., Cuif J-P. 2011. Boron isotopes as pH proxy: A new look at boron speciation in deep-sea corals using ^{11}B MAS NMR and EELS. *Geochim. Cosmochim. Acta* 75, 1003-1012.

Saenger, C., H.P. Affek, T. Felis, N. Thiagarajan, J.M. Lough, and M. Holcomb (2012), Carbonate clumped isotope variability in shallow water corals: Temperature dependence and growth-related vital effects. *Geochim. Cosmochim. Acta*, 99, 224-242. doi: 10.1016/j.gca.2012.09.035.

Saenger, C., Affek H. P., Felis T., Thiagarajan N., Lough J. M., Holcomb M. 2013 Carbonate clumped isotope variability in shallow water corals: Temperature dependence and growth-related vital effects. *Geochim. Cosmochim. Acta*. 99, 224-242.

Schauble, E. A., P. Ghosh, and J. M. Eiler (2006), Preferential formation of 13C–18O bonds in carbonate minerals, estimated using first-principles lattice dynamics *Geochim. Cosmochim. Acta*, 70(10), 2510-2529. doi: 10.1016/j.gca.2006.02.011.

Smith, J.E., Schwarcz, H.P., Risk, M.J., McConnaughey, T.A., and Keller, N., 2000, Paleotemperatures from deep-sea corals: Overcoming 'vital effects': *Palaios*, v. 15, p. 25-32.

Swart P. K., Burns S., Leder S. 1991. Fractionation of the stable isotopes of oxygen and carbon in carbon dioxide during the reaction of calcite with phosphoric acid as a function of temperature and technique. *Chem. Geol.* 86, 89-96.

Tang, J., Dietzel, M., Fernandez, A., Tripati, A. K., & Rosenheim, B. E. (2014). Evaluation of kinetic effects on clumped isotope fractionation (Δ 47) during inorganic calcite precipitation. *Geochim. Cosmochim. Acta*, 134, 120-136.

Revisions 7/25/2016 10:32 AM
Moved up [7]: B.,

Revisions 7/25/2016 10:32 AM
Deleted: Roark, E.

Revisions 7/25/2016 10:32 AM
Moved up [8]: B.,

Revisions 7/25/2016 10:32 AM
Deleted: Guilderson, T.P., Flood-Page, S., Dunbar, R.

Revisions 7/25/2016 10:32 AM
Deleted: Ingram, B.L., Fallon, S.J., and McCulloch, M., 2005, Radiocarbon-based ages and growth rates of bamboo corals from the Gulf of Alaska: Geophysical Research Letters, v. 32, p. 5 pp.

Revisions 7/25/2016 10:32 AM
Formatted: Font:Italic

Revisions 7/25/2016 10:32 AM
Deleted: (

Revisions 7/25/2016 10:32 AM
Deleted:)

Revisions 7/25/2016 10:32 AM
Formatted: Font:Italic

Revisions 7/25/2016 10:32 AM
Deleted: 10.1016/j.gca.2012.09.035

Revisions 7/25/2016 10:32 AM
Moved (insertion) [6]

Revisions 7/25/2016 10:32 AM
Deleted: 10.1016/j.gca.2006.02.011

Revisions 7/25/2016 10:32 AM
Formatted: Font:Italic

Revisions 7/25/2016 10:32 AM
Deleted: Geochimica et Cosmochimica

Revisions 7/25/2016 10:32 AM
Deleted: ,

Revisions 7/25/2016 10:32 AM
Formatted: Font:Italic

Tarutani, T., Clayton, R.N., and Mayeda, T.K., 1969, Effect of Polymorphism and Magnesium Substitution on Oxygen Isotope Fractionation between Calcium Carbonate and Water: *Geochim. Cosmochim. Acta*, v. 33, p. 987.

Thiagarajan, N., Adkins, J., and Eiler, J., 2011, Carbonate clumped isotope thermometry of deep-sea corals and implications for vital effects: *Geochim. Cosmochim. Acta*, v. 75, p. 4416-4425.

Thiagarajan, N., Gerlach D., Roberts M., Burke A, McNichol A., Jenkins W., Subhas A., Thresher R., Adkins J. 2013. Movement of deep-sea coral populations on climatic timescales. 28, 227-236.

Tripati, A. K., R. A. Eagle, N. Thiagarajan, A. C. Gagnon, H. Bauch, P. R. Halloran, and J. M. Eiler (2010), Apparent equilibrium ^{13}C-^{18}O isotope signatures and 'clumped isotope' thermometry in foraminifera and coccoliths, *Geochim. Cosmochim. Acta*, 74(20), 5697-5717. doi: 10.1016/j.gca.2010.07.006.

Tripati, A. K., Hill, P. S., Eagle, R. A., Mosenfelder, J. L., Tang, J., Schauble, E. A., Eiler, J., Ries, J., & Henry, D., 2015. Beyond temperature: Clumped isotope signatures in dissolved inorganic carbon species and the influence of solution chemistry on carbonate mineral composition. *Geochim. Cosmochim. Acta*, 166, 344-371.

Usdowski E., Michaelis J., Bottcher M. E. and Hoefs J. (1991) Factors for the oxygen isotope equilibrium fractionation between aqueous and gaseous CO$_2$, carbonic acid, bicarbonate, carbonate, and water (19°C). *Z. Phys. Chem.* 170, 237–249.

Wacker, U., Fiebig, J., and Schöne, B.R. (2013), Clumped isotope analysis of carbonates: comparison of two different acid digestion techniques, *Rapid Commun. Mass Spectrom.*, 27, 1631-1642. doi:10.1002/rcm.6609.

Wang, D., Wallace, A., Yoreo, J., Dove, P., 2009. Carboxylated molecules regulate magnesium content of amorphous calcium carbonates during calcification. Proceedings of the National Academy of Sciences 106, 21511–21516.

Watkins J. M., Nielson L. C., Ryerson F., DePaolo D., The influence of kinetics on the oxygen isotope composition of calcium carbonate. *Earth Planet. Sci Lett.* 375, 349-360.

Revisions 7/25/2016 10:32 AM
Deleted: Geochimica Et Cosmochimica

Revisions 7/25/2016 10:32 AM
Deleted: ,

Revisions 7/25/2016 10:32 AM
Formatted: Font:Italic

Revisions 7/25/2016 10:32 AM
Formatted: Superscript

Revisions 7/25/2016 10:32 AM
Formatted: Superscript

Revisions 7/25/2016 10:32 AM
Deleted: 10.1016/j.gca.2010.07.006

Revisions 7/25/2016 10:32 AM
Deleted: Geochimica et Cosmochimica

Revisions 7/25/2016 10:32 AM
Formatted: Font:Italic

Revisions 7/25/2016 10:32 AM
Deleted: ,

Revisions 7/25/2016 10:32 AM
Deleted: Urey, H.

Revisions 7/25/2016 10:32 AM
Moved up [5]: C.,

Revisions 7/25/2016 10:32 AM
Deleted: 1947, The Thermodynamic Properties of Isotopic Substances: Journal of the Chemical Society, p. 562-581.

Revisions 7/25/2016 10:32 AM
Formatted: Subscript

Revisions 7/25/2016 10:32 AM
Formatted: Font:Italic

Revisions 7/25/2016 10:32 AM
Deleted: 10.1002/rcm.6609

Revisions 7/25/2016 10:32 AM
Deleted: Wang, Z., E. A. Schauble, and J. M. Eiler (2004), Equilibrium thermodynamics of multiply substituted isotopologues of molecular gases,

Revisions 7/25/2016 10:32 AM
Moved up [2]: *Geochim. Cosmochim.*

Revisions 7/25/2016 10:32 AM
Formatted: English (US)

Revisions 7/25/2016 10:32 AM
Formatted: Font:Italic

Revisions 7/25/2016 10:32 AM
Deleted: Acta, 68(23), 4779-4797. doi: 10.1016/j.gca.2004.05.039

Watson, E. B. 2004. A conceptual model for near-surface kinetic controls on the trace-element and stable-isotope composition of abiogenic calcite. *Geochim. Cosmochim. Acta*, 68, 1473-1488.

Watson, E. B. and Liang Y. 1995. A simple model for sector zoning in slowly-grown crystals: Implications for growth rate and lattice diffusion, with emphasis on accessory minerals in crustal rocks. *Am. mineral.* 80, 1170-1187.

Weber J., and Woodhead, P. 1972. Temperature dependence of oxygen-18 concentration in reef coral carbonates. *J. Geophys. Res.* 77, 463-473.

Zaarur, S., G. Olack, and H.P. Affek 2011. Paleo-environmental implications of clumped isotopes in land snail shells, *Geochim. Cosmochim. Acta*, 75(22), 6859-6869. doi: 10.1016/j.gca.2011.08.044.

Zaarur, S., Affek, H.P., and Brandon, M.T. 2013. A revised calibration of the clumped isotope thermometer, *Earth Planet. Sci. Lett,* v382, 47-57. doi: 10.1016/j.epsl.2013.07.026

Zeebe, R. E., 1999. An explanation of the effect of seawater carbonate concentration on foraminiferal oxygen isotopes. *Geochim. Cosmochim. Acta,* 63, 2001-2007.

Zeebe, R. E. and Wolf-Gladrow. CO_2 in Seawater: Equilibrium, Kinetics, Isotopes. Elsevier Oceanography Series, 65, pp. 346, Amsterdam, 2001

Zeebe R. E. 2007 An expression for the overall oxygen isotope fractionation between the sum of dissolved inorganic carbon and water. *Geochem. Geophys. Geosyst.* 8, Q09002.

Revisions 7/25/2016 10:32 AM
Deleted: (

Revisions 7/25/2016 10:32 AM
Deleted:),

Revisions 7/25/2016 10:32 AM
Deleted: (

Revisions 7/25/2016 10:32 AM
Deleted:),

Revisions 7/25/2016 10:32 AM
Formatted: English (US)

Revisions 7/25/2016 10:32 AM
Deleted: R. E. (2007)

Revisions 7/25/2016 10:32 AM
Deleted: .

Revisions 7/25/2016 10:32 AM
Formatted: Font:Italic

Table captions

Table 1. Thirteen scleractinian and gorgonian deep-sea corals were collected live by submersible diving with depth and temperature measured at the time of collection. Temperature ranges are mean with standard deviation and come from Hawaii Ocean Time Series (Karl and Lukas, 1996) and cruises extracted from the National Ocean Database (Boyer et al., 2013).

Table 2. Coral specimens analyzed for $\delta^{13}C$, $\delta^{18}O$ and Δ_{47}. Δ_{47} is reported relative to the absolute reference frame (ARF). Standard error, 1σ, is reported with number of replicate measurements (n). Individual analyses are reported in Supplementary Table 1. Values are calculated using a 25 to 90 ^{o}C AFF = 0.092 (denoted by 1; Henkes et al., 2013) and AFF = 0.082 (denoted by 2; Defliese et al., 2015 and Passey et al., 2010).

Table 3. Average standard values with standard error reported for the two periods of time when samples were measured compared to accepted values. Δ_{47} values are in ‰ relative to the absolute reference frame. a. winter b. summer 2013. Values are calculated using a 25 to 90 ^{o}C AFF = 0.092 (denoted by 1; Henkes et al., 2013) and AFF = 0.082 (denoted by 2; Defliese et al., 2015 and Passey et al., 2010).

Table 4. Coral specimens analyzed for $\delta^{13}C$, $\delta^{18}O$ and Δ_{47}. Average Δ_{47} for all replicate measurements is reported relative to the absolute (ARF) reference frame. δ_{47} is reported relative to intra-laboratory working gas (WG). a) $\delta^{18}O_{water}$ values are from WOCE and HOTS. b) $\delta^{18}O$ predicted values are calculated using the equations reported in Kim and O'Neil (1997) for calcite and Kim et al. (2007) for aragonite. c) δ_{47} is relative to intralaboratory working gas with a known isotopic composition. d) Δ_{47} predicted value is calculated from the inorganic calibration of Ghosh et al. (2006); similar values are predicted from other inorganic calibrations including Zaarur et al. (2013) and Tripati et al. (2015).

Table 5. Two coral specimens were analyzed using different portions of their skeletons. PIV 146-6 was sampled by micromilling the outer portion of a disk (outer) as well as grinding an entire disk (whole). PV 703-3 was micromilled in both cases, but was milled in both the center and outer portion of a disk. All data and averages are reported as well as standard error, 1σ.

aradhna tripati 8/11/2016 2:53 PM
Formatted: Font:Italic

aradhna tripati 8/11/2016 2:53 PM
Formatted: Subscript

aradhna tripati 8/11/2016 2:53 PM
Formatted: Font:Italic

aradhna tripati 8/11/2016 2:53 PM
Formatted: Subscript

aradhna tripati 8/11/2016 3:25 PM
Formatted: Superscript

aradhna tripati 8/11/2016 2:53 PM
Formatted: Font:Italic

aradhna tripati 8/11/2016 2:53 PM
Formatted: Font:Italic

Figure captions

Figure 1. Sampling locations of three expeditions from which coral specimens were collected by deep-sea submersible diving. Locations approximate Warwick Seamount, Gulf of Alaska (DSRV Alvin, 2004), Hawaiian and Northwest Hawaiian Islands (DSRV Pisces V, 2005 and 2007) and Line Islands (DSRV Pisces IV, 2006).

Figure 2. a) A bamboo coral from Warwick Seamount, ALV 3808-4. The bottommost internode is cut and the disk used for milling along the outer, most recently accreted portion. b) A portion of a radial disk from PV 703-5 in which samples were milled from the center and outer portion.

Figure 3. Scleractinian and gorgonian deep-sea coral compared to deep-sea corals reported in Thiagarajan et al. (2011) and average Δ_{47} values recalculated relative to ARF from Eagle et al. (2013). Sample 703-7 is not included in the calibration is not considered live-collected.

Figure 4. Scleractinian corals from this study and Thiagarajan et al. (2011) are combined (slope: 0.0582±0.008, intercept: 0.0452±0.103, R^2=0.81) and along with gorgonian deep-sea corals are compared to other reported calibrations studies.

Figure 5. Scleractinian and gorgonian corals from this study and Thiagarajan et al. (2011) are compared to the theoretical predictions for Δ_{63} for aragonite, calcite and dolomite. Acid fractionation values were added to convert to Δ_{47}.

Figure 6. Sensitivity analysis of varying acid digestion fractionation factor ($\Delta_{25\text{-}90}$) on results.

Figure 7. Δ_{47} residuals are calculated from average measured Δ_{47} values for each coral relative to the inorganic calibrations of Ghosh et al. (2006), Zaruur et al. (2013) and Dennis and Schrag (2010). δ^{18}O residuals are calculated from average measured δ^{18}O values relative to the calibrations of Kim and O'Neil (1997) and Kim et al. (2007) for calcite and aragonite, respectively.

Figure 8. Δ_{47} residuals are calculated from average measured Δ_{47} values for each coral relative to the biogenic calibrations of Eagle et al. (2013). δ^{18}O residuals are calculated from average measured δ^{18}O values relative to the calibrations of Kim and O'Neil (1997) and Kim et al. (2007) for calcite and aragonite, respectively.

aradhna tripati 8/11/2016 3:36 PM
Deleted: ... [7]

Revisions 7/25/2016 10:32 AM
Deleted: as it was

Revisions 7/25/2016 10:32 AM
Deleted: fully alive when

Revisions 7/25/2016 10:32 AM
Deleted: 643

Revisions 7/25/2016 10:32 AM
Deleted: 288

Revisions 7/25/2016 10:32 AM
Deleted: of Eagle et al. (2013) and Ghosh et al. (2006).

Figure 9. Δ_{47} residuals are calculated from average measured Δ_{47} values for each coral relative to the theoretical calibration of Schauble et al. (2006) paired with theoretical acid digestion fractionations from Guo et al. (2009). $\delta^{18}O$ residuals are calculated from average measured $\delta^{18}O$ values relative to the calibrations of Kim and O'Neil (1997) and Kim et al. (2007) for calcite and aragonite, respectively.

Figure 10. Schematic illustrating general trajectories for different processes on stable isotope signatures (Δ_{63} or Δ_{47} values and $\delta^{18}O$), relative to an arbitrary point. Equilibrium temperature dependence is shown (Ghosh et al., 2006). Note that mixing of DIC from different sources results in curved trajectories (in $\delta^{18}O$ space, mixing is linear whereas in Δ_{47} space can be non-linear) (Eiler and Schauble, 2004; Thiagarajan et al., 2011; Defliese and Lohmann, 2015). Diffusion results in enrichment of clumped species and depletion in $\delta^{18}O$ (Thiagarajan et al., 2011). CO_2 hydration reactions are strongly temperature pH-dependent and also result in enrichment of clumped species and depletion in $\delta^{18}O$ (Affek, 2013; Tang et al., 2014; Tripati et al., 2015). At any given temperature, equilbrium DIC species have differing clumped and oxygen isotope signatures, potentially also giving rise to pH effect (Hill et al., 2014; Tripati et al., 2015). Solid-state diffusion processes (Passey and Henkes, 2012; Henkes et al., 2014), including hypothesized reordering in the interfacial region (Tripati et al., 2015) only influence clumped isotope signatures and not bulk isotopic signatures (e.g., $\delta^{18}O$).

Revisions 7/25/2016 10:32 AM
Deleted: 2015

aradhna tripati 8/11/2016 2:57 PM
Deleted: b

Figure 11. Schematic of the scleractinian coral calcifying region (modified from McConnaughey, 1989; Adkins et al., 2003) illustrating processes that are hypothesized to result in stable isotope signatures observed in corals. Calcium pumping across the cell wall establishes a pH gradient between seawater and the extracellular calcifying fluid. Within the calcifying fluid, carbon can be sourced from CO_2 that is diffusively transported across the cell wall, and/or through seawater leakage. The hydration and/or hydroxylation of CO_2 are slow reactions, particularly at low temperature and at high pH, driving disequilibrium in $\delta^{18}O$ and in clumped isotope signatures. The enzyme carbonic anhydrase will catalyze this reaction, if present and sufficiently active. At a given temperature, both HCO_3^- and CO_3^{2-} ions have distinct clumped isotope and $\delta^{18}O$ signatures, and therefore changes in extracellular calcifying fluid pH may also affect the isotopic composition of minerals, as explored through various models including the pH, surface entrapment, and interfacial models mentioned in the text. Surface kinetic and interfacial processes and properties (e.g., surface speciation,

attachment/detachment rates for isotopologues, the occurrence of defects, the nature of protein and saccharide macromolecules) also affect crystal growth and chemistry.

Page 10: [1] Deleted Revisions 7/25/16 10:32 AM

Passey

Page 10: [1] Deleted Revisions 7/25/16 10:32 AM

Passey

Page 10: [2] Deleted aradhna tripati 8/11/16 3:40 PM

W

Page 10: [2] Deleted aradhna tripati 8/11/16 3:40 PM

W

Page 10: [2] Deleted aradhna tripati 8/11/16 3:40 PM

W

Page 10: [3] Deleted aradhna tripati 8/11/16 3:40 PM

Passey et al., 20132010;

Page 10: [3] Deleted aradhna tripati 8/11/16 3:40 PM

Passey et al., 20132010;

Page 10: [4] Deleted Revisions 7/25/16 10:32 AM

R

Page 10: [4] Deleted Revisions 7/25/16 10:32 AM

R

Page 10: [4] Deleted Revisions 7/25/16 10:32 AM

R

Page 10: [4] Deleted Revisions 7/25/16 10:32 AM

R

Page 10: [4] Deleted Revisions 7/25/16 10:32 AM

R

Page 10: [5] Deleted Revisions 7/25/16 10:32 AM

0631

Page 10: [5] Deleted Revisions 7/25/16 10:32 AM

0631

Page 10: [5] Deleted Revisions 7/25/16 10:32 AM

0631

Page 10: [5] Deleted Revisions 7/25/16 10:32 AM

0631

Page 10: [5] Deleted Revisions 7/25/16 10:32 AM

0631

Page 31: [6] Deleted Revisions 7/25/16 10:32 AM

Noe, S.U., Lembke-Jene, L., and Dullo, W.C., 2008, Varying growth rates in bamboo corals: sclerochronology and radiocarbon dating of a mid-Holocene deep-water gorgonian skeleton (Keratoisis sp.: Octocorallia) from Chatham Rise (New Zealand): Facies, v. 54, p. 151-166.

O'Neil, J.R., R. N. Clayton, and T.K. Mayeda (1969), Oxygen Isotope Fractionation I Divalent Metal Carbonates, J.

Page 36: [7] Deleted aradhna tripati 8/11/16 3:36 PM

Figure 1

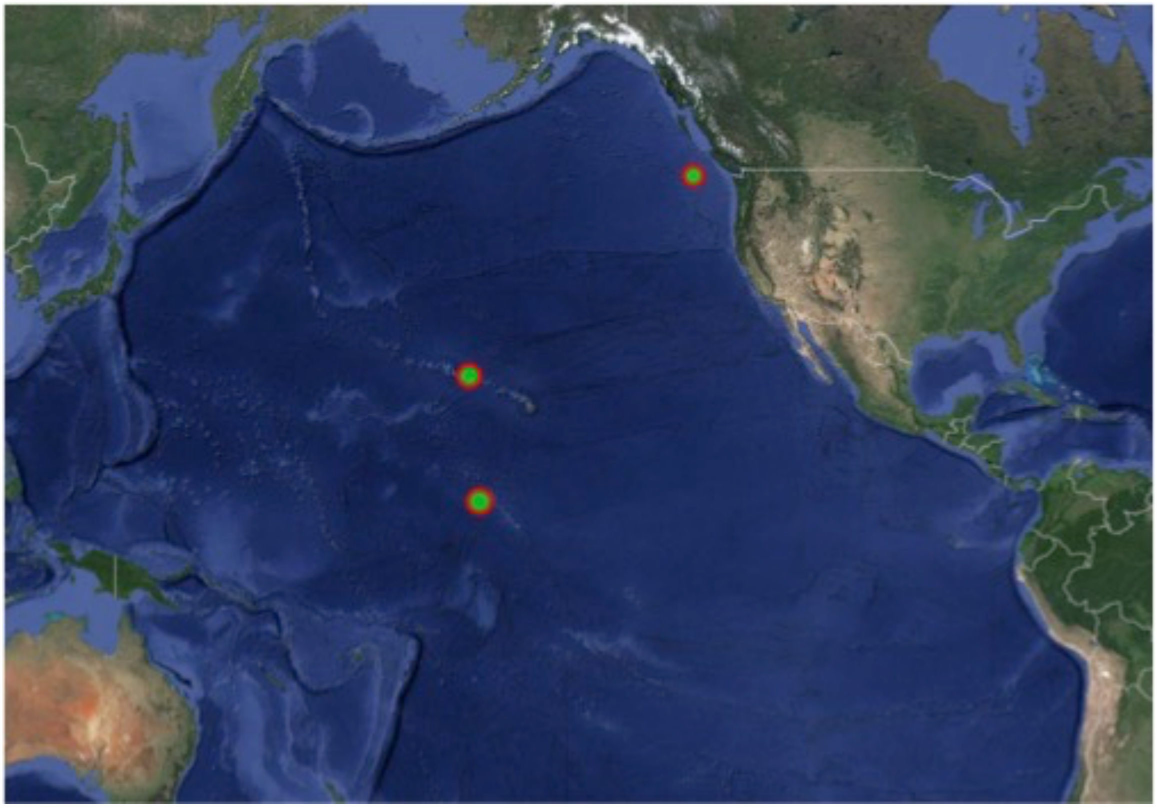

Figure 2

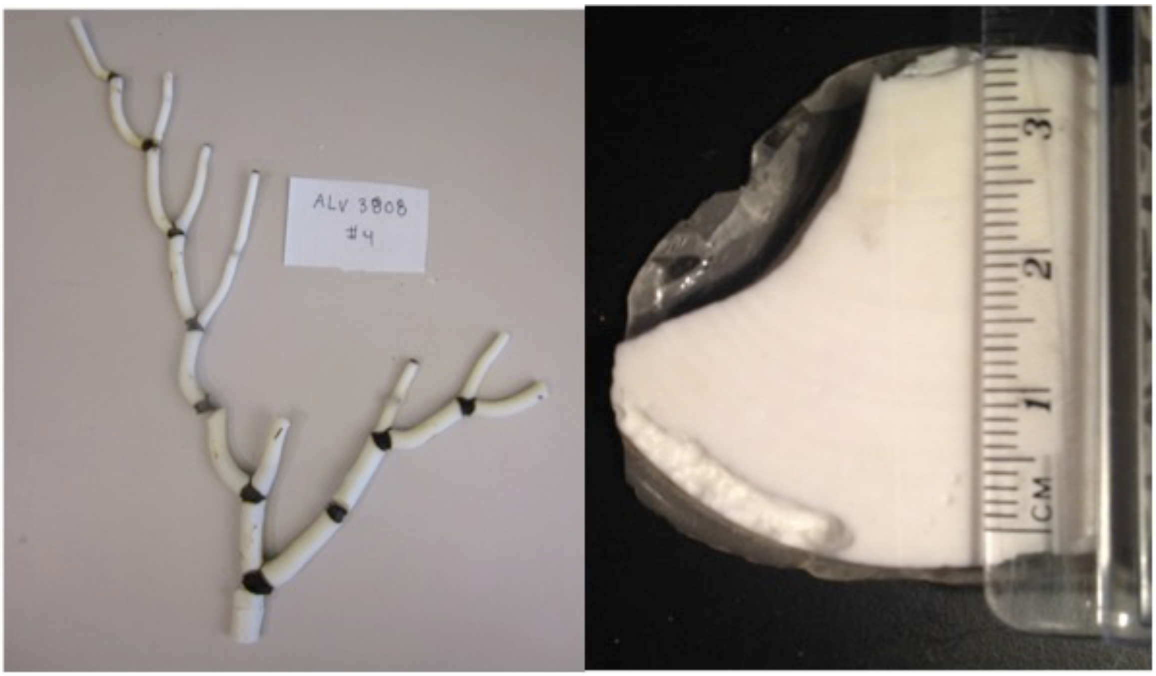

Figure 3

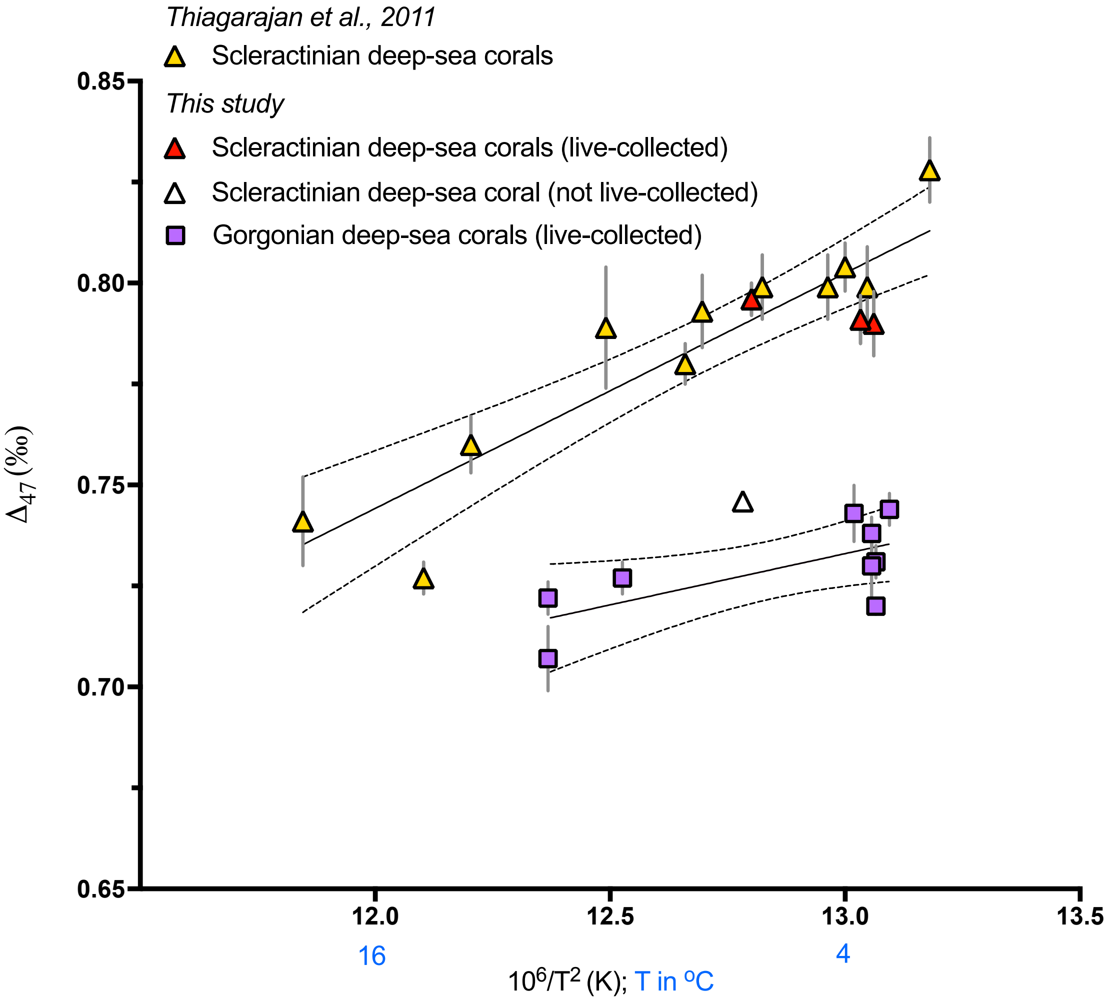
Thiagarajan et al., 2011
△ Scleractinian deep-sea corals
This study
▲ Scleractinian deep-sea corals (live-collected)
△ Scleractinian deep-sea coral (not live-collected)
■ Gorgonian deep-sea corals (live-collected)
0.85
0.80
0.75
0.70
0.65
Δ_{47} (‰)
12.0
12.5
13.0
13.5
16
4
$10^6/T^2$ (K); T in °C

Figure 4

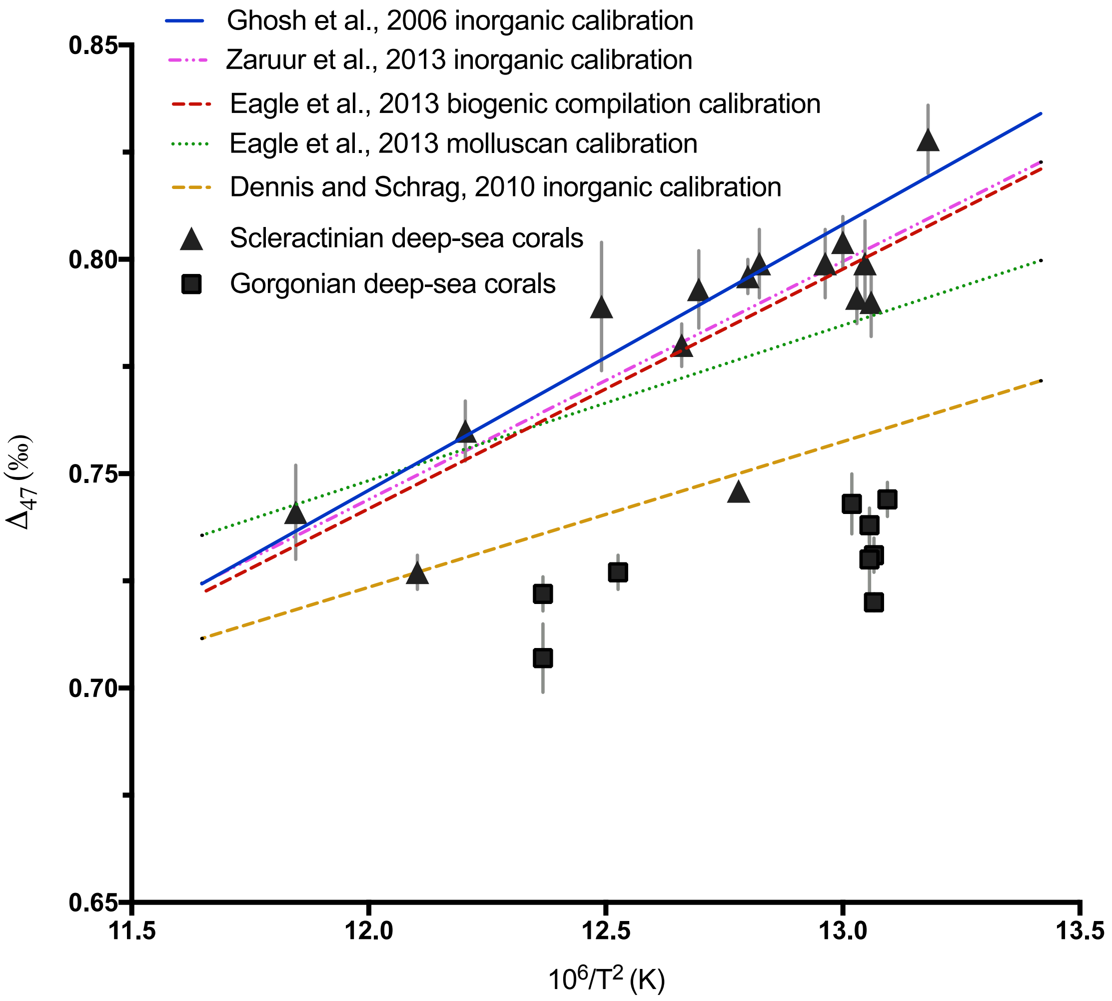
Ghosh et al., 2006 inorganic calibration
Zaruur et al., 2013 inorganic calibration
Eagle et al., 2013 biogenic compilation calibration
Eagle et al., 2013 molluscan calibration
Dennis and Schrag, 2010 inorganic calibration
Scleractinian deep-sea corals
Gorgonian deep-sea corals
Δ_{47} (‰)
0.85
0.80
0.75
0.70
0.65
11.5
12.0
12.5
13.0
13.5
$10^6/T^2$ (K)

Figure 5

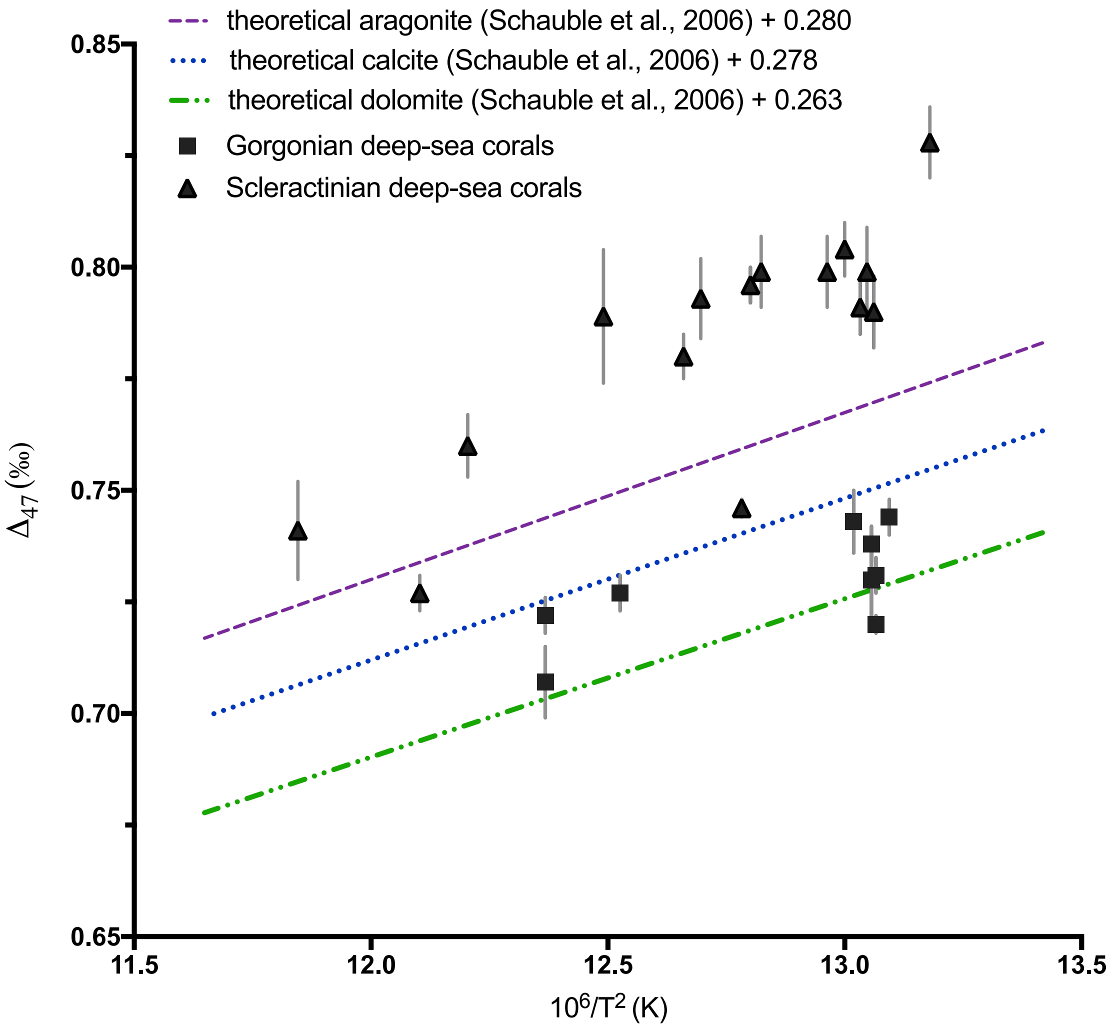
theoretical aragonite (Schauble et al., 2006) + 0.280
theoretical calcite (Schauble et al., 2006) + 0.278
theoretical dolomite (Schauble et al., 2006) + 0.263
Gorgonian deep-sea corals
Scleractinian deep-sea corals
0.85
0.80
0.75
0.70
0.65
Δ_{47} (‰)
11.5
12.0
12.5
13.0
13.5
$10^6/T^2$ (K)

Figure 6

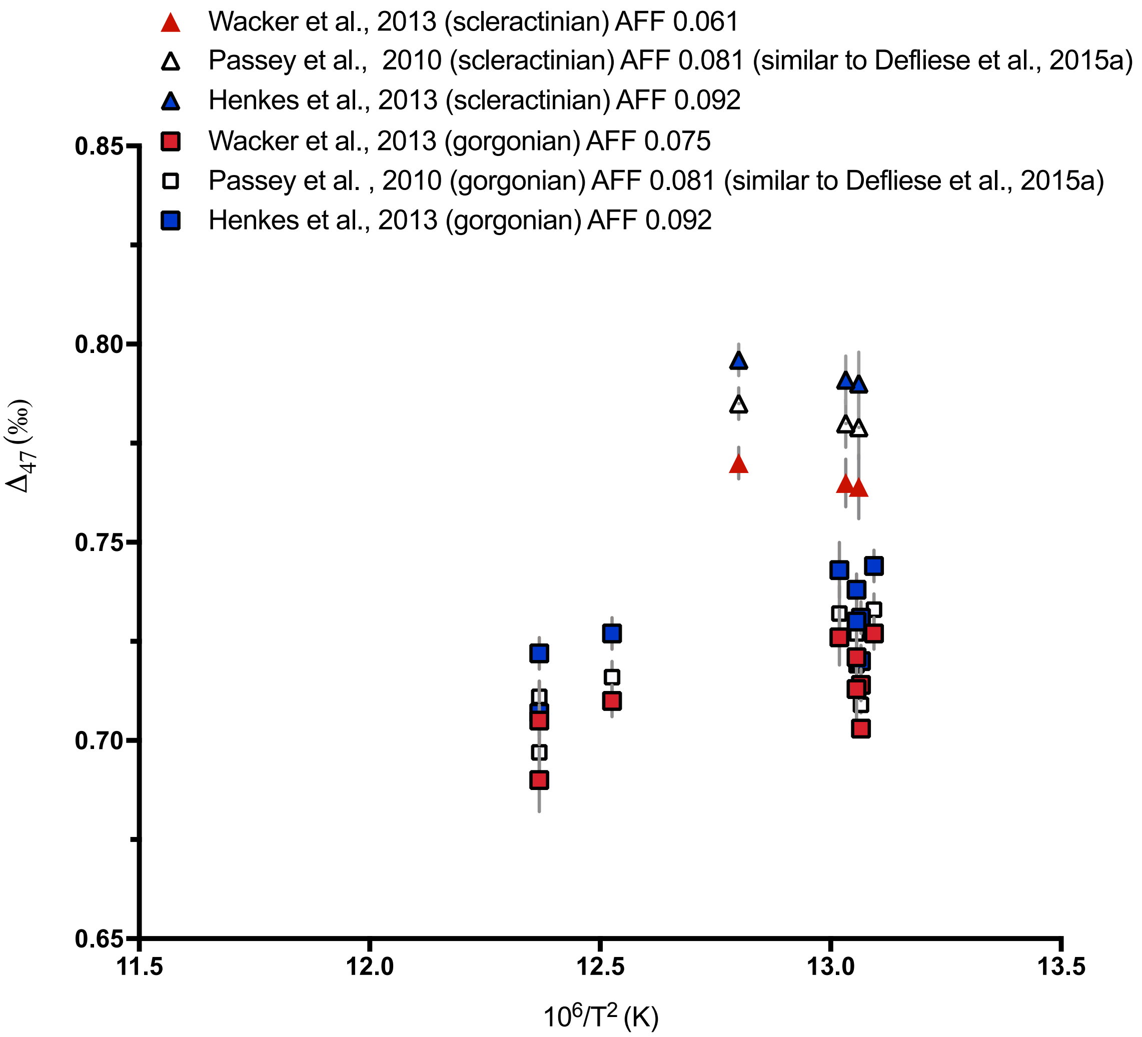
Wacker et al., 2013 (scleractinian) AFF 0.061
Passey et al., 2010 (scleractinian) AFF 0.081 (similar to Defliese et al., 2015a)
Henkes et al., 2013 (scleractinian) AFF 0.092
Wacker et al., 2013 (gorgonian) AFF 0.075
Passey et al. , 2010 (gorgonian) AFF 0.081 (similar to Defliese et al., 2015a)
Henkes et al., 2013 (gorgonian) AFF 0.092
0.85
0.80
0.75
0.70
0.65
Δ47 (‰)
11.5
12.0
12.5
13.0
13.5
10⁶/T² (K)

Figure 7

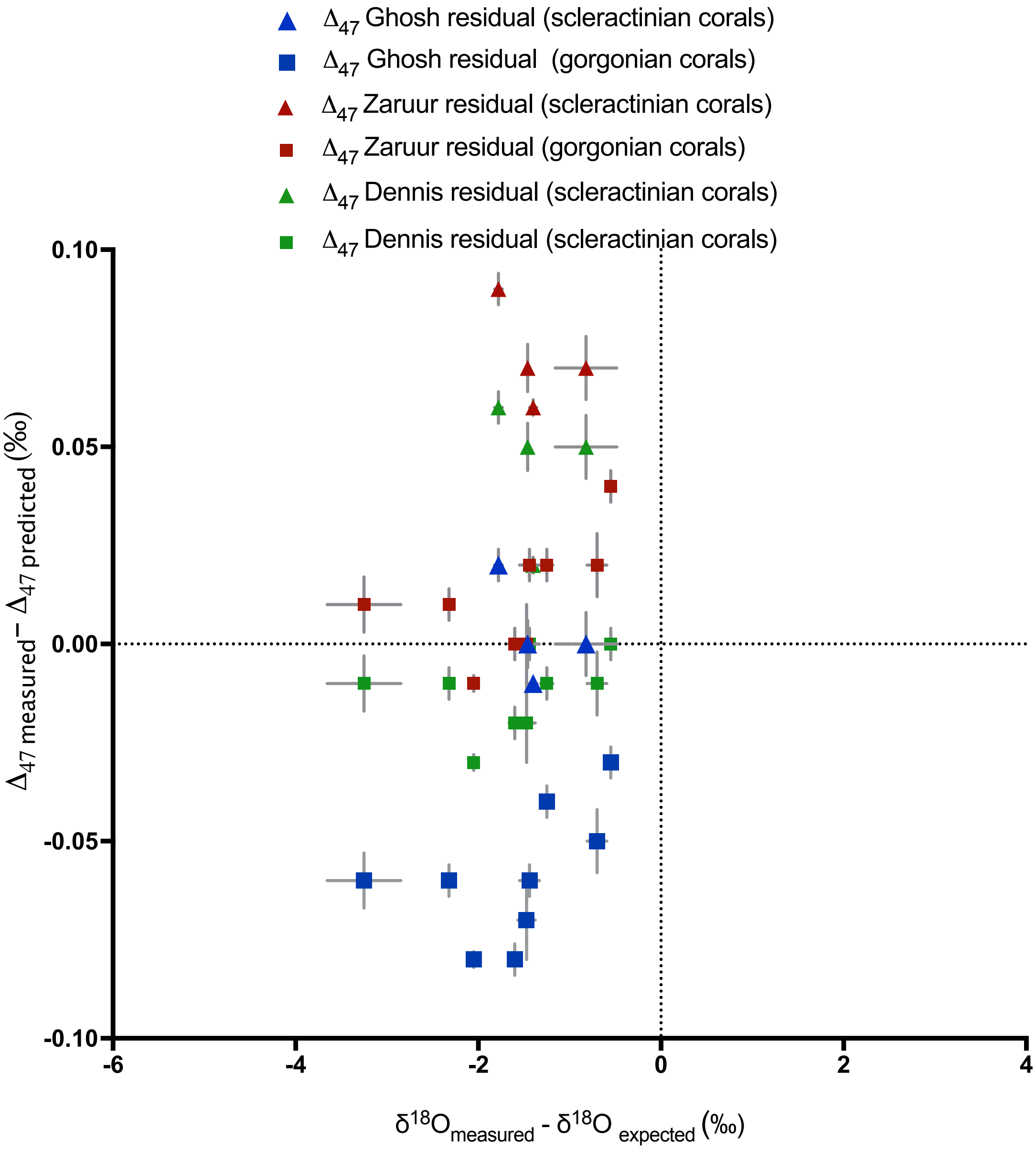

Δ47 Ghosh residual (scleractinian corals)
Δ47 Ghosh residual (gorgonian corals)
Δ47 Zaruur residual (scleractinian corals)
Δ47 Zaruur residual (gorgonian corals)
Δ47 Dennis residual (scleractinian corals)
Δ47 Dennis residual (scleractinian corals)
0.10
0.05
0.00
-0.05
-0.10
Δ47 measured− Δ47 predicted (‰)
-6
-4
-2
0
2
4
δ18Omeasured - δ18O expected (‰)

Figure 8

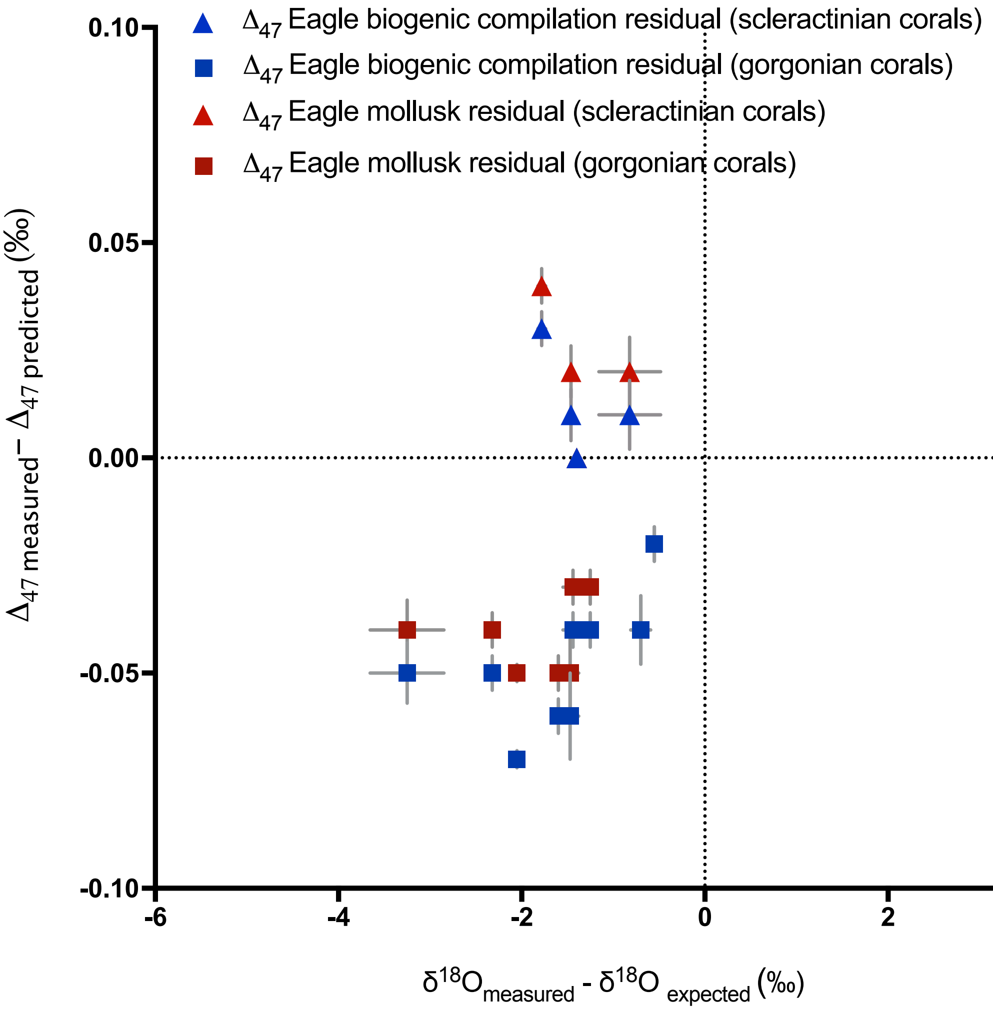
▲ Δ_{47} Eagle biogenic compilation residual (scleractinian corals)
■ Δ_{47} Eagle biogenic compilation residual (gorgonian corals)
▲ Δ_{47} Eagle mollusk residual (scleractinian corals)
■ Δ_{47} Eagle mollusk residual (gorgonian corals)
$\Delta_{47\,measured} - \Delta_{47\,predicted}$ (‰)
0.10
0.05
0.00
-0.05
-0.10
-6
-4
-2
0
2
4
$\delta^{18}O_{measured} - \delta^{18}O_{expected}$ (‰)

Figure 9

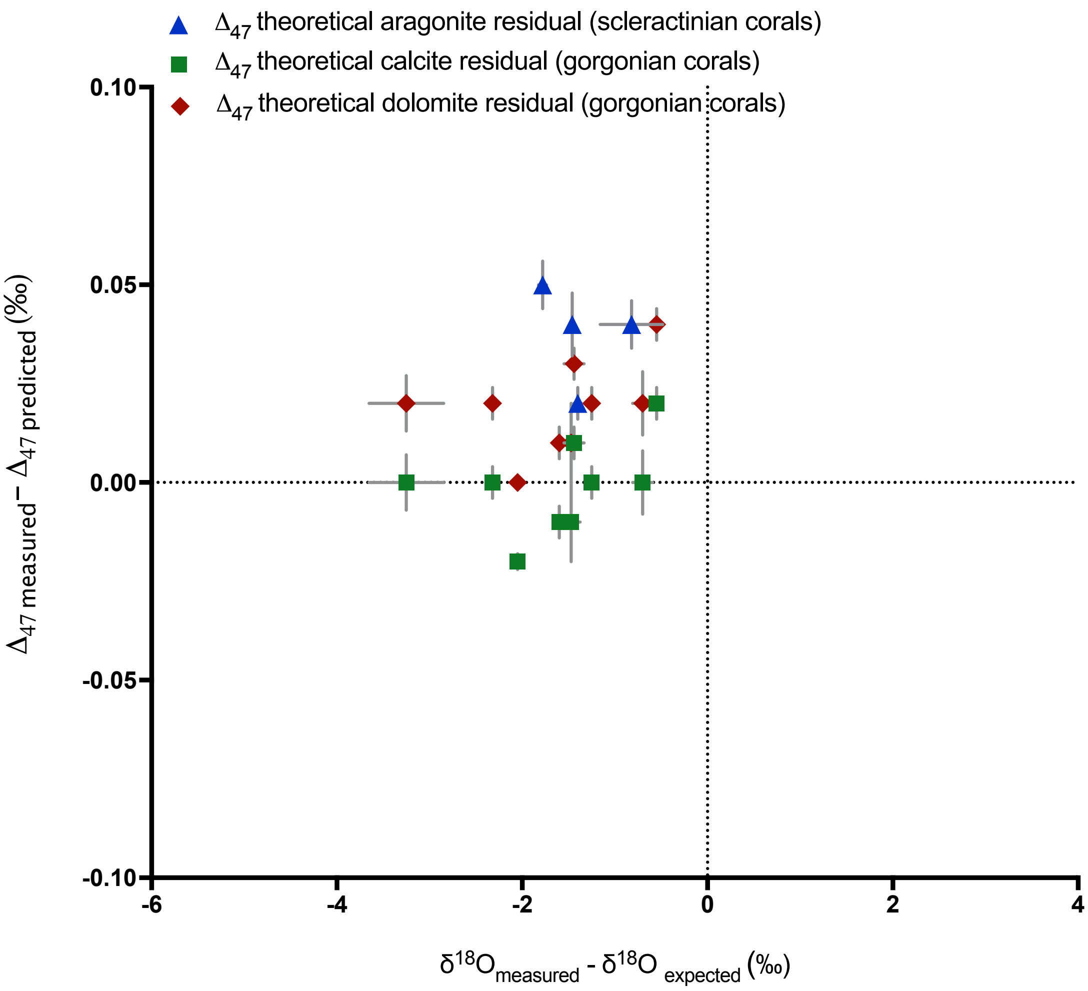

▲ Δ_{47} theoretical aragonite residual (scleractinian corals)
■ Δ_{47} theoretical calcite residual (gorgonian corals)
◆ Δ_{47} theoretical dolomite residual (gorgonian corals)
Δ_{47} measured − Δ_{47} predicted (‰)
0.10
0.05
0.00
-0.05
-0.10
-6
-4
-2
0
2
4
$\delta^{18}O_{measured}$ - $\delta^{18}O_{expected}$ (‰)

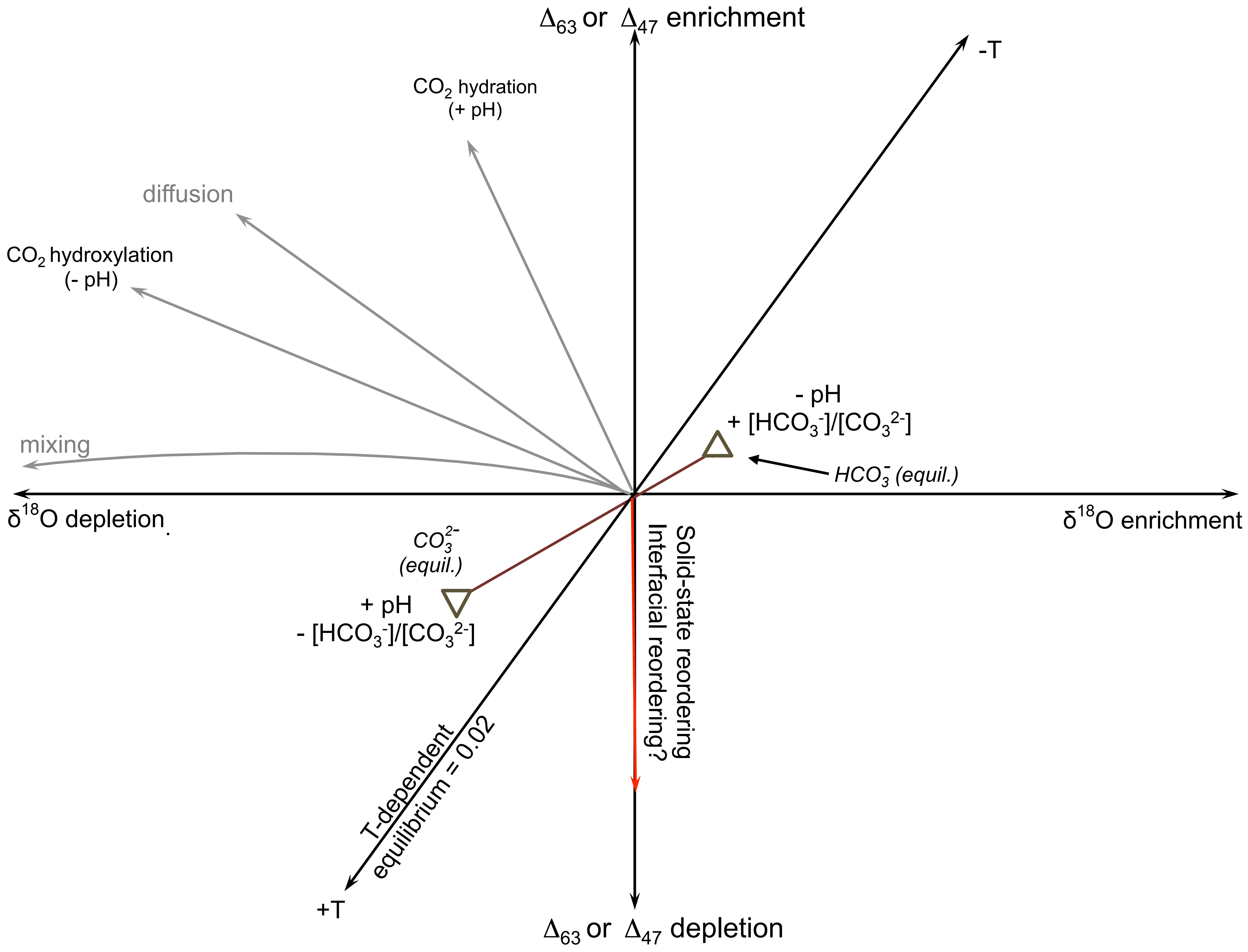

Δ_{63} or Δ_{47} enrichment
-T
CO_2 hydration
(+ pH)
diffusion
CO_2 hydroxylation
(- pH)
- pH
+ $[HCO_3^-]/[CO_3^{2-}]$
HCO_3^- (equil.)
mixing
$\delta^{18}O$ depletion
$\delta^{18}O$ enrichment
CO_3^{2-}
(equil.)
+ pH
- $[HCO_3^-]/[CO_3^{2-}]$
Solid-state reordering
Interfacial reordering?
T-dependent
equilibrium = 0.02
+T
Δ_{63} or Δ_{47} depletion

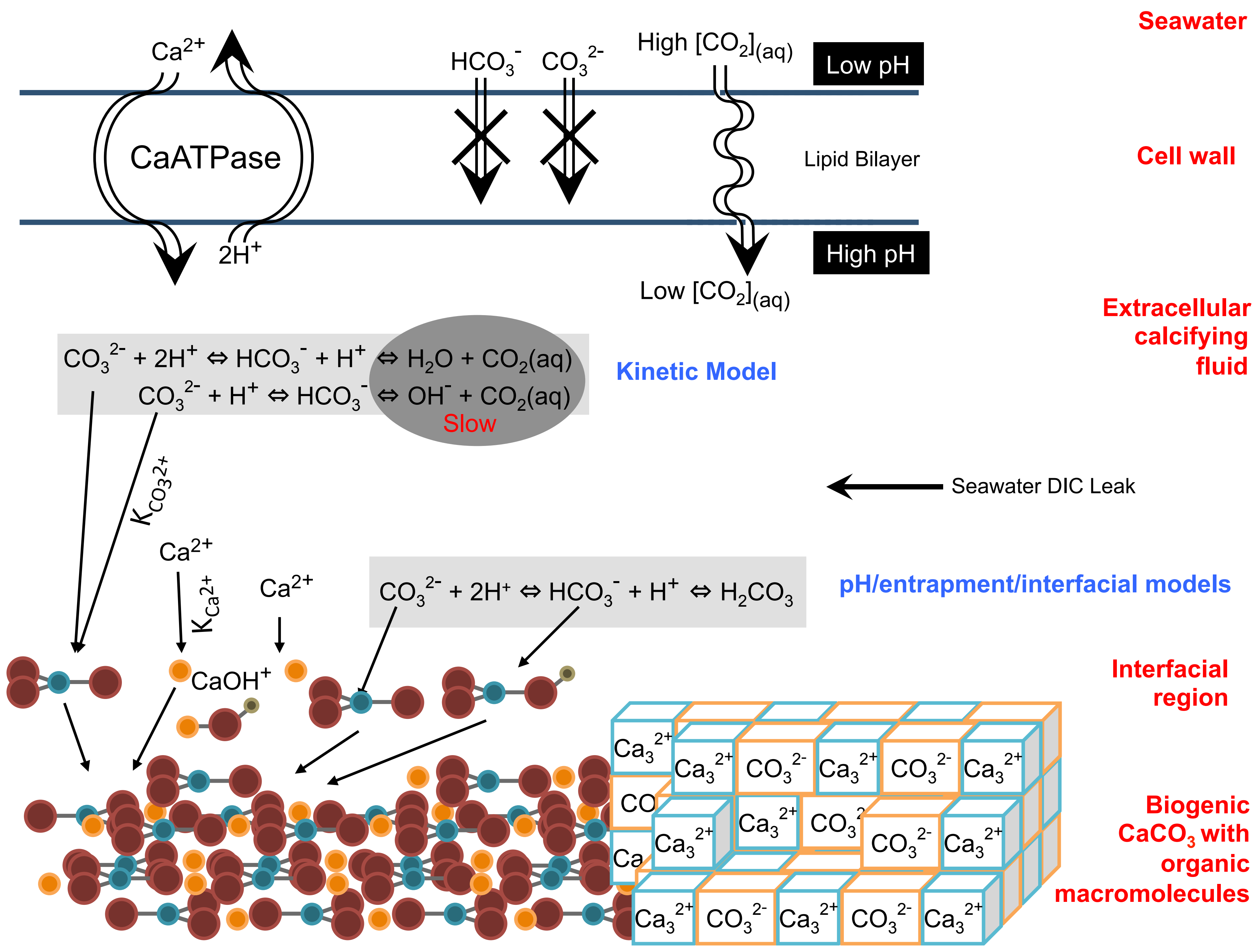
Seawater
Cell wall
Extracellular calcifying fluid
Interfacial region
Biogenic $CaCO_3$ with organic macromolecules
Ca^{2+}
CaATPase
$2H^+$
HCO_3^-
CO_3^{2-}
High $[CO_2]_{(aq)}$
Low pH
Lipid Bilayer
High pH
Low $[CO_2]_{(aq)}$
$CO_3^{2-} + 2H^+ \Leftrightarrow HCO_3^- + H^+ \Leftrightarrow H_2O + CO_2(aq)$
$CO_3^{2-} + H^+ \Leftrightarrow HCO_3^- \Leftrightarrow OH^- + CO_2(aq)$
Slow
Kinetic Model
Seawater DIC Leak
$K_{CO_3^{2+}}$
Ca^{2+}
$K_{Ca^{2+}}$
Ca^{2+}
$CO_3^{2-} + 2H^+ \Leftrightarrow HCO_3^- + H^+ \Leftrightarrow H_2CO_3$
pH/entrapment/interfacial models
$CaOH^+$
Ca_3^{2+}
CO_3^{2-}

Table 1

ID	Order	Coral	Location	Latitude	Longitude	depth (m)	T (°C)	T range (°C)
ALV 3806-1	Gorgonacea	Isididae	Warwick, AK	48°04’N	132°48’W	872	3.2	3.4±0.1
ALV 3808-1	Gorgonacea	Isididae	Warwick, AK	48°04’N	132°48’W	758	3.5	3.5±0.1
ALV 3808-3	Gorgonacea	Isididae	Warwick, AK	48°04’N	132°48’W	720	3.5	3.7±0.1
ALV 3808-4	Gorgonacea	Isididae	Warwick, AK	48°04’N	132°48’W	704	3.6	3.7±0.1
ALV 3808-5	Gorgonacea	Isididae	Warwick, AK	48°04’N	132°48’W	634	3.6	3.8±0.2
PV 703- 5	Gorgonacea	Coralliidae	Twin Banks, NWHI	23°07N	163°08W	942	4	4.2±0.1
PV 592-1	Gorgonacea	Isididae	Big Island, HI	19°48 N	156°07'W	386	9.4	10.3±0.2
PV 694-13	Gorgonacea	Isididae	East French Frigate Shoals, NWHI	23°54'N	165°23'W	356	11.2	10.6±0.6
PV 694-3	Gorgonacea	Isididae	East French Frigate Shoals, NWHI	23°54'N	165°23'W	351	11.2	11.1±0.7
PV 703-2	Scleractinia	*E.rostrata*	Twin Banks, NWHI	23°07N	163°08W	1108	3.7	3.7±0.1
PIV 146-6	Scleractinia	*E.rostrata*	Kingman Reef	06° 26.0 N	162° 27.5 W	788	4	5.5±0.2
PIV 148-2	Scleractinia	*E.rostrata*	Palmyra Atoll	05° 50.784 N	162° 06.741 W	588	6.5	6.9±0.4
PV 703-7	Scleractinia	*E.rostrata*	Twin Banks, NWHI	23°07N	163°08W	534	6.7	6.7±0.3

Table 2

ID	Order	mineral	n	δ^{13}C	δ^{18}O	Δ_{47}		
				(‰ VPDB)	(‰ VPDB)	(‰ ARF; 90°C results)	(‰ ARF; adj. 25°C[1])	(‰ ARF; adj. 25°C
ALV 3806-1	Gorgonacea	high-Mg calcite	8	-3.74 (±0.091)	0.76 (±0.109)	0.663 (±0.004)	0.744 (±0.004)	0.734 (±0.004)
ALV 3808-1	Gorgonacea	high-Mg calcite	3	-3.15 (±0.024)	0.53 (±0.064)	0.650 (±0.004)	0.731 (±0.004)	0.721 (±0.004)
ALV 3808-3	Gorgonacea	high-Mg calcite	2	-4.58 (±0.04)	0.08 (±0.025)	0.639 (±0.002)	0.720 (±0.002)	0.710 (±0.002)
ALV 3808-4	Gorgonacea	high-Mg calcite	6	-3.15 (±0.208)	0.66 (±0.095)	0.649 (±0.01)	0.730 (±0.01)	0.720 (±0.01)
ALV 3808-5	Gorgonacea	high-Mg calcite	3	-5.87 (±0.131)	-0.21 (±0.043)	0.657 (±0.004)	0.738 (±0.004)	0.728 (±0.004)
PV 703- 5	Gorgonacea	high-Mg calcite	6	-6.35(±0.543)	-1.09 (±0.345)	0.662 (±0.007)	0.743 (±0.007)	0.733 (±0.007)
PV 592-1	Gorgonacea	high-Mg calcite	2	-2.42 (±0.068)	-0.18 (±0.029)	0.646 (±0.004)	0.727 (±0.004)	0.717 (±0.004)
PV 694-13	Gorgonacea	high-Mg calcite	4	-0.71 (±0.019)	0.10 (±0.018)	0.641 (±0.004)	0.722 (±0.004)	0.712 (±0.004)
PV 694-3	Gorgonacea	high-Mg calcite	5	-4.19 (±0.108)	-0.05 (±0.154)	0.626 (±0.008)	0.707 (±0.008)	0.697 (±0.008)
PV 703-2	Scleractinia	aragonite	8	-1.91 (±0.19)	2.11 (±0.338)	0.709 (±0.008)	0.790 (±0.008)	0.780 (±0.008)
PIV 146-6	Scleractinia	aragonite	7	-2.90 (±0.166)	1.40 (±0.083)	0.710 (±0.006)	0.791 (±0.006)	0.781 (±0.006)
PIV 148-2	Scleractinia	aragonite	7	-3.90 (±0.351)	0.70 (±0.044)	0.715 (±0.004)	0.796 (±0.004)	0.786 (±0.004)
PV 703-7	Scleractinia	aragonite	3	-3.10 (±0.065)	0.40 (±0.038)	0.665 (±0.002)	0.746 (±0.002)	0.736 (±0.002)

Table 3

		Δ_{47} UCLA	Δ_{47} UCLA	Accepted Δ_{47} (Caltech)
Standard	n	(‰ ARF; adj. 25°C[1])	(‰ ARF; adj. 25°C[2])	(‰ ARF; adj. 25°C)
Cararra marble[a]	8	0.395 (±0.008)	0.385 (±0.008)	0.395
Cararra marble[b]	15	0.390 (±0.005)	0.380 (±0.005)	0.395
Carmel chalk[a]	7	0.688 (±0.004)	0.678 (±0.004)	0.697
Carmel chalk[b]	13	0.695 (±0.004)	0.685 (±0.004)	0.697
102-GC-AZ01[a]	5	0.729 (±0.004)	0.719 (±0.004)	0.713
102-GC-AZ01[b]	3	0.699 (±0.006)	0.689 (±0.006)	0.713
TV01/TV03[b]	7	0.720 (±0.007)	0.710 (±0.007)	0.713

Table 4

ID	$\delta^{18}O_{coral}$ (‰ VPDB)	$\delta^{18}O_{water}$ (‰ VPDB)[a]	$\delta^{18}O$ predicted (‰ VPDB)[b]	δ_{47} (‰ WG)[c]	Δ_{47} (‰ ARF; adj. 25°C)	Δ_{47} predicted (‰ ARF; adj. 25°C)[d]
ALV 3806-1	0.78 (±0.123)	-0.2	2.6	14.79	0.744 (±0.004)	0.833
ALV 3808-1	0.53 (±0.064)	-0.2	2.53	15.12	0.731 (±0.004)	0.831
ALV 3808-3	0.08 (±0.025)	-0.2	2.53	13.2	0.720 (±0.002)	0.831
ALV 3808-4	0.66 (±0.095)	-0.2	2.51	15.24	0.730 (±0.01)	0.831
ALV 3808-5	-0.21 (±0.043)	-0.2	2.51	11.66	0.738 (±0.004)	0.831
PV 703- 5	-1.70 (±0.165)	-0.05	2.26	10.11	0.743 (±0.007)	0.828
PV 592-1	-0.18 (±0.029)	0.1	0.87	15.1	0.727 (±0.004)	0.797
PV 694-13	0.10 (±0.018)	0.1	0.45	16.97	0.722 (±0.004)	0.786
PV 694-3	-0.05 (±0.154)	0.1	0.45	17.03	0.707 (±0.008)	0.786
PV 703-2	2.00 (±0.318)	-0.1	3.13	18	0.790 (±0.008)	0.830
PIV 146-6	1.40 (±0.083)	-0.1	3.06	16.289	0.791 (±0.006)	0.828
PIV 148-2	0.70 (±0.044)	0.1	2.28	14.62	0.796 (±0.004)	0.813
PV 703-7	0.40 (±0.038)	0.1	1.6	14.94	0.746 (±0.002)	0.796

Table 5

ID	n	δ^{13}C (‰ VPDB)	δ^{18}O (‰ VPDB)	Δ_{47} predicted (‰ ARF; adj. 25°C)[d]
PIV 146-6 (outer)	4	-2.67 (±0.161)	1.33 (±0.02)	0.796 (±0.007)
PIV 146-6 (whole)	3	-3.37 (±0.086)	1.77 (±0.042)	0.820 (±0.010)
PIV 146-6 (average)	7	-2.90 (±0.166)	1.40 (±0.083)	0.808 (±0.008)
PV 703- 5 (center)	3	-7.76 (±0.038)	-1.70 (±0.165)	0.760 (±0.010)
PV 703-5 (outer)	3	-4.95 (±0.116)	-0.47 (±0.025)	0.740 (±0.005)
PV 703-5 (average)	6	-6.35(±0.543)	-1.09 (±0.345)	0.750 (±0.007)

Supplement – Kimball et al., 2015. Biogeosciences Discussions.

Table S1: Raw data for equilibrated gases, standards, and samples.

Figure S1: Equilibrated gas lines for February 2013.

Figure S2: Equilibrated gas lines for May-July 2013.

All data collected at UCLA

Table S1

Counter	Date	Sample ID	spec #'s	d13C (PDB)	d13C stdev	d18O gas (SMOW)	d18O stdev	d47 (v. Oz)	d47 stdev	D47 (v. Oz)	D47 stdev	D47 sterror	d48 (v. Oz)	D48 (v. Oz)	D48 stdev
	02/07/12	TV01	3160	2.271	0.004	29.996	0.014	10.527	0.016	-0.149	0.011	0.004	10.687	0.930	0.132
	2/1/13	86 Breakseal heated CO2 tank	2919	-37.281	0.003	3.260	0.027	-54.485	0.042	-1.076	0.031	0.011	-44.669	-2.673	0.122
	02/02/13	102-GC-A201	2935	0.335	0.004	23.967	0.009	2.561	0.030	-0.221	0.024	0.009	-2.029	0.005	0.092
	2/2/13	69 Heated reg DI+tank CO2	2964	-28.438	0.006	24.745	0.020	-25.170	0.022	-0.942	0.022	0.008	-0.682	-0.036	0.096
	2/2/13	66 Unheated Oztech	2973	-3.863	0.018	23.614	0.024	-1.561	0.050	0.062	0.019	0.007	-2.547	0.192	0.099
	2/2/13	64 heated Oztech	2981	-3.671	0.002	22.220	0.008	-3.631	0.044	-0.809	0.041	0.015	-5.862	-0.413	0.146
	02/03/13	Carmel Chalk	3005	-2.371	0.003	34.599	0.010	10.567	0.019	-0.182	0.014	0.005	20.348	1.557	0.112
	2/3/13	Breakseal 92 heated tank	3022	-28.066	0.002	23.965	0.009	-25.550	0.036	-0.925	0.038	0.013	-2.099	0.064	0.094
high voltage bellows overcomp?	2/3/13	Breakseal 67 Oztech 25C	3030	-3.263	0.003	26.693	0.008	2.055	0.026	0.037	0.019	0.007	3.605	0.338	0.112
	2/3/13	78 reg DI +tank CO2 heated	3039	-28.013	0.004	26.854	0.009	-22.704	0.030	-0.933	0.030	0.011	3.667	0.197	0.082
D47 and D48 are high	2/6/13	79 heated tank CO2 + reg DI	3126	-28.061	0.003	27.808	0.018	-21.742	0.054	-0.848	0.043	0.015	6.496	1.158	0.327
	2/6/13	75 heated tank CO2 + reg DI	3140	-28.460	0.004	24.944	0.018	-25.020	0.039	-0.965	0.025	0.009	-0.326	-0.068	0.167
	02/08/13	102-GC-A201	3205	0.247	0.003	23.849	0.017	2.382	0.018	-0.196	0.023	0.008	-1.997	0.268	0.186
	2/8/13	98 Seawater+Oztech	3240	-3.951	0.002	34.956	0.013	9.633	0.019	0.068	0.024	0.008	21.082	1.593	0.130
	02/08/13	Fast HAGA	3254	3.044	0.002	32.861	0.008	14.117	0.035	-0.176	0.032	0.011	16.607	1.217	0.084
	02/09/13	Carmel Chalk	3262	-2.290	0.003	34.502	0.010	10.529	0.035	-0.202	0.029	0.010	20.129	1.529	0.157
	02/13/13	102-GC-AZ01	3477	0.278	0.005	23.894	0.018	2.532	0.064	-0.121	0.048	0.017	-1.649	0.529	0.190
	2/13/13	509-CO2-5.99mB-H	3497	-37.384	0.004	4.568	0.009	-53.438	0.018	-1.194	0.017	0.006	-42.476	-2.983	0.149
	2/14/13	100 Bone dry CO2 5.86 UH	3542	-37.868	0.005	2.671	0.014	-54.834	0.028	-0.259	0.026	0.009	-45.774	-2.656	0.155
	02/14/13	Carmel Chalk	3555	-2.244	0.008	34.670	0.013	10.758	0.020	-0.186	0.014	0.005	20.499	1.567	0.153
	02/15/13	Carrera Marble	3590	2.285	0.003	37.307	0.017	17.608	0.035	-0.388	0.030	0.011	25.971	1.808	0.271
	02/15/13	101 bone dry tank CO2 - heated	3611	-37.456	0.001	4.424	0.005	-53.630	0.016	-1.179	0.018	0.006	-42.784	-3.018	0.072
	02/16/13	146-6	3636	-2.832	0.004	40.636	0.013	16.252	0.043	-0.057	0.035	0.012	33.021	2.279	0.158
	2/16/13	bone dry tank CO2 - heated	3648	-37.478	0.003	3.589	0.019	-54.450	0.029	-1.176	0.034	0.012	-44.443	-3.091	0.186
	02/16/13	513 bone dry tank CO2 - heated	3648	-37.478	0.003	3.590	0.018	-54.443	0.026	-1.171	0.035	0.012	-44.436	-3.086	0.193
	2/16/13	501 Evap DI + Oz H	3656	-3.949	0.007	40.853	0.013	14.740	0.024	-0.679	0.029	0.010	33.330	2.166	0.146
	2/16/13	102 Bonedry CO2 heated	3664	-38.482	0.006	2.197	0.022	-56.741	0.035	-1.184	0.024	0.009	-47.100	-3.098	0.181
	2/16/13	TV-01	3676	2.294	0.004	30.154	0.011	10.703	0.030	-0.154	0.024	0.008	11.044	0.976	0.144
	2/17/13	103 Bonedry heated	3697	-37.467	0.007	3.826	0.024	-54.212	0.040	-1.175	0.030	0.011	-43.748	-2.836	0.152
	2/18/13	514 Bonedry CO2 6 mB - UH	3762	-37.547	0.002	3.019	0.006	-54.195	0.026	-0.259	0.025	0.009	-45.090	-2.634	0.044
	2/18/13	106 Bonedry CO2 5.55 mB H	3770	-37.311	0.007	3.378	0.009	-54.462	0.030	-1.141	0.021	0.007	-44.639	-2.877	0.252
	2/18/13	694-3	3778	-1.129	0.002	38.977	0.009	16.186	0.036	-0.139	0.029	0.010	29.507	2.052	0.132
GC column changed	2/19/13	Antartic Mollusc	3786	1.737	0.003	43.283	0.007	23.422	0.025	-0.017	0.024	0.008	38.687	2.655	0.186
GC column changed	2/19/13	Antartic Mollusc	3786	1.737	0.003	43.283	0.007	23.422	0.025	-0.017	0.024	0.008	38.687	2.655	0.186
	02/19/13	108 Bonedry CO2 5.5 mB UH	3797	-37.060	0.002	3.117	0.014	-53.599	0.030	-0.215	0.027	0.010	-44.684	-2.407	0.206
	2/20/13	Spel-2-8E	3805	-9.571	0.003	32.409	0.005	1.300	0.034	-0.260	0.032	0.011	15.935	1.486	0.076
	02/20/13	102-GC-AZ01	3813	0.443	0.002	23.759	0.008	2.490	0.025	-0.187	0.025	0.009	-2.315	0.123	0.149

	02/20/13	90 CO2 tank 6.11 mB H	3821	-28.194	0.003	24.274	0.006	-25.437	0.026	-0.989	0.020	0.007	-1.723	-0.160	0.124
	2/20/13	3808-4	3831	-2.907	0.003	40.032	0.004	15.499	0.032	-0.133	0.028	0.010	31.761	2.219	0.086
	2/20/13	Antarctic Mollusc	3839	1.774	0.003	43.241	0.012	23.421	0.046	-0.014	0.040	0.014	38.774	2.818	0.096
	2/20/13	Antarctic Mollusc	3839	1.774	0.003	43.241	0.012	23.421	0.046	-0.014	0.040	0.014	38.774	2.818	0.096
	2/21/13	516 Oz+Evap DI H	3847	-3.683	0.002	42.620	0.008	16.722	0.032	-0.713	0.025	0.009	36.839	2.166	0.182
	2/21/13	146-6	3855	-2.663	0.004	40.600	0.010	16.367	0.032	-0.072	0.027	0.010	32.925	2.254	0.200
	2/21/13	148-2	3863	-2.409	0.004	40.257	0.009	16.307	0.024	-0.040	0.022	0.008	32.179	2.190	0.098
	2/21/13	110 Evap DI+oz UH	3872	-3.600	0.005	44.962	0.011	19.955	0.032	0.095	0.024	0.008	42.209	2.851	0.135
	2/21/13	518 Bonedry UH	3882	-37.295	0.003	3.233	0.012	-53.723	0.017	-0.229	0.017	0.006	-44.582	-2.529	0.126
	2/21/13	519 Bonedry UH	3891	-37.340	0.003	3.403	0.007	-53.645	0.022	-0.276	0.030	0.011	-44.352	-2.627	0.124
	2/22/13	592-1	3916	-2.390	0.003	39.210	0.006	15.203	0.028	-0.119	0.025	0.009	30.210	2.292	0.158
	2/22/13	3808-4	3924	-2.914	0.004	40.120	0.022	15.622	0.027	-0.092	0.024	0.008	32.191	2.467	0.166
	2/22/13	520 CO2 bonedry UH	3933	-37.709	0.003	3.227	0.018	-47.380	0.037	-0.227	0.095	0.034	-44.620	-2.236	0.911
	2/22/13	109 Oz+Evap DI H	3941	-3.834	0.002	42.474	0.007	16.419	0.016	-0.723	0.016	0.006	36.519	2.137	0.094
	2/22/13	522 CO2 Heated	3952	-37.790	0.005	4.074	0.009	-54.207	0.030	-1.100	0.034	0.012	-42.845	-2.386	0.158
	2/22/13	Carrera Marble	3961	2.193	0.002	36.988	0.006	17.196	0.019	-0.390	0.018	0.006	25.395	1.863	0.105
	2/23/13	703-2	3969	-1.873	0.009	41.513	0.015	18.100	0.039	-0.024	0.041	0.014	35.081	2.585	0.153
	2/23/13	502 CO2 tank Heated	3988	-37.459	0.002	4.289	0.011	-53.765	0.028	-1.182	0.032	0.011	-42.898	-2.869	0.088
	2/23/13	115 Oz+Evap DI UH	3999	-3.913	0.002	47.415	0.004	22.174	0.040	0.181	0.039	0.014	47.467	3.201	0.111
changed acid	2/23/13	TV01	4007	2.464	0.004	30.063	0.006	10.774	0.023	-0.157	0.019	0.007	10.794	0.905	0.087
	02/23/13	Spel 2-8-E	4016	-9.518	0.002	32.299	0.006	1.263	0.027	-0.240	0.024	0.008	15.491	1.261	0.117
	2/24/13	703-5 outer	4032	-4.759	0.004	38.879	0.009	12.528	0.039	-0.143	0.031	0.011	29.152	1.910	0.126
	2/24/13	3808-5	4040	-5.606	0.003	39.128	0.008	11.957	0.022	-0.132	0.023	0.008	29.765	2.030	0.125
	2/24/13	3806-1	4048	-4.139	0.002	39.669	0.007	13.932	0.033	-0.132	0.034	0.012	30.987	2.170	0.117
47 (neg. T) same as last Oz+Eva	2/24/13	114 Oz + Evap heated	4057	-3.748	0.003	48.058	0.008	23.002	0.032	0.206	0.031	0.011	49.165	3.596	0.175
	02/24/13	Carrera Marble	4065	2.239	0.003	36.980	0.008	17.192	0.026	-0.431	0.022	0.008	25.234	1.720	0.129
	2/24/13	3803-3	4074	-4.619	0.004	39.383	0.006	13.169	0.026	-0.140	0.026	0.009	30.395	2.148	0.114
	2/25/13	Carrera Marble	4110	2.282	0.002	36.930	0.010	17.179	0.023	-0.436	0.023	0.008	24.937	1.527	0.144
	2/25/13	523	4127	-37.387	0.004	4.131	0.015	-53.818	0.010	-1.150	0.023	0.008	-43.073	-2.738	0.151
	02/26/13	102-GC-AZ01	4143	0.436	0.004	23.829	0.018	2.543	0.034	-0.198	0.037	0.013	-1.750	0.553	0.101
	2/26/13	524-tank-heated	4159	-37.277	0.002	4.588	0.003	-53.312	0.027	-1.189	0.029	0.010	-42.233	-2.771	0.196
changed acid	2/26/13	Fast HAGA	4168	3.068	0.002	32.765	0.004	14.047	0.020	-0.174	0.022	0.008	16.384	1.184	0.118
	2/26/13	Carmel Chalk	4176	-2.155	0.002	34.640	0.008	10.810	0.022	-0.191	0.024	0.009	20.319	1.448	0.181
	2/26/13	703-5 outer	4184	-4.923	0.003	38.834	0.006	12.339	0.044	-0.128	0.046	0.016	29.173	2.017	0.075
	2/27/13	116-Oz+Evap-5.7mB-U	4221	-3.616	0.004	48.473	0.005	23.512	0.019	0.172	0.022	0.008	49.576	3.194	0.068
*only 7 acquisitions	2/27/13	526 CO2 5.54 mB UH	4231	-32.547	13.356	7.392	11.976	-39.468	24.558	-0.222	0.093	0.033	-35.971	-1.752	1.730
	02/28/13	TV01	4241	2.468	0.002	30.095	0.004	10.804	0.022	-0.164	0.020	0.007	10.863	0.911	0.137
	2/28/13	112 Evap DI + Oz 5.91 mB UH	4266	-3.648	0.003	48.587	0.006	23.598	0.024	0.178	0.022	0.008	49.813	3.204	0.089
	2/28/13	118 Bonedry CO2 5.97 UH	4275	-37.415	0.006	3.076	0.015	-53.939	0.022	-0.179	0.024	0.008	-44.623	-2.261	0.437

	2/28/13	Antarctic mollusc	4285	1.750	0.003	43.257	0.003	23.385	0.030	-0.040	0.030	0.011	38.497	2.521	0.138
	03/01/13	47407 coral	4293	-1.976	0.003	41.513	0.010	17.978	0.019	-0.044	0.018	0.006	34.749	2.264	0.098
	3/1/13	703-2	4301	-2.056	0.002	41.435	0.014	17.838	0.029	-0.029	0.032	0.011	34.712	2.377	0.091
*only 7 acquisitions!	3/1/13	705-3 inner	4309	-7.683	0.002	37.877	0.014	7.586	0.021	-0.126	0.053	0.019	27.106	1.629	0.669
	3/1/13	533 Evap DI + Oz UH 6.02 mB	4317	-4.397	0.003	44.413	0.004	18.692	0.026	0.161	0.026	0.009	40.912	2.658	0.084
	3/1/13	CM	4325	2.247	0.002	36.967	0.009	17.157	0.028	-0.460	0.027	0.010	25.083	1.597	0.112
	3/1/13	534 Evap DI+Oz UH 5.86mB	4334	-3.756	0.003	44.458	0.006	19.384	0.021	0.177	0.021	0.007	41.201	2.847	0.045
changed acid	3/1/13	102-GC-AZOL	4343	0.550	0.003	23.955	0.009	2.787	0.034	-0.189	0.032	0.011	-1.816	0.242	0.236
	3/2/13	spel-2-8-E	4351	-9.775	0.003	32.372	0.010	1.081	0.009	-0.244	0.011	0.004	15.704	1.331	0.108
	3/2/13	592-1	4367	-2.448	0.006	39.069	0.009	14.997	0.026	-0.128	0.023	0.008	29.884	2.246	0.680
V too low??/7 acquisitions	3/2/13	535 Evap DI+Oz UH 5.51 mB	4375	-3.444	0.002	43.420	0.010	16.340	0.042	0.168	0.077	0.027	39.225	2.567	1.045
	3/2/13	123 Bonedry UH 6.21mB	4383	-37.533	0.003	3.576	0.010	-53.721	0.021	-0.338	0.024	0.008	-44.141	-2.750	0.055
	3/2/13	148-2	4392	-2.724	0.002	40.131	0.003	15.842	0.032	-0.070	0.029	0.010	31.741	2.008	0.094
	3/2/13	146-6	4400	-2.511	0.004	40.606	0.009	16.555	0.016	-0.039	0.016	0.006	32.968	2.283	0.116
	3/3/13	Carmel Chalk	4408	-2.157	0.003	34.656	0.005	10.818	0.027	-0.197	0.027	0.009	20.371	1.466	0.081
	3/3/13	703-5 outer	4426	-5.160	0.003	38.788	0.008	12.057	0.032	-0.131	0.029	0.010	28.965	1.905	0.109
	3/3/13	3804-4	4444	-2.982	0.002	40.003	0.010	15.419	0.026	-0.112	0.028	0.010	31.658	2.174	0.160
	3/3/13	CM	4453	2.206	0.004	37.046	0.012	17.222	0.030	-0.434	0.027	0.010	25.365	1.720	0.149
	3/4/13	3808-1	4462	-3.198	0.003	39.745	0.012	14.935	0.029	-0.127	0.032	0.011	31.221	2.249	0.164
	3/4/13	3808-5	4471	-6.013	0.003	39.026	0.012	11.461	0.029	-0.128	0.023	0.008	29.578	2.048	0.135
	3/4/13	Carrer Marble	4480	2.163	0.003	36.911	0.015	17.055	0.024	-0.425	0.025	0.009	25.205	1.827	0.172
	3/4/13	119 Bonedry UH	4489	-37.327	0.003	3.672	0.010	-53.338	0.036	-0.237	0.034	0.012	-44.017	-2.812	0.095
	3/4/13	120 Bonedry H	4498	-37.738	0.002	3.811	0.007	-54.368	0.025	-1.055	0.025	0.009	-43.308	-2.347	0.122
	03/04/13	125 Evap DI Oztech UH	4510	-13.785	0.003	32.252	0.007	-2.596	0.029	0.101	0.035	0.012	15.529	1.410	0.136
	3/5/13	527 tank CO2 - Unheated	4526	-37.519	0.003	2.456	0.008	-54.713	0.022	-0.262	0.021	0.007	-46.330	-2.811	0.225
	3/6/13	SPEL-28-E	4545	-9.068	0.003	32.378	0.009	1.793	0.023	-0.226	0.024	0.008	15.557	1.171	0.196
	3/6/13	3808-4 1	4553	-2.955	0.005	40.296	0.018	15.767	0.033	-0.083	0.029	0.010	32.307	2.241	0.187
Sample mislabeled as 538 in Aq.	3/6/13	528-CO2-5.42mB-U	4566	-37.501	0.004	3.099	0.020	-54.081	0.040	-0.265	0.034	0.012	-44.963	-2.660	0.150
	3/6/13	536-Evap+Oz-5.39mB-U	4575	-3.042	0.005	43.663	0.009	19.312	0.026	0.192	0.025	0.009	39.907	3.123	0.126
	3/6/13	3808-1	4584	-3.120	0.004	39.930	0.013	15.210	0.023	-0.113	0.016	0.006	31.588	2.248	0.151
	3/7/13	carmel chalk	4600	-2.151	0.003	34.691	0.020	10.863	0.039	-0.192	0.044	0.015	20.482	1.509	0.128
	3/7/13	539-Evap DI Oz-6.15-H	4614	-28.125	0.003	38.084	0.019	-11.887	0.028	-0.903	0.026	0.009	27.407	1.846	0.183
	3/7/13	703-5 inner	4624	-7.780	0.004	37.495	0.009	8.184	0.034	-0.157	0.037	0.013	26.377	1.886	0.168
	3/7/13	703-5 inner	4632	-7.807	0.005	37.291	0.023	7.971	0.022	-0.141	0.031	0.011	26.164	2.074	0.143
	3/7/13	3803-4	4641	-4.186	0.005	39.568	0.016	13.763	0.043	-0.154	0.032	0.011	30.628	2.016	0.130
	3/8/13	CM	4649	2.224	0.005	37.039	0.012	17.223	0.018	-0.444	0.021	0.008	25.248	1.620	0.151
	3/8/13	3808-1	4657	-3.136	0.007	39.956	0.020	15.214	0.015	-0.119	0.015	0.005	31.712	2.318	0.135
	3/8/13	3806-1	4666	-4.026	0.006	39.615	0.020	14.012	0.036	-0.109	0.022	0.008	31.072	2.358	0.184
	3/8/13	3806-1	4666	-4.026	0.006	39.615	0.020	14.012	0.036	-0.109	0.022	0.008	31.072	2.358	0.184

	3/8/13	703-2	4674	-3.055	0.013	40.006	0.013	15.441	0.025	-0.023	0.025	0.009	32.138	2.635	0.171
	3/8/13	542 Evap DI + Oz 5.8- UH	4683	-28.243	0.005	40.216	0.012	-9.134	0.032	-0.097	0.025	0.009	31.947	2.158	0.078
	3/9/13	CM	4699	2.306	0.008	37.128	0.026	17.392	0.037	-0.445	0.025	0.009	25.561	1.753	0.111
7 acquisitions	3/9/13	545 Evap DI UH 4719	4719	-3.661	0.003	45.889	0.005	18.313	0.025	0.180	0.075	0.027	44.048	2.488	1.010
	3/10/13	Carmel Chalk	4740	-2.160	0.003	34.705	0.008	10.891	0.027	-0.170	0.022	0.008	20.533	1.531	0.167
	3/10/13	533-tank CO2-5.65mB-H	4749	-37.398	0.005	3.780	0.014	-54.177	0.021	-1.161	0.023	0.008	-43.883	-2.886	0.170
	3/10/13	544-Evap DI+Oz-6.32mB-UH	4758	-3.649	0.004	45.917	0.005	20.952	0.024	0.188	0.021	0.007	44.053	2.793	0.098
	3/10/13	540-Evap DI+Oz-6.97mB-H	4767	-27.936	0.004	40.123	0.008	-9.712	0.021	-0.893	0.015	0.005	31.304	1.709	0.136
	03/11/13	542-Evap DIoz-6.52mB-UH	4789	-4.021	0.006	46.413	0.013	21.074	0.032	0.183	0.018	0.006	45.122	2.871	0.058
	3/11/13	543-Evap DIoz-6.33mB-UH	4798	-3.636	0.003	46.152	0.009	21.222	0.015	0.211	0.016	0.006	44.547	2.817	0.098
	5/19/13	SPEL-2-8-E	7205	-9.672	0.007	32.512	0.012	1.230	0.018	-0.333	0.017	0.006	16.254	1.602	0.235
	5/19/13	596 Evap DI oz 6.37mB UH	7215	-4.173	0.003	46.394	0.007	20.849	0.032	0.130	0.031	0.011	45.409	3.184	0.088
	5/20/13	579 Evap DI oz UH	7264	-4.081	0.006	45.408	0.021	20.041	0.033	0.208	0.018	0.006	43.947	3.669	0.278
	5/20/13	Carmel Chalk	7272	-2.150	0.007	34.801	0.016	10.893	0.039	-0.271	0.027	0.010	20.793	1.601	0.115
	5/21/13	CM	7306	2.340	0.027	37.114	0.037	17.335	0.062	-0.519	0.025	0.009	25.803	2.017	0.155
	5/21/13	598 bonedry 6.7mB uh	7343	-37.430	0.002	3.539	0.009	-53.672	0.029	-0.352	0.025	0.009	-44.390	-2.936	0.071
	5/22/13	Carmel Chalk	7351	-2.174	0.009	34.743	0.016	10.816	0.031	-0.267	0.031	0.011	20.543	1.468	0.143
	5/23/13	Carmel Chalk	7416	-2.491	0.002	34.881	0.012	10.634	0.026	-0.278	0.025	0.009	20.921	1.573	0.136
	5/23/13	603 Evap DI ox 6.1mB UH	7456	-3.839	0.004	46.620	0.007	21.449	0.022	0.175	0.021	0.007	46.044	3.360	0.103
	5/24/13	CM	7465	2.288	0.005	37.170	0.011	17.359	0.029	-0.500	0.024	0.009	25.679	1.788	0.182
	5/24/13	Carmel Chalk	7473	-2.200	0.004	34.811	0.011	10.866	0.021	-0.261	0.016	0.006	20.779	1.567	0.159
	5/28/13	CM	7683	2.329	0.005	37.120	0.012	17.332	0.028	-0.518	0.019	0.007	25.533	1.741	0.126
	5/30/13	601 Bonedry 5.82mB UH	7754	-37.640	0.008	2.906	0.011	-54.452	0.031	-0.322	0.033	0.012	-45.502	-2.840	0.289
	5/30/13	CM	7762	2.266	0.002	37.128	0.009	17.275	0.025	-0.521	0.024	0.008	25.753	1.942	0.155
	5/31/13	614 Evap + Oz 6.46 mB - H	7798	-3.794	0.003	45.417	0.009	19.333	0.019	-0.772	0.019	0.007	43.063	2.801	0.119
	6/1/13	616 Bonedry 6.35 mB Heated	7830	-37.531	0.003	4.095	0.012	-54.115	0.031	-1.283	0.029	0.010	-43.941	-3.571	0.123
	6/2/13	611 bonedry ?mB UH	7860	-37.490	0.002	3.241	0.007	-54.041	0.028	-0.378	0.030	0.011	-45.264	-3.258	0.132
	6/3/13	609Bone6.11UH	7918	-37.605	0.003	3.332	0.009	-54.053	0.017	-0.369	0.020	0.007	-44.925	-3.082	0.190
	6/4/13	CM	7976	2.314	0.002	37.129	0.009	17.328	0.022	-0.516	0.020	0.007	25.710	1.898	0.127
	6/5/13	Bonedry 6.51mB-H	8049	-37.511	0.003	4.096	0.010	-54.110	0.030	-1.297	0.022	0.008	-44.104	-3.742	0.139
	6/6/13	168 Evap DI Oz 6.58 mB H	8060	-3.698	0.002	45.367	0.003	19.369	0.025	-0.780	0.021	0.007	43.021	2.856	0.119
	6/6/13	Carmel Chalk	8078	-2.185	0.003	34.699	0.010	10.747	0.027	-0.283	0.028	0.010	20.548	1.557	0.100
	6/6/13	Carmel Chalk	8087	-2.136	0.002	34.725	0.007	10.807	0.027	-0.296	0.024	0.009	20.533	1.492	0.120
	6/7/13	CM	8095	2.295	0.004	37.097	0.008	17.263	0.033	-0.530	0.030	0.011	25.430	1.686	0.113
	6/8/13	617 Bonedry 6.11mB UH	8146	-37.783	0.004	3.505	0.010	-54.064	0.027	-0.378	0.029	0.010	-44.810	-3.306	0.070
	6/9/13	CM	8231	2.329	0.014	37.020	0.030	17.244	0.057	-0.506	0.021	0.007	25.261	1.669	0.080
	6/10/13	172 Bonedry - 6.41 mB - H	8260	-37.595	0.002	3.761	0.008	-54.483	0.026	-1.270	0.025	0.009	-44.877	-3.885	0.193
Acid change (2 dummy run prior)	6/10/13	TV03	8271	3.390	0.002	30.286	0.005	11.802	0.023	-0.251	0.019	0.007	11.049	0.721	0.121
	6/11/13	TV01	8312	2.471	0.002	30.246	0.007	10.867	0.027	-0.253	0.028	0.010	11.022	0.775	0.120
	6/11/13	703-2	8347	-1.401	0.007	42.295	0.006	19.244	0.025	-0.121	0.024	0.008	36.858	2.800	0.056

6/12/13	CM	8355	2.329	0.002	37.146	0.008	17.356	0.030	-0.519	0.029	0.010	25.574	1.732	0.114
6/12/13	694-3	8363	-0.352	0.002	39.471	0.006	17.398	0.030	-0.181	0.025	0.009	30.702	2.259	0.123
6/12/13	148-2	8371	-4.183	0.004	39.873	0.012	14.099	0.017	-0.125	0.019	0.007	31.573	2.347	0.112
6/12/13	Bonedry 6.12 UH	8380	-37.590	0.002	3.089	0.008	-54.292	0.024	-0.390	0.025	0.009	-45.718	-3.430	0.125
6/12/13	CM	8391	2.314	0.003	37.156	0.005	17.371	0.034	-0.500	0.038	0.013	25.541	1.680	0.123
6/12/13	694-3	8407	-0.394	0.004	39.452	0.007	17.337	0.026	-0.181	0.021	0.008	30.591	2.188	0.094
6/13/13	TV01	8431	2.441	0.024	30.187	0.044	10.798	0.078	-0.234	0.018	0.006	10.998	0.868	0.140
6/13/13	148-2	8440	-4.440	0.002	40.170	0.005	14.158	0.027	-0.109	0.023	0.008	32.139	2.327	0.146
6/13/13	3806-1	8451	-3.470	0.003	40.384	0.006	15.260	0.033	-0.170	0.029	0.010	32.615	2.373	0.147
6/13/13	TV01	8467	2.585	0.001	30.238	0.007	10.965	0.033	-0.258	0.029	0.010	11.015	0.782	0.086
6/13/13	703-2	8475	-1.423	0.002	42.345	0.005	19.290	0.025	-0.105	0.022	0.008	36.941	2.782	0.105
6/14/13	148-2	8491	-4.685	0.002	40.034	0.008	13.754	0.038	-0.137	0.036	0.013	31.909	2.367	0.146
6/14/13	169 Bonedry - 6.15 mB - H	8502	-37.446	0.004	4.229	0.008	-53.899	0.033	-1.275	0.034	0.012	-43.963	-3.859	0.171
6/14/13	Carmel Chalk	8524	-2.120	0.002	34.858	0.005	10.974	0.024	-0.278	0.020	0.007	20.760	1.458	0.122
6/15/13	TV03	8566	3.138	0.002	30.272	0.005	11.542	0.026	-0.252	0.026	0.009	11.152	0.851	0.131
6/16/13	CM	8607	1.939	0.004	36.897	0.010	16.736	0.025	-0.510	0.024	0.008	25.153	1.802	0.060
6/16/13	Bonedry 6.26 mBUH	8624	-37.596	0.002	3.063	0.007	-54.310	0.034	-0.376	0.036	0.013	-45.895	-3.562	0.082
6/18/13	CM	8702	2.268	0.005	37.114	0.010	17.266	0.017	-0.518	0.020	0.007	25.672	1.890	0.135
6/18/13	618 Bonedry 6.03 mB UH	8738	-37.570	0.010	3.097	0.009	-54.238	0.045	-0.360	0.048	0.017	-45.573	-3.293	0.323
6/18/13	TV03	8746	3.274	0.003	30.357	0.004	11.801	0.020	-0.211	0.017	0.006	11.368	0.898	0.113
6/19/13	Carmel Chalk	8780	-2.017	0.003	35.099	0.005	11.323	0.030	-0.269	0.028	0.010	21.396	1.615	0.138
6/20/13	TV03	8807	3.305	0.019	30.289	0.036	11.737	0.057	-0.236	0.022	0.008	11.140	0.805	0.111
6/20/13	170 Bonedry 6.47H	8817	-37.732	0.003	3.690	0.002	-54.683	0.029	-1.272	0.031	0.011	-45.001	-3.872	0.119
6/20/13	3806-1 (run) (8833)	8833	-3.557	0.002	40.346	0.005	15.150	0.026	-0.157	0.023	0.008	32.518	2.353	0.114
6/20/13	694-13	8841	-0.697	0.003	39.427	0.006	17.027	0.015	-0.170	0.015	0.005	30.730	2.371	0.098
6/21/13	146-6	8849	-3.271	0.003	41.053	0.005	16.198	0.030	-0.094	0.027	0.010	34.114	2.538	0.108
6/21/13	3806-01 (run 2)	8857	-3.528	0.005	40.341	0.006	15.172	0.025	-0.159	0.029	0.010	32.604	2.446	0.136
6/21/13	CM	8865	2.325	0.005	37.109	0.007	17.318	0.029	-0.516	0.029	0.010	25.637	1.865	0.103
6/21/13	694-3 milled	8873	-0.292	0.001	39.014	0.007	16.955	0.033	-0.225	0.027	0.009	29.746	2.210	0.141
6/21/13	3806-1 (run 1)	8892	-3.541	0.002	40.277	0.008	15.084	0.029	-0.171	0.030	0.010	32.453	2.422	0.154
6/21/13	3806-1 (run 2)	8900	-3.726	0.013	40.291	0.024	14.903	0.038	-0.183	0.021	0.007	32.377	2.321	0.092
6/22/13	694-13	8909	-0.709	0.003	39.439	0.008	14.899	0.024	-0.148	0.063	0.022	30.587	1.933	0.785
6/22/13	CM	8917	2.326	0.002	37.161	0.006	17.373	0.014	-0.515	0.013	0.005	25.634	1.761	0.132
6/22/13	703-7 (run 1)	8925	-2.994	0.004	39.783	0.006	15.135	0.028	-0.164	0.024	0.009	31.417	2.365	0.128
6/22/13	703-7 (run 2)	8933	-3.186	0.002	39.726	0.007	14.880	0.036	-0.174	0.032	0.011	31.234	2.298	0.158
6/22/13	703-7 (run 3)	8941	-3.194	0.004	39.647	0.011	14.797	0.028	-0.171	0.024	0.009	31.177	2.393	0.233
6/22/13	694-13	8949	-0.748	0.002	39.412	0.007	16.952	0.034	-0.179	0.031	0.011	30.598	2.272	0.127
6/22/13	179 Bonedry CO2 6.79mB UH	8958	-37.585	0.001	3.512	0.009	-53.903	0.026	-0.413	0.026	0.009	-45.045	-3.566	0.127
6/22/13	CM	8966	2.222	0.002	37.126	0.006	17.253	0.024	-0.497	0.025	0.009	25.604	1.800	0.127
6/23/13	694-3 (run2)	8982	-0.419	0.003	39.432	0.009	17.292	0.041	-0.181	0.040	0.014	30.749	2.381	0.088

6/23/13	148-2 (run 1)	8991	-4.469	0.003	40.106	0.008	14.051	0.031	-0.123	0.026	0.009	32.204	2.512	0.133
6/23/13	148-2 (run 2)	8999	-4.398	0.004	40.104	0.013	14.123	0.029	-0.118	0.020	0.007	32.039	2.357	0.097
6/23/13	CM	9008	2.317	0.003	37.219	0.009	17.454	0.042	-0.484	0.037	0.013	25.847	1.858	0.075
6/23/13	703-2 (old)	9024	-1.884	0.283	40.084	3.185	17.603	0.027	-0.130	0.057	0.020	34.518	2.636	0.086
6/24/13	703-2 (new)	9032	-1.506	0.004	42.214	0.010	19.068	0.017	-0.113	0.016	0.006	36.734	2.835	0.071
6/24/13	146-6 (old)	9040	-2.383	0.008	40.632	0.008	16.616	0.038	-0.128	0.038	0.014	33.492	2.742	0.112
6/24/13	TV03	9048	3.339	0.015	30.388	0.008	11.873	0.028	-0.233	0.022	0.008	11.732	1.198	0.130
6/24/13	180-Bonedry-5.94-UH	9059	-37.525	0.003	2.836	0.008	-54.437	0.012	-0.351	0.010	0.003	-46.278	-3.512	0.128
6/24/13	694-13	9067	-0.734	0.006	39.377	0.009	16.927	0.038	-0.183	0.032	0.011	30.620	2.362	0.099
6/24/13	3808-5	9075	-5.981	0.003	39.179	0.007	11.562	0.024	-0.208	0.023	0.008	30.049	2.211	0.148
6/24/13	3808-4	9084	-2.948	0.007	40.023	0.009	15.378	0.022	-0.205	0.019	0.007	31.904	2.376	0.159
6/25/13	3808-3	9094	-4.540	0.002	39.436	0.008	13.228	0.022	-0.210	0.018	0.006	30.790	2.430	0.142
6/25/13	CM	9102	2.302	0.002	37.197	0.008	17.383	0.016	-0.517	0.017	0.006	25.863	1.916	0.111
6/25/13	Adamossi (run 1)	9111	1.832	0.010	43.420	0.013	23.569	0.020	-0.099	0.025	0.009	39.388	3.068	0.180
6/25/13	Adamossi (run 2)	9121	1.818	0.001	43.432	0.005	23.569	0.051	-0.097	0.050	0.018	39.329	2.988	0.124
6/26/13	Adamossi (run 3)	9129	1.826	0.004	43.450	0.009	23.586	0.043	-0.107	0.044	0.015	39.421	3.042	0.166
6/26/13	620 Evap + Oz - 5.97 mB - H	9138	-3.777	0.005	42.539	0.009	16.480	0.018	-0.781	0.019	0.007	37.081	2.556	0.094
6/27/13	703-2 (old) run 2	9189	-2.073	0.003	41.139	0.011	17.450	0.034	-0.103	0.026	0.009	34.539	2.780	0.159
6/27/13	TV03	9197	3.326	0.002	30.248	0.020	11.707	0.031	-0.246	0.022	0.008	11.334	1.076	0.169
6/27/13	146-6 (new) (run1)	9208	-3.426	0.004	40.994	0.006	15.954	0.020	-0.128	0.017	0.006	34.605	3.128	0.113
6/27/13	146-6 (new) (run2)	9216	-3.415	0.002	41.073	0.009	16.072	0.028	-0.099	0.033	0.012	34.243	2.626	0.081
6/28/13	694-13 (run 2)	9232	-0.658	0.004	39.485	0.009	16.977	0.359	-0.187	0.019	0.007	31.386	2.521	0.094
6/28/13	CM	9240	2.345	0.009	37.161	0.011	17.373	0.026	-0.532	0.025	0.009	25.938	2.058	0.137
6/29/13	171 Bonedry 6.13mB H	9311	-37.636	0.008	3.763	0.017	-54.542	0.024	-1.291	0.029	0.010	-44.817	-3.824	0.156
7/3/13	178 Bonedry- 6.53 mB- UH	9529	-37.864	0.002	3.192	0.007	-54.477	0.027	-0.416	0.027	0.009	-46.048	-3.976	0.122
7/5/13	176 Bonedry 5.97 mB-H	9641	-37.763	0.004	2.908	0.011	-55.473	0.036	-1.282	0.039	0.014	-47.058	-4.469	0.121
7/7/13	183 Bonedry CO2 6.33mB UH	9747	-37.759	0.002	2.383	0.008	-55.136	0.038	-0.396	0.034	0.012	-47.661	-4.057	0.099
7/10/13	185 Bonedry CO2- 6.51 mB- UH	9940	-37.856	0.002	2.651	0.007	-54.975	0.021	-0.400	0.027	0.010	-47.040	-3.939	0.139
7/11/13	623 Evap DI oz 5.77mB UH	9981	-3.834	0.004	46.136	0.015	20.890	0.020	0.092	0.018	0.007	45.307	3.579	0.097
7/14/13	Bonedry174 CO2 6.38mB H	10156	-37.638	0.002	4.306	0.004	-54.059	0.040	-1.330	0.040	0.014	-44.135	-4.190	0.155
7/16/13	624 Evap DI + Oz 5.9mB UH	10271	-3.777	0.023	46.662	0.047	21.448	0.087	0.072	0.024	0.008	46.375	3.595	0.142
7/18/13	626 Evap.DI+oz 6.17mB H	10372	-3.884	0.002	46.050	0.016	19.889	0.041	-0.756	0.030	0.011	45.033	3.480	0.125
7/18/13	177 Bonedry 6.22 mB UH	10409	-37.540	0.003	2.941	0.010	-54.417	0.015	-0.421	0.019	0.007	-46.543	-3.996	0.174
7/20/13	627 Evap DI+Oz 6.11mB H	10440	-3.860	0.002	45.605	0.008	19.481	0.021	-0.745	0.024	0.008	44.038	3.379	0.150
7/21/13	184 Bonedry 6.25 UH	10462	-37.362	0.004	3.866	0.014	-53.358	0.021	-0.420	0.023	0.008	-44.654	-3.860	0.140
7/28/13	632 Evap DI+Oz 6.35mB UH	10484	-3.814	0.003	46.665	0.007	21.466	0.051	0.122	0.043	0.015	46.285	3.503	0.193

Fig. S1

		from multiple regression	
line		intercept - observed	intercept - theoretical
25oC		0.05506	0.9252
1000oC		-0.8145	0.0266
common slope	0.005981		

emp. Transfer function	
slope	1.033396
intercept	0.868301

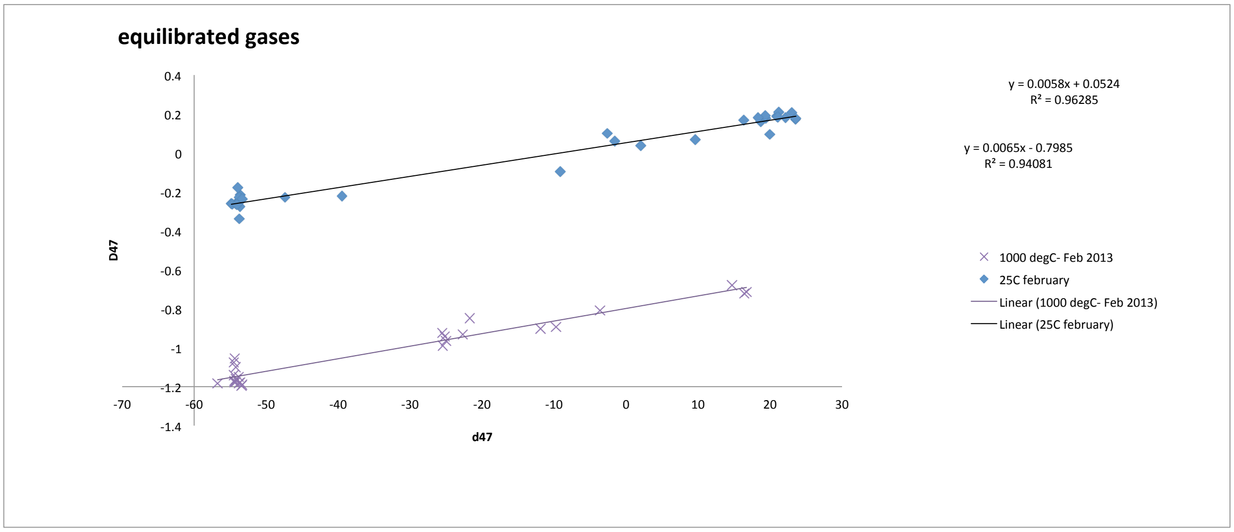

Fig. S2

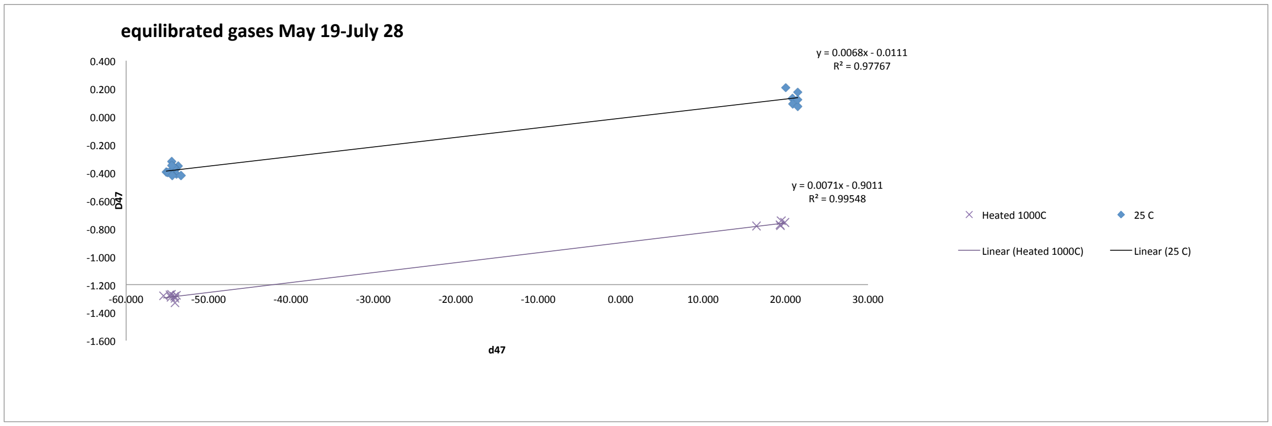

May 19 - July 28

Population 1	line		intercept - observed	intercept - theoretical	emp. Transfer function	
	25oC		-0.007724	0.9252	slope	1.001475577
	1000oC		-0.905	0.0266	intercept	0.932935397
	common slope	0.006952				